UNIVERSITY OF LJUBLJANA
FACULTY OF MATHEMATICS AND PHYSICS
DEPARTMENT OF PHYSICS

Nejc Košnik

STANDARD MODEL AND SIGNATURES OF NEW PHYSICS IN WEAK AND RADIATIVE DECAYS OF HEAVY MESONS

Doctoral thesis

ADVISOR: prof. dr. Svjetlana Fajfer

Ljubljana, 2010

UNIVERZA V LJUBLJANI
FAKULTETA ZA MATEMATIKO IN FIZIKO
ODDELEK ZA FIZIKO

Nejc Košnik

STANDARDNI MODEL IN SLEDI NOVE FIZIKE V ŠIBKIH IN RADIACIJSKIH RAZPADIH TEŽKIH MEZONOV

Doktorska disertacija

MENTOR: prof. dr. Svjetlana Fajfer

Ljubljana, 2010

Abstract

We study rare decays of heavy B and D mesons in the standard model and several new physics models. For the extremely rare process $b \to dd\bar{s}$ we use the experimental limit of $B^- \to \pi^-\pi^-K^+$ to constrain parameter space of model with Z' gauge boson and MSSM with broken R_p-parity. We predict upper bounds of several two-body hadronic B^- decay branching fractions which turn out to be of the order 10^{-7} in the case of Z' model.

For the $c \to u\ell^+\ell^-$, where $\ell = e, \mu$ we study spectra and decay widths of $D \to P\gamma$ and $D_{(s)} \to \pi(K)\ell^+\ell^-$. We model the long distance amplitude with the intermediate resonances using the Breit-Wigner shape. We find new bounds on the new physics parameters coming from the $D^+ \to \pi^+\mu^+\mu^-$ experimental upper bound and predict decay spectra and widths of the $D_s \to K\ell^+\ell^-$. We find MSSM with broken R_p-parity and the model with singlet leptoquark in SM representation $(3, 1, -1/3)$ have best prospects to be probed in experimental searches.

We use a combined heavy quark, large energy, and chiral symmetry of QCD and make a prediction of photon spectra of $B \to K\eta\gamma$ in a kinematic region with hard photon and one soft meson. Precision of future experiments will allow for probing $b \to s\gamma$ transition in this kinematical region.

In experimental analyses of $B^- \to D^0\ell\bar{\nu}$ decay there is a background of events with additional undetectable soft photon. We find that D^{0*} contributes dominantly in this respect due to small mass splitting between D^{0*} and D^0. Future experiments should be able to detect photons of energy below 100 MeV in order to extract V_{cb} with precision of order 1%.

Keywords: weak decays of heavy mesons, flavour changing neutral current, new physics searches, radiative decays

PACS (2008): 13.20.-v, 13.20.He, 13.20.Fc, 13.25.Hw

Povzetek

V tezi raziščemo razpade težkih mezonov B in D v okviru standardnega modela in nekaterih modelov nove fizike. Za izjemno redek proces $b \to dd\bar{s}$ uporabimo obstoječo zgornjo eksperimentalno mejo razpada $B^- \to \pi^-\pi^-K^+$, da omejimo parametre modelov nove fizike, kot sta model z dodatnim umeritvenim bozonom Z' in minimalni supersimetrični standardni model s kršeno parnostjo R_p. Napovemo zgornje meje razvejitvenih razmerij za nekatere dvodelčne hadronske razpadne kanale mezona B^-. Le-te so v primeru modela z bozonom Z' reda 10^{-7}.

Raziščemo spektre in razpadne širine razpadov $D \to P\gamma$ in $D_{(s)} \to \pi(K)\ell^+\ell^-$, kjer je $\ell = e, \mu$, ki temeljijo na procesu $c \to u\ell^+\ell^-$. Dolgosežne prispevke amplitude modeliramo z vmesnimi resonančnimi stanji in Breit-Wignerjevim nastavkom. Izhajajoč iz zgornje eksperimentalne meje razvejitvenega razmerja razpada $D^+ \to \pi^+\mu^+\mu^-$, izpeljemo nove meje parametrov za minimalni supersimetrični model s kršeno parnostjo R_p in model s skalarnim leptokvarkom v reprezentaciji $(3, 1, -1/3)$. S temi parametri napovemo tudi spektre in razpadne širine razpadov $D_s \to K\ell^+\ell^-$. Omenjena modela nove fizike imata tudi največ možnosti zaznave v eksperimentih.

Za radiacijski razpad $B \to K\eta\gamma$ v kinematičnem območju z visokoenergijskim fotonom in enim počasnim mezonom, z uporabo simetrije težkih kvarkov, efektivne teorije visoke energije, in kiralne simetrije kvantne kromodinamike, napovemo fotonski spekter. V prihodnosti bodo eksperimenti lahko merili prehod $b \to s\gamma$ v omenjenem kinematičnem območju.

V eksperimentalnih analizah $B^- \to D^0\ell\bar{\nu}$ ima pomembno vlogo dodatni foton, ki ga eksperiment ne zazna in tako prispeva k ozadju semileptonskega razpada. Ugotovimo, da je zaradi majhne razlike mas mezonov D^{0*} in D dominantni mehanizem takšnega ozadja resonančni proces preko vmesnega D^{0*}. Spodnji rez na fotone nizkih energij bi moral biti nižje od 100 MeV, da bi lahko iz analize semileptonskega razpada ugotovili vrednost matričnega elementa V_{cb} z natančnostjo okrog 1%.

Ključne besede: šibki razpadi težkih mezonov, okus spreminjajoči nevtralni tokovi, iskanje nove fizike, radiacijski razpadi

PACS (2008): 13.20.-v, 13.20.He, 13.20.Fc, 13.25.Hw

I acknowledge the financial support of the Slovenian Research Agency and throughout completion of this thesis. Parts of this work have been completed with the financing from FLAVIAnet network, whose support I also acknowledge.

Above all, I am deeply grateful to my advisor prof. Svjetlana Fajfer for all the support, stimulating discussions, and patient guidance throughout my graduate study. It is to say that without her immense help this work would have never seen the light of day.

My thanks go to Jernej Kamenik, Damir Bećirević, Ilja Doršner, Saša Prelovšek, and Tri-Nang Pham with whom I completed parts of this work and meanwhile learned a great deal about physics. For fruitful discussions I also thank Miha Nemevšek, Jure Drobnak, and Jure Zupan. Special thank goes to Damir Bećirević who allowed me to complete a part of this thesis at LPT Orsay.

During the making of this work I have enjoyed a stimulating atmosphere at the Department of Theoretical Physics of Jožef Stefan Institute, where I've spent a good time in the company of my colleagues and friends. In this respect, I thank Matej Kanduč, Samir El Shawish, and Ana Hočevar for making the coffee and lunch breaks lively.

Last but definitely not least, I would like to thank Alenka for her patience and support during the last few months.

Contents

Notation

Greek indices μ, ν, ... run over the spacetime coordinates $0, 1, 2, 3$.

Spacetime metric $g^{\mu\nu}$ is diagonal with elements $-g^{00} = g^{11} = g^{22} = g^{33} = -1$.

Covariant derivative operator is $\partial_\mu = \frac{\partial}{\partial x^\mu}$. d'Alambertian ∂^2 is defined as $\partial_\mu \partial^\mu$.

The four-dimensional Levi-Civita tensor $\epsilon^{\mu\nu\alpha\beta}$ is totally antisymmetric and has $\epsilon^{0123} = +1$.

Dirac gamma matrices γ^μ satisfy the anticommutation relation $\gamma^\mu\gamma^\nu + \gamma^\nu\gamma^\mu = 2g^{\mu\nu}$. We define $\gamma_5 = i\gamma^0\gamma^1\gamma^2\gamma^3 = -i/4!\,\epsilon_{\mu\nu\alpha\beta}\gamma^\mu\gamma^\nu\gamma^\alpha\gamma^\beta$.

Left- and right-handed projection operators are defined as $P_{L,R} = (1 \mp \gamma_5)/2$.

We use units where $\hbar = c = 1$.

H.c. denotes a Hermitian conjugate of the preceding expression.

Chapter 1

Introduction

The standard model of particle physics has been established as a satisfactory theory of smallest verifiable distances and time scales. It is a model with 19 free parameters which have been overconstrained by hundreds of measured observables collected during the last three decades. Still to date there has been no direct experimental evidence of an observable that would, including experimental and theoretical uncertainties, deviate more than 3 standard deviations from the standard model predictions. The only exception is the observation of neutrino mixing, which cannot be explained with massless neutrinos of the standard model.

1.1 Standard model and beyond

Further indirect experimental evidence supporting incompleteness of the standard model (SM) originate from cosmological and astrophysical observations. Namely, SM lacks dark matter particle which should not be a baryon and must interact very weakly. However, there exists a possibility that axions of quantum chromodynamics could comprise the required dark matter. The observed abundance of matter with respect to antimatter in the present day universe requires baryogenesis with stronger breaking of charge-parity (CP) symmetry violation than is present in the SM.

One aspect of the SM experimental tests has been to look for new energy thresholds where new degrees of freedom would become relevant. In this way, the gauge structure of SM was confirmed directly at the weak scale ~ 100 GeV at the Large Electron Positron collider (LEP), where the weak bosons and neutral currents were first discovered. The electroweak-breaking sector of the SM should be directly studied at Fermilab and the Large Hadron Collider (LHC) in the forthcoming years with typical energy of partonic reactions of the order 1 TeV. On the other hand, Yukawa sector of the SM exposes its richness in the quark flavor changing interactions, which are well suited for study in hadron and τ lepton weak decays and are accessible at energies much below the weak scale. From theoretical perspective, hadron states are bound by a genuinely nonperturbative phenomenon of strong interactions — confinement — which is interesting in its own right, but in this case blurs the view of electroweak dynamics that drives the decay. Nonperturbative hadronic dynamics, whose quantitative treatment makes theoretical predictions rather uncertain, thus stands between a clean comparison of observables' measured values and predictions

of SM or of a theory that would supersede SM at energies above the electroweak scale.

Conceptual reasons have also been put forward for considering SM as merely an effective low-energy theory of its yet unknown ultraviolet completion. Certainly SM would fail to describe physical phenomena at the Planck scale ($M_P \simeq 10^{19}$ GeV), at which gravity should be reconciled with principles of quantum mechanics. In principle, SM could hold up to almost M_P but in this case the fundamental scalar field in the SM — the Higgs doublet — which breaks the electroweak symmetry and provides masses for gauge bosons and fermions, seems unnaturally light. The *hierarchy problem* is the problem of instability of Higgs mass term, which is, due to being a coupling of relevant operator, naturally expected to be driven to the SM cut-off scale Λ. Namely, first order additive quantum corrections to the Higgs mass scale as Λ^2 and setting $\Lambda \simeq M_P$ requires excessive fine-tuning of the tree-level Higgs mass term. On the other hand, Higgs mass should not be too far from the electroweak scale in order to satisfy all experimental constraints coming in particular from the electroweak precision observables [1]. The common opinion about hierarchy problem is that there should be a scale close to or not far above 1 TeV, at which SM might loose its validity and is to be replaced by a more fundamental theory, usually termed *new physics* (NP) in the literature. Currently there are many viable possibilities about what the NP may be like, however none of them is clearly preferred over others owing to good agreement of SM predictions with experimental data.

1.2 Flavour physics

Presently available experimental data from LEP, Fermilab experiments, B-factories, and other low energy experiments as well as astrophysical and cosmological observations impose important constraints on NP models. The experiments based on the colliding e^+e^- beams measured a whole plethora of quark flavor changing processes, driven by the tree-level charged weak currents as well as flavor changing neutral currents (FCNC) which lead to rare meson decays and neutral meson mixing. Violation of CP symmetry has been observed both in meson mixing amplitudes and directly in the decay amplitudes. Important contributions have also come from Fermilab experiments, most notably the discovery of B_s meson mixing.

1.2.1 Flavour sector of the standard model

The number of quark generations N is a free parameter in the SM, and so are the quark masses and quark flavour mixing parameters. Anomaly cancellation condition [2] only requires that we have an equal number of quark and lepton generations, while the asymptotic freedom of quantum chromodynamics requires $N \leq 8$. It was pointed out by Kobayashi and Maskawa [3] before the third generation of quarks was discovered, that one needs at least $N = 3$ generations of quarks to accommodate one CP-violating phase in the Cabibbo-Kobayashi-Maskawa (CKM) matrix [3, 4]. Thus the observed phenomenon of CP violation is not a prediction of the SM but rather a consequence of observation of 3 generations. To put it differently, for observation of 3 generations SM predicts there should be exactly one real parameter

describing all CP violating phenomena[1]. The magnitude of mixing is parameterized by 3 angles in the CKM matrix, which are known to be small, i.e. the CKM matrix is, to within $\lambda = 0.22$ error, diagonal. The flavour changing transitions are hierarchically suppressed as λ, λ^2, and λ^3 for the respective transitions between generations $1 \leftrightarrow 2$, $2 \leftrightarrow 3$, and $3 \leftrightarrow 1$. Since the angles are free parameters, SM cannot provide a reason for their smallness, and neither can for huge disparity between quark masses which span over 5 orders of magnitude. Questioning the reason behind the measured flavour parameters is meaningful only in a suitable NP model.

1.2.2 Flavour changing neutral currents

The Glashow-Iliopoulos-Maiani (GIM) mechanism of SM suppresses FCNCs through sums over intermediate quark flavours which contribute to the process at loop order. Presence of FCNCs in the SM amplitude is recognized by a fermion line running through the Feynman graph connecting two fermions of different generation but same charge. GIM is directly related to unitarity of the CKM matrix and thus an inherent property of SM amplitudes. It is broken only by the nondegenerate quarks masses. NP models with new sources of flavor violation generally lack a mechanism analogous to GIM, thus leading to severe experimental constraints on flavour violation parameters of the NP model or potentially result in a clean signal of NP with small SM background. Moreover, since FCNCs are loop-induced they are sensitive to short distance dynamics that might play a role in quantum corrections. One well-known example is the study of dependence of the $B \to K^*\gamma$ decay width upon the top quark mass [6].

However, all observables that involve quark flavour change confirm the CKM mixing mechanism among the six quark flavours and is best illustrated by the unitarity triangle shown on Figure 1.1. Absence of deviations at few percent level requires a highly nontrivial flavour structure of NP around the 1 TeV scale, whereas scale of a generic NP model is to be of the order 100 TeV or above. The above-mentioned flavour constraints are in tension with the hierarchy problem as they force the NP scale far above 1 TeV. The problem has been addressed in a model independent framework called minimal flavour violation [8, 9], where the flavour structure of NP is exactly aligned with the SM, i.e., the SM flavour group is broken only by the SM Yukawa couplings.

1.2.3 Heavy meson decays

Heavy B (D) meson contains a heavy valence b (c) quark and another light valence anti-quark. Mass above 5 GeV allows the B meson to decay weakly into numerous final states resulting in many observables where one could find signatures of physics beyond the SM. The CKM flavour mixing mechanism has been thoroughly tested in K and B decay observables [10], the most important of the latter we list in the following. Exclusive and inclusive charm decays can be used to constrain V_{cb}, while charmless B decays constrain V_{ub}. Time dependent CP asymmetry in $B \to J/\psi K_S$

[1] Another source of CP violation is the θ term of quantum chromodynamics, which is however constrained by the electric dipole moment of the neutron ($|d_n| < 3 \times 10^{-26}$ ecm) which implies $\theta < 10^{-9}$ [5].

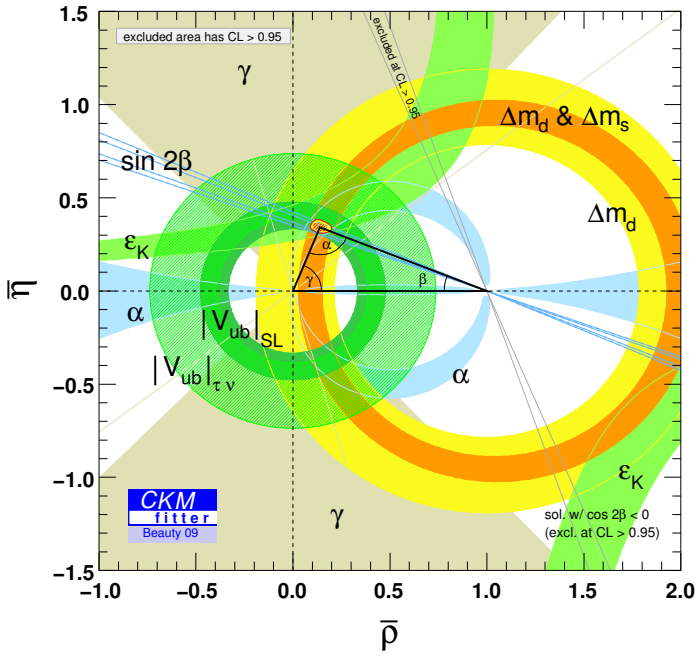

Figure 1.1: Unitarity of the CKM matrix is globally satisfied [7].

depends on the phase difference between the B^0–$\bar{B}^0$ mixing amplitude and the decay amplitude and provides a very precise measurement of $\sin 2\beta$ (see Figure 1.1). Decay widths of several $B \to DK$ decay channels and hadronic channels $B \to \pi\pi, \rho\pi, \rho\rho$ provide constraints on the respective angles γ and α. The ratio of mass splittings determined in B^0 and B_s mixing is a measure of $|V_{td}/V_{ts}|$.

Semileptonic and leptonic charm meson decays can probe magnitudes of $|V_{cd}|$ and $|V_{cs}|$. Very recently also neutral charm meson mixing has been measured [11–15], offering various new possibilities in the up-type quarks FCNCs. However, the $c \leftrightarrow u$ FCNC process is dominated by d and s quarks in the loop (b quark contributions Cabibbo suppressed by factor λ^5) and light hadronic resonances dominate the decay widths.

From the theoretical viewpoint, large masses of heavy quarks, compared to the QCD scale ($m_Q \gg \Lambda_{\mathrm{QCD}} \approx 200$ MeV), admit considering a limit, where we treat the them as infinitely massive and thus static. In this case QCD is symmetric under heavy quark spin and flavour rotations and consequently different form factors between heavy mesons are related to a single Isgur-Wise function [16, 17]. In the framework of heavy quark effective theory (HQET) one can systematically incorporate the $1/m_Q$ symmetry breaking terms and α_s radiative corrections. When heavy meson decays to an energetic light hadron via heavy to light quark transition $Q \to q$, the light quark is almost on the light cone where additional symmetries arise.

1.3 Goals and methods

Considering the existing results from B-factories, with LHCb almost in the physics run, and recent approval of the Belle 2 experiment, precision of D and B meson decay observables will improve considerably. The two new experiments will hopefully find an evidence for NP or provide a good handle for discrimination between NP models.

In this thesis we set out to analyse rare decays of B and D mesons in framework of SM and several NP models. We shall provide for considered decay channels a comparison between the SM prediction and experimental results (or bounds at 90% confidence level (CL) if the decay in question has not yet been discovered). Afterwards we study what would be the impact on observables of particular NP model. Among these we will consider minimal supersymmetric standard model with (MSSM) and without ($\not{R}_p$MSSM) R_p-parity conservation, models with extra Z' neutral gauge boson, models with additional singlet up-type quark (EQS), and class of models with scalar weak singlet leptoquark (LQ).

For meson decays dynamical heavy degrees of freedom like W bosons, t quark, and short distance NP dynamics are integrated out and absorbed in the short distance Wilson coefficients of operator product expansion [18, 19]. Where necessary we will account for the QCD corrections in the effective Lagrangian. For matrix elements between meson states we will either use form factors calculated by dispersive methods (QCD sum rules, light-cone sum rules), lattice QCD, or use form factors determined experimentally. Whenever feasible we shall utilize underlying symmetries of QCD which arise in specific kinematic circumstances. For heavy quarks interacting with light degrees of freedom this is the aforementioned heavy quark symmetry and in the case of energetic light quark the large energy effective theory, whereas low energy light degrees of freedom interact as dictated by chiral symmetry of QCD.

1.4 Structure of thesis

In Chapter 2 we restate the mechanism of flavour violation in SM and outline the procedure of separating short distance from long distance dynamics when treating weak meson decays in SM. Relevant aspects of NP models will be described when needed, *in situ*.

Chapter 3: Rare process $b \to dd\bar{s}$. Quark transition $b \to dd\bar{s}$ and the corresponding hadronic decay channels would be too rare to be detected if SM was a complete theory. Currently, the best bound is obtained in $B^- \to \pi^-\pi^-K^+$ channel. Experimental evidence would serve as indisputable proof of NP, but already existing bounds on branching ratios can be used to constrain some NP models and predict viability of searches in other hadronic modes.

Chapter 4: Neutral currents in charm and $D \to P\ell^+\ell^-$. Semileptonic decay channel $D \to \pi\ell^+\ell^-$ and $D_s \to K\ell^+\ell^-$ encompass the $c \to u\ell^+\ell^-$ process and are sensitive to FCNCs of up-type quarks. With existing bounds on parameters of NP models there is still some room for signals in the kinematical region with low and high invariant mass of the dilepton pair.

Chapter 5: Dalitz plot analysis of $B \to K\eta\gamma$ decay. We focus on two corners of Dalitz plot with one or other meson soft. We predict the photon spectra in the two regions in the SM.

Chapter 6: Radiative background of $B \to D\ell\bar{\nu}$. This exclusive decay channel is used to extract the magnitude of V_{cb}. We explore the impact on precision of V_{cb} measurement if the resonant D^* meson decays into an unobserved photon and a D meson.

In Chapter 7 we summarize the results and draw conclusions. Intermediate derivations and too long expressions are relegated to appendices whenever their presence would bother the main line of thought.

Chapter 2

Flavour violation at low energies

2.1 Flavour violation in the standard model

In this section we will demonstrate how flavour violation arises in the standard model (SM). SM is a realization of relativistic quantum field theory consistent with Lorentz invariance and causality and has built in basic postulates of quantum mechanics like positivity and unitarity [20–22]. Structure of the SM interactions is completely specified with local gauge group $G = SU(3)_c \times SU(2)_W \times U(1)_Y$ and its fermionic representations:

$$\begin{aligned} &E(1,2)_{-1/2} = \begin{pmatrix} \nu_L \\ \ell_L \end{pmatrix}, && \ell_R(1,1)_{-1}, \\ &Q(3,2)_{1/6} = \begin{pmatrix} u_L^1 \\ d_L^1 \end{pmatrix}, \begin{pmatrix} u_L^2 \\ d_L^2 \end{pmatrix}, \begin{pmatrix} u_L^3 \\ d_L^3 \end{pmatrix}, && \\ &u_R(3,1)_{2/3} = \begin{pmatrix} u_R^1 & u_R^2 & u_R^3 \end{pmatrix}, && d_R(3,1)_{-1/3} = \begin{pmatrix} d_R^1 & d_R^2 & d_R^3 \end{pmatrix}, \end{aligned} \tag{2.1}$$

where the numbers in the brackets denote representations of the respective color, weak isospin, and weak hypercharge groups. The above gauge structure repeats itself in three generations of matter, which are distinct only by the Yukawa couplings in the SM Lagrangian (2.3). The Lagrangian density of SM is commonly split into four terms

$$\mathcal{L} = \mathcal{L}_{\text{kin}} + \mathcal{L}_{\text{gauge}} + \mathcal{L}_{\text{Yuk}} + \mathcal{L}_{\text{EWB}}. \tag{2.2}$$

These, in the order as written above, correspond to gauge-covariant kinetic terms of fermions, kinetic terms of gauge bosons, and Yukawa couplings between fermions and Higgs field. To break the electroweak symmetry and allow for masses of the gauge bosons and fermions, an additional scalar field ϕ — the Higgs scalar – in the representation $(1,2)_{1/2}$ is introduced [23–26]. The electroweak symmetry breaking potential, present in $\mathcal{L}_{\text{EWB}}$, then triggers the Higgs field to develop a spacetime-uniform vacuum expectation value (VEV). Parameters responsible for fermion masses an flavour changing interactions of quarks are contained in

$$\mathcal{L}_{\text{Yuk}} = -\bar{Q}\phi Y^d d_R - \bar{Q} i\tau^2 \phi^* Y^u u_R - \bar{E}\phi Y^e e_R + \text{H.c.}, \tag{2.3}$$

where $Y^{d,u,e}$ are the 3×3 dimensionless Yukawa matrices in generation space. The Higgs field has develops a VEV

$$\langle \phi \rangle_0 = \begin{pmatrix} 0 \\ v/\sqrt{2} \end{pmatrix}, \tag{2.4}$$

and mass terms for the fermions arise in the Yukawa potential

$$\mathcal{L}_{\text{Yuk}} \ni -\frac{v}{\sqrt{2}}\, \bar{d}_L Y^d d_R - \frac{v}{\sqrt{2}}\, \bar{u}_L Y^u u_R - \frac{v}{\sqrt{2}}\, \bar{e}_L Y^e e_R + \text{H.c.}\,. \tag{2.5}$$

In order to operate with conventional Feynman rules with flavour-diagonal propagators, we have to work in the mass-basis of fermion fields. For a general complex matrix Y two unitary matrices $\mathcal{U}$ and $\mathcal{V}$ can always be found such that $Y = \mathcal{U}^\dagger D \mathcal{V}$, where D is diagonal. We express the Yukawa matrices in terms of physical fermion masses and unitary rotations

$$Y^u = \mathcal{U}_L^\dagger \,\text{diag}(m_u, m_c, m_t)\, \mathcal{U}_R, \tag{2.6a}$$

$$Y^d = \mathcal{D}_L^\dagger \,\text{diag}(m_d, m_s, m_b)\, \mathcal{D}_R, \tag{2.6b}$$

$$Y^e = \mathcal{E}_L^\dagger \,\text{diag}(m_e, m_\mu, m_\tau)\, \mathcal{E}_R, \tag{2.6c}$$

and absorb the rotations in fermion fields $u_{L,R} \to \mathcal{U}_{L,R}^\dagger u_{L,R}$, $d_{L,R} \to \mathcal{D}_{L,R}^\dagger d_{L,R}$, $e_{L,R} \to \mathcal{E}_{L,R}^\dagger e_{L,R}$ in order to make the mass terms (2.5) diagonal. The flavour rotations connecting the weak- and mass-basis fields cancel out in the kinetic and neutral current terms of the SM Lagrangian because of their unitarity. This cancellation does not occur in the quark charged current coupled to W boson where the remnant physical parameter is the misalignment between rotations of up-type and down-type left-handed quarks[1]

$$\mathcal{L}_{\text{kin}} \ni -\frac{g}{\sqrt{2}} W_\mu^+ \, \bar{u}_i \gamma^\mu P_L (\mathcal{U}_L \mathcal{D}_L^\dagger)_{ij} d_j + \text{H.c.}, \tag{2.7}$$

The CKM matrix $V = \mathcal{U}_L \mathcal{D}_L^\dagger$ thus contains all parameters of the SM flavour changing interactions.

2.1.1 CKM matrix

The CKM matrix for N quark doublets is described by a total of $N(N-1)/2$ Euler angles and $N(N+1)/2$ phase factors. We may redefine the phases of each up- and down-type quark fields — $2N$ of them — and get eliminate $2N-1$ phases from the CKM matrix and end up with altogether

$$(N-1)^2 = \underbrace{N(N-1)/2}_{\text{Euler angles}} + \underbrace{(N-2)(N-1)/2}_{\text{phases}} \tag{2.8}$$

real parameters. Based on observed CP violation in K^0–$\bar{K}^0$ mixing and the above-mentioned phase counting, Kobayashi and Maskawa [3] proposed existence of the

[1] We work here in the unitary gauge to avoid complications with flavour changing couplings of Goldstone modes.

third quark generation before even charm quark was discovered. For the $N = 3$ SM, three angles θ_{12}, θ_{23}, θ_{13}, and phase δ are conventionally taken as

$$V = \begin{pmatrix} c_{12}c_{13} & s_{12}c_{13} & s_{13}e^{-i\delta} \\ -s_{12}c_{23} - c_{12}s_{23}s_{13}e^{i\delta} & c_{12}c_{23} - s_{12}s_{23}s_{13}e^{i\delta} & s_{23}c_{13} \\ s_{12}s_{23} - c_{12}c_{23}s_{13}e^{i\delta} & -c_{12}s_{23} - s_{12}c_{23}s_{13}e^{i\delta} & c_{23}c_{13} \end{pmatrix} \tag{2.9}$$

with $c_{ij} \equiv \cos\theta_{ij}$, $s_{ij} \equiv \sin\theta_{ij}$. Note that the CP phase is absent from CKM matrix when $s_{13} = 0$. Experiments have established the smallness of all mixing angles, meaning that CKM matrix is diagonal up to λ corrections, a fact which we demonstrate below. Hierarchy of CKM elements becomes more lucid in the Wolfenstein parameterization [27] which is a power expansion in $\lambda \equiv s_{12}$ along with redefined parameters [28, 29] $s_{23} \equiv A\lambda^2$, $s_{13}e^{-i\delta} \equiv A\lambda^2(\rho - i\eta)$:

$$V = \begin{pmatrix} 1 - \frac{\lambda^2}{2} & \lambda & A\lambda^3(\rho - i\eta) \\ -\lambda & 1 - \frac{\lambda^2}{2} & A\lambda^2 \\ A\lambda^3(1 - \rho - i\eta) & -A\lambda^2 & 1 \end{pmatrix} + \mathcal{O}(\lambda^4). \tag{2.10}$$

Working to λ^3 order we can take $\lambda = 0.226 \pm 0.001$, value of Cabibbo angle $\cos\theta_c$, while other parameters' values are [28] $A = 0.81 \pm 0.02$, $\rho = 0.14^{+0.03}_{-0.02}$, and $\eta = 0.36 \pm 0.02$. Mutual orthogonality relations between columns $\sum_k V_{ki}V^*_{kj} = \delta_{ij}$ and rows $\sum_k V_{ik}V^*_{jk} = \delta_{ij}$ of V can be depicted as six unitarity triangles, of which the one corresponding to product between the first and the third column is commonly used to illustrate the unitarity triangle analyses (Figure 1.1).

2.2 Operator product expansion in weak decays

Weak decays of heavy mesons are processes involving a typical kinematical energy scales of at most few GeV. In contrast, the dynamical degrees of freedom triggering a weak decay are the weak gauge bosons of a mass ~ 100 GeV or even heavier NP degrees of freedom. Full theory treatment becomes rather awkward due to large disparity of scales in the problem. Thus, to facilitate calculations of decay amplitudes and in particular their QCD renormalization effects one works instead with effective f-flavour theory, where $f = 5, 4, \ldots$ is the number of dynamical quark fields at the chosen renormalization scale μ. To this end, we will integrate over the W boson field in the generating functional in the presence of external weak currents $J^\pm_\mu$. We integrate over the weak gauge bosons degrees of freedom whereas the weak currents of fermions are here treated as external fields [29]

$$Z_W[J^+_\mu] = \int \mathcal{D}W^+\mathcal{D}W^- \exp\left[i\int d^4x \left(\mathcal{L}_W + \frac{g}{\sqrt{2}}(J^+_\mu W^{+\mu} + J^-_\mu W^{-\mu})\right)\right]. \tag{2.11}$$

Coupling constant of the $SU(2)$ weak isospin is denoted g. The functional integral measure is defined as [30]

$$\mathcal{D}W^\pm = N(\epsilon)\prod_x dW^\pm_0(x)\, dW^\pm_1(x)\, dW^\pm_2(x)\, dW^\pm_3(x), \tag{2.12}$$

where Π_x denotes the product over the points of infinitesimally discretized space-time with spacing ϵ [2].

$$\mathcal{L}_W = -\frac{1}{2}(\partial_\mu W^+_\nu - \partial_\nu W^+_\mu)(\partial^\mu W^{-\nu} - \partial^\nu W^{-\mu}) + m_W^2 W^+_\mu W^{-\mu}, \tag{2.13}$$

$$J^+_\mu = V_{ij}\bar{u}_{iL}\gamma_\mu d_{jL} + \bar{\nu}_{iL}\gamma_\mu \ell_{iL}, \qquad J^-_\mu = (J^+_\mu)^\dagger. \tag{2.14}$$

We work in the unitary gauge of the electroweak interactions, where the Goldstone scalars are absorbed by the longitudinal components of weak bosons. The kinetic terms can be rewritten using per partes integration and dropping the surface terms

$$\begin{aligned} -\partial_\mu W^+_\nu \partial^\mu W^{-\nu} + \partial_\mu W^+_\nu \partial^\nu W^{-\nu} + m_W^2 W^+_\mu W^{-\mu} & \\ \longrightarrow W^+_\nu \partial^2 W^{-\nu} - W^+_\nu \partial^\nu \partial_\mu W^{-\mu} + m_W^2 W^+_\mu W^{-\mu} & \\ = W^+_\mu K^{\mu\nu}(x,y) W^-_\nu, & \end{aligned} \tag{2.15}$$

$$K^{\mu\nu}(x,y) \equiv \delta^4(x-y)\left[(\partial^2_{(y)} + m_W^2) g^{\mu\nu} - \partial^\mu_{(y)}\partial^\nu_{(y)}\right], \tag{2.16}$$

where the introduced operator K is the inverse Feynman propagator of the W boson

$$\int d^4y\, K_{\mu\alpha}(x,y)\, i\Delta^{\alpha\nu}(y,z) = g^\nu_\mu\, i\delta^{(4)}(x-z), \tag{2.17}$$

$$i\Delta_{\mu\nu}(x,y) = \int \frac{d^4p}{(2\pi)^4} \frac{-i\left(g_{\mu\nu} - \frac{p_\mu p_\nu}{m_W^2}\right)}{p^2 - m_W^2 + i\epsilon} e^{-ip\cdot(x-y)} \tag{2.18}$$

Schematic structure of the action functional is then

$$S[W^+, W^-] = W^+_x K_{xy} W^-_y + \frac{g}{\sqrt{2}}(J^+_x W^+_x + J^-_x W^-_x), \tag{2.19}$$

and may be completed into a square with obvious substitutions

$$\tilde{W}^+_x = W^+_x + \frac{g}{\sqrt{2}} J^-_y \Delta_{yx}, \tag{2.20a}$$

$$\tilde{W}^-_x = W^-_x + \frac{g}{\sqrt{2}} \Delta_{xy} J^+_y. \tag{2.20b}$$

Expressed in terms of the new variables (2.20) the action becomes

$$S[\tilde{W}^+, \tilde{W}^-] = \tilde{W}^+_x K_{xy} \tilde{W}^-_y - \frac{g^2}{2} J^-_x \Delta_{xy} J^+_y. \tag{2.21}$$

At this point, we can integrate over the $\tilde{W}$ fields in the functional integral

$$\begin{aligned} Z_W[J^+_\mu] = \int \mathcal{D}\tilde{W}^+ \mathcal{D}\tilde{W}^- \exp\Big[i \int d^4x\, d^4y \Big(\tilde{W}^+_\mu(x) K^{\mu\nu}(x,y) \tilde{W}^-_\nu(y) & \\ - \frac{g^2}{2} J^-_\mu(x) \Delta^{\mu\nu}(x,y) J^+_\nu(y) \Big)\Big], & \end{aligned} \tag{2.22}$$

[2] The normalization constant $N(\epsilon)$ cancels out in the physical results.

to find nonlocal interaction for the fermions

$$S_{\text{nonlocal}} = \frac{-ig^2}{2} \int d^4x\, d^4y\, J_\mu^-(x) \Delta^{\mu\nu}(x,y) J_\nu^+(y). \tag{2.23}$$

Now follows the crucial step — expanding the nonlocal operator under the integral in terms of local operators, with consecutive highers orders carrying additional powers of $1/m_W^2$. Higher order terms will necessary involve derivatives to account for nonlocality, whereas the leading term is a point-like interaction

$$S_{\text{nonlocal}} = \frac{-ig^2}{2m_W^2} \int d^4x\, d^4y \left[J_\mu^-(x) g^{\mu\nu} \delta(x-y) J_\nu^+(y) + \mathcal{O}(1/m_W^2) \right]. \tag{2.24}$$

We read off the leading order term in the *operator product expansion* (OPE) [18, 19] to be

$$\mathcal{L}_{\text{OPE}} = -\frac{4G_F}{\sqrt{2}} J_\mu^-(x) J^{+\mu}(x) + \mathcal{O}(1/m_W^2) \times (\text{higher } D \text{ operators}). \tag{2.25}$$

Of particular importance for weak decays are dimension-5 and 6 operators. For definiteness we focus here on the dimension-6 composite operators

$$\mathcal{L}_{\text{dim-6}} = -\frac{4G_F}{\sqrt{2}} \sum_i C_i(\mu) Q_i(\mu), \tag{2.26}$$

$$Q_i = (\bar{\psi}_{i_1} \Gamma_i \psi_{i_2})(\bar{\psi}_{i_3} \Gamma_i' \psi_{i_4}). \tag{2.27}$$

Here i_1,i_2,i_3, and i_4 denote species of particles, while Γ_i, Γ_i' are matrices in the Dirac spinor space whose combination is scalar under homogeneous Lorentz transformation (barring discrete transformations like time-reversal and parity). Dimensionless Wilson coefficients $C_i(\mu)$ depend on the renormalization scale μ, couplings, and masses of heavy particles. On the other hand, composite operators' μ-dependence is indirect through μ-dependence of the renormalized fermion fields. We should emphasize that renormalization scale μ (also called factorization scale) is an artificially introduced momentum scale, separating long distance dynamics (momentum scales below μ) from short distance scales (scales above μ) [29]. For a process in question we first choose a complete set of effective operators which will, together with their corresponding Wilson coefficients, reproduce the invariant amplitudes of the full theory below the *matching scale* Λ up to terms suppressed with additional powers of $1/\Lambda^2$. Calculating hadronic amplitude amounts to determining the Wilson coefficients and then evaluating matrix elements of the composite operators between hadronic asymptotic states

$$\mathcal{A}_{i\to f} = -\frac{4G_F}{\sqrt{2}} \sum_i C_i(\mu) \left\langle f \left| Q_i(\mu) \right| i \right\rangle. \tag{2.28}$$

Any possible hadronic states in asymptotic states $|i\rangle$, $|f\rangle$ require the matrix elements to be calculated in nonperturbative regime of QCD, which is notoriously difficult to solve. The only ab-initio technique is a discrete formulation of QCD on four dimensional lattice which employs direct evaluation of correlation functions using the Feynman path integral representation [31, 32] analytically continued to

imaginary time. From the point of view of OPE, the important feature of matrix elements is their dependence on renormalization scale μ, which is cancelled against μ-dependence of Wilson coefficients in the final expression for the amplitude. In practice however, the nonperturbative methods are usually performed at a single value of $\mu = m_{\text{had}}$, namely at typical momentum scale of hadronic process. Correspondingly also the Wilson coefficients' values should be known at scale μ_{had}. In Appendix A we outline the procedure of composite operator renormalization as applied to the $b \to dd\bar{s}$ transition.

2.3 Low energy QCD

Having separated the short distance dynamics by performing the perturbative OPE and QCD renormalization procedure, we now have at hand the necessary set of short distance Wilson coefficients, whereas the matrix elements in (2.28) must involve some nonperturbative QCD method. In parameterizing the matrix elements we are guided by the Lorentz covariance of quark bilinears which must be manifest in the resulting form factor decomposition[3]. We will first introduce the customary form factor decomposition for transitions of pseudoscalar or vector to vacuum ($P, V \to 0$), pseudoscalar to pseudoscalar meson ($P \to P'$) and pseudoscalar to vector ($P \to V$). Later on we will briefly delve into the underlying symmetries of QCD which can impose further constraints on the form factors.

2.3.1 Hadronic form factors

Decay constants

The standard decay constants of the pseudoscalar P and vector mesons V are defined

$$\left\langle 0 \left| \bar{q}'\gamma^\mu\gamma^5 q \right| P(p) \right\rangle = i f_P p^\mu, \tag{2.29a}$$

$$\left\langle 0 \left| \bar{q}'\gamma^\mu\gamma^5 q \right| V(\epsilon, p) \right\rangle = g_V \epsilon^\mu, \tag{2.29b}$$

where $\bar{q}'q$ are the flavours of P or V. Polarization vector of vector particle is denoted ϵ, $\epsilon^2 = -1$, $\epsilon \cdot p = 0$.

Transitions between pseudoscalars

In semileptonic decays with one hadron in the final state we may encounter a quark bilinear inserted between the two meson states. We will use the standard form

[3] Also the parity transformation properties must be preserved by the form factor decomposition since we consider hadronic states as purely QCD bound states, not allowing for parity violation.

factor parameterization [33, 34] between two pseudoscalar mesons

$$\begin{aligned}\left\langle P'(p') \,\middle|\, \bar{q}'\gamma^\mu(1\pm\gamma_5)q \,\middle|\, P(p)\right\rangle =& F_+(q^2)\left((p+p')^\mu - \frac{m_P^2-m_{P'}^2}{q^2}q^\mu\right) \\ &+ F_0(q^2)\frac{m_P^2-m_{P'}^2}{q^2}q^\mu,\end{aligned} \tag{2.30}$$

$$\left\langle P'(p') \,\middle|\, \bar{q}'\sigma^{\mu\nu}(1\pm\gamma_5)q \,\middle|\, P(p)\right\rangle = is(q^2)\left[(p+p')^\mu q^\nu - q^\mu(p+p')^\nu \pm i\epsilon^{\mu\nu\alpha\beta}(p+p')_\alpha q_\beta\right], \tag{2.31}$$

where $q = p - p'$ is the momentum transfer.

Pseudoscalar to vector transitions

Matrix elements between a pseudoscalar and a vector meson are decomposed as customary

$$\left\langle V(\epsilon,p') \,\middle|\, \bar{q}'\gamma^\mu q \,\middle|\, P(p)\right\rangle = \frac{2V(q^2)}{m_P+m_V}\epsilon^{\mu\nu\alpha\beta}\epsilon^*_\nu p_\alpha p'_\beta, \tag{2.32a}$$

$$\begin{aligned}\left\langle V(\epsilon,p') \,\middle|\, \bar{q}'\gamma^\mu\gamma^5 q \,\middle|\, P(p)\right\rangle =& i\epsilon^{\nu*}\Bigg[2m_V A_0(q^2)\frac{q^\mu q^\nu}{q^2} \\ &+ (m_P+m_V)A_1(q^2)\left(g^{\mu\nu} - \frac{q^\mu q^\nu}{q^2}\right) \\ &- \frac{A_2(q^2)}{(m_P+m_V)}\left((p+p')^\mu - \frac{m_P^2-m_V^2}{q^2}q^\mu\right)q^\nu\Bigg],\end{aligned} \tag{2.32b}$$

$$\begin{aligned}\left\langle P(p') \,\middle|\, \bar{q}'q_\mu\sigma^{\mu\nu}(1\pm\gamma_5)q \,\middle|\, V(\epsilon,p)\right\rangle =& i\epsilon_\lambda\Bigg[-2iT_1(q^2)\epsilon^{\nu\mu\rho\lambda}p_\mu p'_\rho \\ &\pm T_2(q^2)\left((m_V^2-m_P^2)g^{\lambda\nu} - q^\lambda(p+p')^\nu\right) \\ &\pm T_3(q^2)q^\lambda\left(q^\nu - \frac{q^2}{m_V^2-m_P^2}(p+p')^\nu\right)\Bigg].\end{aligned} \tag{2.33a}$$

2.3.2 Heavy quark symmetry

Hadronic phenomena are effects determined by QCD in the nonperturbative regime, namely at scale Λ_{QCD}, where the perturbative expansion in powers of α_s cannot be used. Typical energy of quark and gluon degrees of freedom in a hadron are of order Λ_{QCD}. A heavy quark Q and accompanying light antiquark q comprise a heavy-light mesons, and since $m_Q \gg \Lambda_{\mathrm{QCD}}$ the heavy quark acts as almost static triplet colour charge interacting with dynamical light degrees of freedom [16, 17]. Accordingly, momentum of heavy quark is split into kinematic part owing to velocity of the parent hadron and a small residual fluctuation $k \sim \Lambda_{\mathrm{QCD}}$

$$p_Q = m_Q v + k. \tag{2.34}$$

On the level of QCD Lagrangian of heavy quarks (c, b) we can introduce new velocity dependent fields which have the momentum scales of order m_Q factored out [35]

$$h_v(x) = e^{im_Q v\cdot x}\frac{1+\not{v}}{2}Q(x) \tag{2.35}$$

$$H_v(x) = e^{im_Q v\cdot x}\frac{1-\not{v}}{2}Q(x), \tag{2.36}$$

where $Q(x)$ is a quark field of QCD. Projectors $(1\pm\not{v})/2$ project out the particle and antiparticle components of Dirac spinors, and H_v corresponds to small components which would vanish exactly in the limit $m_Q \to \infty$. Lagrangian of QCD expressed with new fields is [35]

$$\mathcal{L}_{\mathrm{HQET}} = \bar{h}_v iv\cdot D h_v + \bar{h}_v i\not{D}_\perp \frac{1}{iv\cdot D + 2m_Q - i\epsilon} i\not{D}_\perp h_v, \tag{2.37a}$$

$$D_\perp^\mu = D^\mu - v\cdot D\, v^\mu.$$

We have used D as standard covariant derivative of QCD. In the exact heavy quark symmetry limit (HQS) only the first term survives. It is manifestly independent of quark mass and owing to the absence of Dirac gamma matrices interaction with gluons are independent of the heavy quark spin. Spin-independence implies that physical states of heavy-light mesons are grouped into doublets of according to spin of light degrees of freedom $\mathbf{j}_\ell$ which is summed with the heavy quark spin $\mathbf{j}_h$ into total spin of a hadron

$$\mathbf{J} = \mathbf{j}_h + \mathbf{j}_\ell. \tag{2.38}$$

The two degenerate doublet members' spin difference comes from $\pm 1/2$ contribution of heavy spin. The ground state $\mathbf{j}_\ell = 1/2$ doublet can be represented by a velocity-dependent field

$$H_a(v) = \frac{1+\not{v}}{2}\left(\not{P}_a^*(v) - \gamma_5 P_a(v)\right) \tag{2.39}$$

with v the meson velocity and a the flavour of light antiquark. The factor $(1+\not{v})/2$ projects out the large quark components, fields P_a^* and P_a annihilate vector and pseudoscalar mesons, whereas Dirac matrices γ^μ and γ^5 are added to ensure that field $H_a(v)$ transforms as a fermionic bilinear under the Lorentz group. $H_a(v)$ are useful entities for incorporating the chiral symmetry of QCD, which couples to the light quark indices a.

2.3.3 Chiral perturbation theory

Chiral perturbation theory (CHPT) is the effective theory of QCD valid below the chiral symmetry breaking scale $\Lambda_\chi \sim 1$ GeV. Perturbative expansion in α_s is meaningless in this regime and because of confinement also the quark degrees of freedom cannot be used. We consider Lagrangian of QCD in the approximation where we neglect masses of light quarks

$$\mathcal{L}^0_{\mathrm{QCD}} = \bar{\psi}\gamma^\mu\left(i\partial_\mu + g_s\frac{\lambda^a}{2}G^a_\mu\right)\psi - \frac{1}{4}G^a_{\mu\nu}G^{a\mu\nu}, \quad \psi = \begin{pmatrix} u & d & s\end{pmatrix}^T. \tag{2.40}$$

Here g_s is the strong coupling constant, λ^a are the standard Gell-Mann generators of $SU(3)_c$ fundamental representation, whereas G^a_μ is the gluon field[4]. The above Lagrangian is invariant with respect to $SU(3)_L \times SU(3)_R \times U(1)_V \times U(1)_A$ global transformations. The $U(1)_V$ symmetry, acting as a phase rotation of all quarks simultaneously, is conserved even with quarks massive and its generator is the baryon number. The $U(1)_A$ is broken by the Abelian anomaly [36]. Remaining $G = SU(3)_L \times SU(3)_R$ is the group of chiral transformations that act independently on the left- and right-handed components of the quark fields

$$\psi_{L,R} \to g_{L,R}\psi_{L,R}. \tag{2.41}$$

The chiral group transformations (2.41) can equivalently be parameterized with the vector $g_V \equiv g_{L+R}$ and axial $g_A \equiv g_{R-L}$ transformations. The global symmetry of dynamics should be imprinted in degeneracy of physical states. The vector subgroup g_V when acting on physical states spans the familiar octet of pseudoscalar mesons [37, 38], which are quite far from being degenerate because of questionable assumption of massless s quark. Once we consider only u and d as massless the g_V becomes the isospin $SU(2)$ symmetry which manifests itself in highly degenerate multiplets of hadrons (i.e. mass splittings in the nucleon doublet and pion triplet are tiny).

Global axial symmetry g_A, on the other hand, would, if conserved predict degeneracy also between multiplets of opposite parities. No such degeneracies are observed in the physical spectrum, which indicates that g_A must be broken somehow. The central idea of CHPT lies in the assumption of axial symmetry breaking by the vacuum expectation value of the quark condensate $\langle 0 \,|\, \psi\bar{\psi} \,|\, 0 \rangle \neq 0$ and in identifying the broken generators with Goldstone bosons [39, 40], which are the lightest pseudoscalar mesons of the spectrum. To construct the effective theory one has to include in the Lagrangian all terms with Goldstone fields that are symmetric under G [41] and devise power counting to be able to truncate the expansion. Higher dimension operators are suppressed by more powers of p/Λ_χ [42], where p is a typical momentum of the process. Very convenient method to construct the terms in the effective Lagrangian is the CCWZ formalism [43]. The group element G is a product of axial and vector generators

$$g = e^{\xi_a A^a} e^{\eta_a V^a}. \tag{2.42}$$

Group generators can be taken as $V^a = i\lambda^a/2$ and $A^a = V^a\gamma_5$ where λ^a are the Gell-Mann matrices. G is broken into $H = SU(3)_V$, and the Goldstone boson fields are represented by coordinates ξ_a of the coset space G/H. We study the transformations of the broken subgroup elements $u(\xi_a) \equiv e^{\xi_a A^a}$, defined by

$$gu(\xi_a) \equiv u(\xi'_a)e^{\eta'_a V^a} \equiv u(\xi'_a)h(g, \xi_a). \tag{2.43}$$

Transformation of $u(\xi_a)$ is found to be nonlinear

$$u(\xi_a) \to u(\xi'_a) = gu(\xi_a)h^{-1}(g, \xi_a) = h(g, \xi_a)u(\xi_a)L(g)^{-1}, \tag{2.44}$$

[4]Gluon field strength is $G^a_{\mu\nu} = \partial_\mu G^a_\nu - \partial_\nu G^a_\mu + g_s f^{abc} G^a_\mu G^b_\nu$, where f^{abc} are $SU(3)$ structure constants.

where $g \in G$ is arbitrary and $L(g)$ denotes g with left and right components interchanged. Group element h belongs to the unbroken group H. A useful block of building invariants is $\Sigma \equiv u^2$ field which transforms as

$$\Sigma(\xi_a) = u(\xi_a)^2 \to g_R u(\xi_a) h^{-1}(g, \xi_a)\, h(g, \xi_a) u(\xi_a) g_L^{-1} = g_R \Sigma(\xi_a) g_L^{-1} \tag{2.45}$$

and can be parameterized as

$$\Sigma = e^{i\sqrt{2}\Pi/f}. \tag{2.46}$$

We fix our parameterization of the Goldstone boson fields by specifying matrix Π which contains the octet of pseudoscalar mesons

$$\Pi = \frac{1}{\sqrt{2}} \pi_a \lambda^a = \begin{pmatrix} \frac{\pi^0}{\sqrt{2}} + \frac{\eta_8}{\sqrt{6}} & \pi^+ & K^+ \\ \pi^- & -\frac{\pi^0}{\sqrt{2}} + \frac{\eta_8}{\sqrt{6}} & K^0 \\ K^- & \bar{K}^0 & -\frac{2\eta_8}{\sqrt{6}} \end{pmatrix}. \tag{2.47}$$

Parameter f with dimension of mass is introduced to cancel the pseudoscalar fields mass-dimension. The unique chiral invariant with two derivatives that reproduces the conventional normalization of kinetic terms is

$$\frac{f^2}{4} \partial_\mu \Sigma^{ab} (\partial^\mu \Sigma^\dagger)_{ba}. \tag{2.48}$$

To generalize the framework to include also explicit breaking of G, we find in the first order of light quark masses

$$\mathcal{L}_2 = \frac{f^2}{4} \partial_\mu \Sigma^{ab} (\partial^\mu \Sigma^\dagger)_{ba} + \lambda_0 (\hat{m}_{ab} \Sigma^{ab} + (\Sigma^\dagger)_{ab} \hat{m}_{ba}). \tag{2.49}$$

Light quark mass-matrix is here $\hat{m} = \mathrm{diag}(m_u, m_d, m_s)$. The chiral noninvariant term accounting for the finite quark masses shares the same transformation properties under G as quark mass terms in the QCD Lagrangian [44, 45]. Expanding the leading chiral-order Lagrangian (2.49) leads to interactions of even number of pions whose vertices are accompanied by one power of external momentum p. In the low energy limit the leading order Lagrangian dominates as the terms with higher number of derivatives contain more powers of p. The power counting even works for loop integrals in the effective theory [41].

Heavy meson CHPT

In our calculation in Chapter 5 we shall encounter the amplitude for emission of soft Goldstone boson off a heavy meson line. One can combine both chiral symmetry of QCD and the heavy quark symmetry to construct the heavy meson chiral perturbation theory (HMχPT) (c.f. [46] and references therein). We use the velocity dependent heavy meson fields $H_a(v)$ for the ground state negative parity-doublet (2.39). They transform under the unbroken light flavour group H as

$$H_a \to H_b (h^{-1})_{ba}. \tag{2.50}$$

Fields H_a can be combined into chiral invariants together with the derivatives of Goldstone fields

$$\mathcal{A}_\mu = \frac{i}{2}\left(u^\dagger \partial_\mu u - u\partial_\mu u^\dagger\right), \tag{2.51}$$

$$\mathcal{V}_\mu = \frac{i}{2}\left(u^\dagger \partial_\mu u + u\partial_\mu u^\dagger\right). \tag{2.52}$$

Leading order effective Lagrangian is

$$\mathcal{L}_{\mathrm{HM}\chi\mathrm{PT}} = \left\langle H_a(v) v_\mu (\delta_{ab} i\partial^\mu + \mathcal{V}^\mu_{ab})\bar{H}_b(v)\right\rangle + g\left\langle H_a(v)\mathcal{A}^\mu_{ab}\gamma_\mu\gamma_5\bar{H}_b(v)\right\rangle, \tag{2.53}$$

$$\bar{H}_a(v) \equiv \gamma^0 H_a^\dagger(v)\gamma^0 = \left(\not{P}^{*\dagger}_a(v) + \gamma_5 P^\dagger_a(v)\right)\frac{1+\not{v}}{2}. \tag{2.54}$$

Brackets $\langle \ldots \rangle$ denote traces over Dirac indices. The above Lagrangian contains vertices with two heavy meson lines along with even number of Goldstones (terms with $\mathcal{V}$), which are entirely fixed from the symmetry. Interaction with odd number of Goldstones, contained in $\mathcal{A}$, introduces a coupling constant g that can be extracted from experiment or calculated with nonperturbative methods.

Chapter 3

Rare process $b \to dd\bar{s}$

In the standard model (SM) the only source of flavour violation is the Cabibbo-Kobayashi-Maskawa (CKM) matrix whose unitarity ensures that flavour changing currents are charged. Moreover, the multiple W exchanges, which may lead to flavour changing neutral currents (FCNCs), are suppressed by the Glashow-Iliopoulos-Maiani (GIM) mechanism. Some of the FCNC processes including the neutral meson mixing require effective operators with flavour structures that are driven by box diagrams at leading order. These involve double W boson exchange between the two internal quark lines and therefore these diagrams are suppressed by two independent GIM sums. The quark-level process $b \to dd\bar{s}$ is mediated by box diagram in the SM and, as expected from the above arguments, is rendered negligible in the SM.

In this chapter we will study the $b \to dd\bar{s}$ and its corresponding hadronic decay channels in the context of SM and some of the well known new physics (NP) scenarios: the minimal supersymmetric standard model (MSSM), supersymmetry with violated R-parity ($\not{R}_p$MSSM), and the model with family nonuniversal Z' gauge boson (Z'). In contrast with the SM, in some some of the NP models inclusive and exclusive branching fractions of $b \to dd\bar{s}$ transition may be enhanced to a level close to current experimental sensitivity. Currently the $b \to dd\bar{s}$ mediated exclusive decay channel $B^- \to K^+\pi^-\pi^-$ has been searched for in both B-factories [47, 48] and the strongest bound to this date has been set by BaBar collaboration whose analysis based on 426×10^{-6} fb^{-1} data sample yields [49]

$$\mathcal{B}(B^- \to \pi^-\pi^- K^+) < 9.5 \times 10^{-7} \text{ at } 90\% \text{ C.L. .} \tag{3.1}$$

The literature on the subject is rich and focuses also on the analogous process $b \to ss\bar{d}$ [50–56].

3.1 Effective Hamiltonian

The most convenient approach to the problem is to employ the operator product expansion to obtain the effective Hamiltonian. The virtue of effective Hamiltonian is its versatility in the sense that a complete basis of effective operators can embed all low-energy effects of a generic short distance dynamics. Moreover, QCD renormalization calculation of effective operators is more feasible in the effective rather

than in the full theory. We start with

$$\mathcal{H}_{\text{eff.}} = \sum_{n=1}^{5} \left[C_n \mathcal{O}_n + \tilde{C}_n \tilde{\mathcal{O}}_n \right], \tag{3.2}$$

written as a linear combination of four-quark operators with flavour structure $(\bar{d}b)(\bar{d}s)$ and accompanied by their respective Wilson coefficients

$$\begin{aligned}
\mathcal{O}_1 &= (\bar{d}_L^\alpha \gamma^\mu b_L^\alpha)\,(\bar{d}_R^\beta \gamma_\mu s_R^\beta), \\
\mathcal{O}_2 &= (\bar{d}_L^\alpha \gamma^\mu b_L^\beta)\,(\bar{d}_R^\beta \gamma_\mu s_R^\alpha), \\
\mathcal{O}_3 &= (\bar{d}_L^\alpha \gamma^\mu b_L^\alpha)\,(\bar{d}_L^\beta \gamma_\mu s_L^\beta), \\
\mathcal{O}_4 &= (\bar{d}_R^\alpha b_L^\alpha)(\bar{d}_L^\beta s_R^\beta), \\
\mathcal{O}_5 &= (\bar{d}_R^\alpha b_L^\beta)(\bar{d}_L^\beta s_R^\alpha).
\end{aligned} \tag{3.3}$$

We denote with $\tilde{\mathcal{O}}_i$ the chirally-flipped set of operators obtained from $\mathcal{O}_i$ by interchange $L \leftrightarrow R$. Color contractions of the quark fields are indicated by repeated indices α and β. For convenience we supplemented the operator basis introduced in [57] with additional scalar operators $\mathcal{O}_{4,5}, \tilde{\mathcal{O}}_{4,5}$, which are however redundant and can be reduced to $\mathcal{O}_{2,1}, \tilde{\mathcal{O}}_{2,1}$ via Fierz transformation

$$\mathcal{O}_{4,5} = -\frac{1}{2}\mathcal{O}_{2,1}, \qquad \tilde{\mathcal{O}}_{4,5} = -\frac{1}{2}\tilde{\mathcal{O}}_{2,1}. \tag{3.4}$$

3.1.1 QCD corrections

Given an underlying full theory valid at short distances we perform matching to the effective theory (8.8) by equating the 4-quark 1-particle irreducible Green functions calculated in both theories. In this way we obtain the short-distance Wilson coefficients, as described in Sections 2.2 and A.1. In Appendix A also the anomalous dimension matrix of operators $\mathcal{O}_{1\ldots3}$ are determined in leading order in α_s and leading logarithm approximation. For the $\mathcal{O}_{1,\ldots,5}$ we get

$$\gamma = \frac{\alpha_s}{2\pi} \begin{pmatrix} 1 & -3 & 0 & 0 & 0 \\ 0 & -8 & 0 & 0 & 0 \\ 0 & 0 & 2 & 0 & 0 \\ 0 & 0 & 0 & -8 & 0 \\ 0 & 0 & 0 & -3 & 1 \end{pmatrix}. \tag{3.5}$$

The operator $\mathcal{O}_3$ does not mix into its color-flipped counterpart (which has color contractions between the two currents), which is due to the two $\bar{d}_L$ fields and Fierz rearrangement, equal to the original $\mathcal{O}_3$. Obviously, with (3.4) the anomalous dimensions for $\mathcal{O}_{1,2}$ and $\mathcal{O}_{5,4}$ are the same. We solve the renormalization group equations which govern evolution of the Wilson coefficients as the renormalization scale runs from Λ down to $\mu \simeq m_b$, where the hadronic matrix elements are calculated [1]. These corrections might be substantial due to large separation between

[1] We will consistently denote Λ and μ for the matching scale and the scale where hadronic matrix elements are calculated, namely $\mu \simeq m_b$.

scales $\Lambda \gtrsim m_W$ and $\mu \simeq m_b$. The resulting evolution matrix

$$U(\mu,\Lambda) = T_g \exp\left[\int_{g(\Lambda)}^{g(\mu)} dg' \frac{\gamma^T(g')}{\beta(g')}\right] \tag{3.6}$$

then relates the Wilson coefficients at the scale μ to their values obtained at the matching scale

$$C_i(\mu) = U(\mu,\Lambda)_{ij} C_j(\Lambda). \tag{3.7}$$

Using the standard parametrization of the beta function (A.10) we obtain the sub-blocks of the evolution matrix from where we can directly read the Wilson coefficients at scale μ. The QCD corrections mix the operator $\mathcal{O}_1$ into $\mathcal{O}_2$

$$C_1(\mu) = \left[\frac{\alpha_s(\mu)}{\alpha_s(\Lambda)}\right]^{-1/\beta_0} C_1(\Lambda), \tag{3.8a}$$

$$C_2(\mu) = \frac{1}{3}\left(\left[\frac{\alpha_s(\mu)}{\alpha_s(\Lambda)}\right]^{8/\beta_0} - \left[\frac{\alpha_s(\mu)}{\alpha_s(\Lambda)}\right]^{-1/\beta_0}\right) C_1(\Lambda) + \left[\frac{\alpha_s(\mu)}{\alpha_s(\Lambda)}\right]^{8/\beta_0} C_2(\Lambda), \tag{3.8b}$$

while C_3 is multiplicatively renormalized

$$C_3(\mu) = \left[\frac{\alpha_s(\mu)}{\alpha_s(\Lambda)}\right]^{-2/\beta_0} C_3(\Lambda). \tag{3.9}$$

We reproduce the mixing behaviour reported in [57]. To find mixing of C_4 and C_5 one is to substitute in expressions (3.8) $C_1 \to C_5$ and $C_2 \to C_4$. The beta-function coefficient $\beta_0 = (33 - 2f)/3$ depends on f, the number of dynamical quark flavours between scales μ and Λ. Evolution matrix depends on whether the matching scale Λ is above m_t and when this is the case we compose U from consecutive evolution matrices valid at $f = 6$ and $f = 5$

$$U(\mu,\Lambda)|_{\Lambda > m_t} = U(\mu, m_t)|_{f=5} U(m_t,\Lambda)|_{f=6}. \tag{3.10}$$

Note that expressions (3.8),(3.9) assume that the number of dynamical quark flavours f is constant between μ and Λ. Renormalization of the Wilson coefficients $\tilde{C}_{1,\dots,5}$ of chirally-flipped operators is governed by the same set of equations as for $C_{1,\dots,5}$.

3.2 Inclusive decay width

In this section we will calculate inclusive decay width of $b \to dd\bar{s}$ in frameworks of SM, MSSM, $\not{R}_p$MSSM, and the Z' model. Model with down-type singlet quark has been studied in [58]. First we will match the full theory onto the effective Hamiltonian (8.8) at scale Λ to find relevant Wilson coefficients C_i (we denote these without the scale argument). The RGE techniques, described in the last section, are then applied to obtain a set of $C_i(\mu)$, $\tilde{C}_i(\mu)$ in the given framework. Finally, we express the inclusive decay width in terms of relevant parameters of the underlying theory and its numerical value, if the parameters are already bounded from other observables.

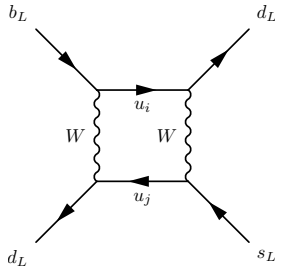

Figure 3.1: Box diagram generating $b \to dd\bar{s}$ in the SM.

3.2.1 Standard model

In the SM process $b \to dd\bar{s}$ is mediated by box diagram 3.1 with two W bosons exchanged between the quark lines. The leading term of the order $1/m_W^2$ in the OPE is local and thus independent of external momenta [59] so we set the external momenta to zero in calculating the box diagram of Figure 3.1. One should in principle also add nonlocal contributions of $\mathcal{H}_{\text{eff.}}^{(\bar{c}b)(\bar{d}c)}$ and $\mathcal{H}_{\text{eff.}}^{(\bar{c}s)(\bar{d}c)}$, which have been shown to be smaller than short distance contributions for decay $B \to K^-K^-\pi^+$ [54, 55] and we choose to neglect them as they cannot change the order of magnitude of our predictions. All the vertices are of the $(V-A)\otimes(V-A)$ color-singlet type so only $\mathcal{O}_3$ is generated at scale $\Lambda \simeq m_W$. Note that we used the SM with dynamical t quark and integrated out both W and t at common scale m_W.

$$C_3^{\text{SM}} = \frac{G_F^2 m_W^2}{8\pi^2} \sum_{i,j} \lambda_i \tilde{\lambda}_j f\left(x_i, x_j\right) \tag{3.11}$$

The sum runs over the charge 2/3 quark flavours $(i,j = u,c,t)$ with CKM weights $\lambda_i = V_{ib}V_{id}^*$ and $\tilde{\lambda}_j = V_{js}V_{jd}^*$. Remaining dependence on masses of the quarks in the loop is contained in function $f(x_i, x_j)$ [2], where $x_i \equiv m_{u_i}^2/m_W^2$

$$f(x,y) = -\frac{3xy}{(x-1)(y-1)} + \frac{xy}{x-y}\left[\left(1 - \frac{6x-3}{(x-1)^2}\right)\ln x - [x \to y]\right]. \tag{3.12}$$

The above $f(x,y)$ suppresses contributions of light quarks in the loop (see however Section A.2). Intricate hierarchy of quark masses and CKM factors in (3.11) renders negligible all but two of the terms. Relative size of all 9 terms contributing to C_3^{SM}, using the simple Cabibbo angle $\lambda = \cos\theta_c = 0.22$ power-counting is given below. The two important ones are with $i = t$ and $j = c$ or t. Two top quarks contribute dominantly although the Cabibbo suppression is $\sim \lambda^8$. The subleading contribution comes from top and charm in the loop and its milder ($\sim \lambda^4$) Cabibbo suppression is compensated by small value of $f(x_t, x_c)$ and is at par with the dominant contribution. With the abovegiven Wilson coefficient (3.11), adapted for the $b \to ss\bar{d}$ decay, our numerical value of C_3^{SM} agrees with the expressions reported in [50]. In analogy with K^0–$\bar{K}^0$ and B^0–$\bar{B}^0$ mixing processes we do not expect the QCD corrections to change significantly the decay rate [60]. Indeed, the RG evolution (3.9) only

[2] For inherent ambiguity in the choice of $f(x,y)$ that is related to GIM cancellation, see Section A.2.

i \ j	u	c	t
u	4×10^{-7}	5×10^{-6}	2×10^{-8}
c	5×10^{-6}	5×10^{-2}	1×10^{-3}
t	9×10^{-6}	0.4	1

(3.13)

Table 3.1: Hierarchy of contributions of virtual quarks in the SM box diagram for $b \to dd\bar{s}$.

changes $C_3^{\rm SM}$ by a negligible factor of 0.9. Using values for the parameters from the Particle Data Group [28], we get

$$C_3^{\rm SM} \approx 5.3 \times 10^{-13}\ {\rm GeV}^{-2}. \tag{3.14}$$

To obtain the decay width, one has to consider two distinct cases, namely when: (i) the two final state d quarks have the same color and they cannot be distinguished, or else, (ii) when d quarks' colors are different and we can tell which one belongs to which of the currents in $\mathcal{O}_3$. In the end, these two cases have to be summed incoherently, i.e., on the level of decay width. The resulting inclusive decay rate, averaged and summed over spins and colors of quarks is

$$\Gamma_{\rm incl.}^{\rm SM} = \frac{\left|C_3^{\rm SM}\right|^2 m_b^5}{384\pi^3} \tag{3.15}$$

which amounts to $\mathcal{B}(b \to dd\bar{s})_{\rm SM} = (8 \pm 2) \times 10^{-14}$. This is far below the current and foreseeable experimental sensitivity and discovery of this decay mode would undoubtedly be a signal of NP.

3.2.2 Minimal supersymmetric SM

In the supersymmetric extensions of the SM the $b \to dd\bar{s}$ process can be mediated by additional diagrams involving squarks and gluinos in the box [61]. The contribution depends on the quark-squark-gluino vertices which are flavour nonconserving in the mass-basis of fields [62]. A universal framework for dealing with these flavour violating interactions in the general low-scale supersymmetry is the mass insertion approximation (MIA) [63] where one chooses a mass-basis for squarks where the vertices with gluino are flavour diagonal, whereas the squark mass matrix and the squark propagator are flavour nondiagonal. One can expand the squark propagator in powers of a (matrix) parameter $\delta_{ij} = \Delta_{ij}/(m_{\tilde{d}_i} m_{\tilde{d}_j})$, where Δ_{ij} are the off-diagonal terms in the squark mass matrix and $m_{\tilde{d}_j}$ are the squark masses. Single insertion in the squark line is denoted by a cross (see Figure 3.2).

We will use Wilson coefficients of the effective $\Delta S = 2$ Hamiltonian derived in [61] and adapt them for the process $b \to dd\bar{s}$. The left-handed squark contributions, $(\delta^d_{ij})_{LL}$, contribute to the $\mathcal{O}_3$ operator:

$$C_3^{\rm MSSM} = -\frac{\alpha_s^2}{216\bar{m}^2_{\tilde{q}}}(\delta^d_{13})_{LL}(\delta^d_{12})_{LL}\left[24x f_6(x) + 66\tilde{f}_6(x)\right] \tag{3.16}$$

Here $x \equiv \bar{m}^2_{\tilde{d}}/m^2_{\tilde{g}}$ is the squared ratio of average squark mass to the mass of gluino and the loop functions f_6 and $\tilde{f}_6$ are [61]

$$f_6(x) = \frac{6(1+3x)\ln x + x^3 - 9x^2 - 9x + 17}{6(x-1)^5}, \tag{3.17a}$$

$$\tilde{f}_6(x) = \frac{6x(1+x)\ln x - x^3 - 9x^2 + 9x + 1}{3(x-1)^5}. \tag{3.17b}$$

The recent limits on $\delta^{d*}_{21}\delta^d_{13}$ [64–66] disallow significant contributions from the mixed and the right-handed squark mass insertion terms. Therefore, we only include the dominant left-left insertions given in the expression (3.16). We follow [65] and take $x = \bar{m}^2_{\tilde{d}}/m^2_{\tilde{g}} = 1$ and the corresponding values of $\left|\left(\delta^d_{13}\right)_{LL}(x=1)\right| \leq 0.14$ and $\left|\left(\delta^d_{21}\right)_{LL}(x=1)\right| \leq 0.042$ [61]. We take for the average mass of squarks $\bar{m}_{\tilde{d}} = 500$ GeV and for the strong coupling constant $\alpha_s = 0.11$, and find

$$\left|C_3^{\mathrm{MSSM}}\right| < 1.6 \times 10^{-12}\ \mathrm{GeV}^{-2}. \tag{3.18}$$

Using then (3.15) and substituting for the C_3^{MSSM} Wilson coefficient one finds that in the MSSM the branching fraction of $b \to dd\bar{s}$ inclusive decay is at most 7×10^{-13}.

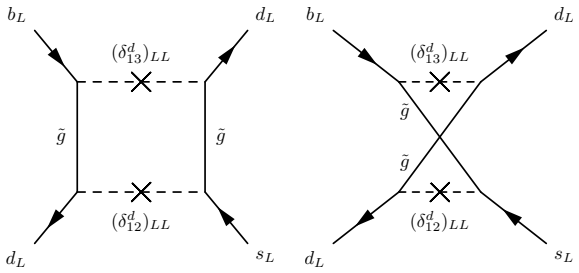

Figure 3.2: The box diagrams in the MSSM with gluinos and down-type squark lines with δ^d_{LL} mass insertions.

3.2.3 MSSM with broken R_p-parity

One way to generalize the MSSM is to relax the implicit assumption of R-parity (R_p) conservation which prevents violation of baryon (B) and lepton (L) numbers. A complete review on the topic is available in [67]. Once the supersymmetric particles are assigned the same B and L numbers as their SM partners, the R_p of a given particle is given in terms of its spin (S), B, and L [68]

$$R_p = (-1)^{2S}(-1)^{3B+L} = \begin{cases} +1 & ; \quad \mathrm{SM} \\ -1 & ; \quad \mathrm{SUSY} \end{cases}, \tag{3.19}$$

which implies that all "normal" particles are R_p even and their superpartners R_p odd. Consequently, in the MSSM supersymmetric particles can only form in pairs and the lightest supersymmetric particle is stable. Another important virtue of R_p conservation is the absence of interaction terms which would violate B or L, and thus the proton is stable in MSSM.

All the above features are not guaranteed in supersymmetric models with R_p violation ($\not{R}_p$MSSM). The superpotential is supplemented by terms with trilinear couplings

$$W_{\not{R}_p} = \frac{1}{2}\lambda_{ijk} L_i L_j E^c_k + \lambda'_{ijk} L_i Q_j D^c_k + \frac{1}{2}\lambda''_{ijk} U^c_i D^c_j D^c_k \tag{3.20}$$

of which λ and λ' violate L while λ'' violates B. Note that the proton cannot decay if at least one of the B, L is conserved [69]. In addition, λ' coupling induces a flavour changing neutral current in the down-type quark sector mediated by a sneutrino exchange

$$\mathcal{L}_{\tilde{\nu}} = -\lambda'_{ijk} \tilde{\nu}_{iL} \bar{d}_{kR} d_{jL} + \text{H.c.} \,. \tag{3.21}$$

In this supersymmetric framework, the tree-level exchange of a sneutrino (Figure 3.3) is expected to be the dominant contribution to $b \to dd\bar{s}$ transition and its OPE at common sneutrino mass scale $\Lambda \simeq m_{\tilde{\nu}}$ is

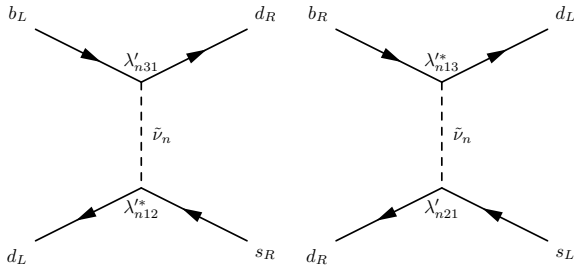

Figure 3.3: Tree-level exchanges of sneutrino via trilinear couplings.

$$C_4^{\not{R}_p} = -\sum_{n=1}^{3} \frac{\lambda'_{n31}\lambda'^*_{n12}}{m^2_{\tilde{\nu}_n}}, \tag{3.22}$$

$$\tilde{C}_4^{\not{R}_p} = -\sum_{n=1}^{3} \frac{\lambda'_{n21}\lambda'^*_{n13}}{m^2_{\tilde{\nu}_n}}. \tag{3.23}$$

The renormalization group evolution of $C_4^{\not{R}_p}$ down to scale $\mu \simeq m_b$ is according to (3.8) with substitutions $C_1 \to 0$ and $C_2 \to C_4^{\not{R}_p}$ (with omission of squarks and gluinos contributions in the QCD beta function). The resulting multiplicative renormalization is contained in f_{QCD}

$$C_4^{\not{R}_p}(m_b) = f_{QCD}(m_{\tilde{\nu}}) C_4^{\not{R}_p} \tag{3.24}$$

where

$$f_{QCD}(\Lambda) = \begin{cases} \left[\frac{\alpha_s(m_b)}{\alpha_s(m_t)}\right]^{24/23} \left[\frac{\alpha_s(m_t)}{\alpha_s(\Lambda)}\right]^{24/21} & ; \quad \Lambda > m_t \\ \left[\frac{\alpha_s(m_b)}{\alpha_s(\Lambda)}\right]^{24/23} & ; \quad \Lambda < m_t \end{cases} . \tag{3.25}$$

In range of common sneutrino mass the f_{QCD} assumes values from $f_{QCD}(200\text{ GeV}) \approx 2$ to $f_{QCD}(1\text{ TeV}) \approx 2.5$ and we will fix $f_{QCD} = 2.2$. Also $\tilde{C}_4^{\not{R}_p}$ is renormalized by f_{QCD}. Inclusive b-quark decay width is then

$$\Gamma^{\not{R}_p}_{\text{incl.}} = \frac{m_b^5 f^2_{QCD}(m_{\tilde{\nu}})}{2048\pi^3} \left(|C_4^{\not{R}_p}|^2 + |\tilde{C}_4^{\not{R}_p}|^2 \right). \tag{3.26}$$

Present experimental bounds on the individual λ' couplings contributing to the Wilson coefficients $C_4^{\not{R}_p}$ and $\tilde{C}_4^{\not{R}_p}$ do not constrain this mode, and we extract the bounds on the relevant combination from exclusive decays in Section 3.4.

3.2.4 Family nonuniversal Z'

In many extensions of the SM [70] an additional neutral gauge boson appears. Heavy neutral bosons are also present in grand unified theories, superstring theories and theories with large extra dimensions [71]. This induces contributions to the effective tree-level Hamiltonian from the operators $\mathcal{O}_{1,3}$ as well as $\tilde{\mathcal{O}}_{1,3}$. Following [70, 71], the Wilson coefficients for the corresponding operators read at the interaction scale $\Lambda \simeq m_{Z'}$

$$C_1^{Z'} = -4\sqrt{2}G_F y B_{12}^{d_L} B_{13}^{d_R}, \qquad \tilde{C}_1^{Z'} = -4\sqrt{2}G_F y B_{12}^{d_R} B_{13}^{d_L}, \tag{3.27a}$$

$$C_3^{Z'} = -4\sqrt{2}G_F y B_{12}^{d_L} B_{13}^{d_L}, \qquad \tilde{C}_3^{Z'} = -4\sqrt{2}G_F y B_{12}^{d_R} B_{13}^{d_R}, \tag{3.27b}$$

where $y = (g_2/g_1)^2(\rho_1 \sin^2\theta + \rho_2 \cos^2\theta)$ and $\rho_i = m_W^2/m_i^2 \cos^2\theta_W$. Here g_1, g_2, m_1 and m_2 stand for the gauge couplings and masses of the Z and Z' bosons, respectively, while θ is their mixing angle. Weinberg angle is denoted θ_W. Again, renormalization group running induces corrections and mixing between the operators. According to the RG evolution equations (3.8) the operator $\mathcal{O}_1\,(\tilde{\mathcal{O}}_1)$ mixes into $\mathcal{O}_2\,(\tilde{\mathcal{O}}_2)$ and for typical mass of $m_{Z'} \gtrsim 500$ GeV their Wilson coefficients at the scale $\mu \simeq m_b$ are expressed in terms of f_{QCD} given in (3.25)

$$C_1^{Z'}(m_b) = [f_{QCD}(m_{Z'})]^{-1/8}\, C_1^{Z'} \tag{3.28a}$$

$$C_2^{Z'}(m_b) = \frac{1}{3}\left(f_{QCD}(m_{Z'}) - [f_{QCD}(m_{Z'})]^{-1/8}\right) C_1^{Z'}, \tag{3.28b}$$

whereas the value of $C_3(m_b)$ is

$$C_3^{Z'}(m_b) = [f_{QCD}(m_{Z'})]^{-1/4}\, C_3^{Z'}. \tag{3.29}$$

In particular, for a Z' boson scale of $m_{Z'} \simeq 500$ GeV [70] one gets numerically $f_{QCD}(m_{Z'}) \simeq 2.3$ and

$$\begin{aligned} &C_1^{Z'}(m_b) = 0.90 C_1^{Z'}, \qquad C_3^{Z'}(m_b) = 0.81 C_3^{Z'}, \\ &C_2^{Z'}(m_b) = 0.47 C_1^{Z'}. \end{aligned} \tag{3.30}$$

Again, the chirally flipped operators $\tilde{\mathcal{O}}_{1,2,3}$ are renormalized in the same manner.

The inclusive $b \to dd\bar{s}$ decay width is given in the closed form as

$$\Gamma_{\text{incl.}}^{Z'} = \frac{m_b^5}{768\pi^3}\left[\frac{1}{3}(f_{QCD}^2 + 8 f_{QCD}^{-1/4})(|C_1^{Z'}|^2 + |\tilde{C}_1^{Z'}|^2) + 2 f_{QCD}^{-1/2}(|C_3^{Z'}|^2 + |\tilde{C}_3^{Z'}|^2)\right] \tag{3.31}$$

In Section 3.4 we discuss bounds on Wilson coefficients $C_{1,3}^{Z'}$ and $\tilde{C}_{1,3}^{Z'}$ which might be estimated from the $B^- \to \pi^-\pi^- K^+$ decay rate.

3.3 Exclusive B^- decay modes

We only consider the charged B meson decays driven by the $b \to dd\bar{s}$ transition, since the antiquark $\bar{u}$ is a spectator in this process and one should not worry about possible contributions of the SM penguins. In calculating decay widths of the B^- meson decay channels driven by the $b \to dd\bar{s}$ transition, we will make use of form factors available in the literature. Alternative approach taken in [55] exploits the $SU(3)$ flavour symmetry of light quarks to relate the amplitudes to the measured ones.

3.3.1 Vacuum saturation of matrix elements

Since we aim for $\sim 30\%$ precision we can use the vacuum saturation (VSA, also called naïve factorization) approximation assuming that vacuum state, inserted between the two currents, contributes dominantly with respect to other states [33, 72, 73]. The matrix elements in VSA are factorized and it is clear that long distance contributions between the two hadronic currents are neglected. Obtained matrix elements of single current operators are then decomposed into standard form factors (see Section 2.3.1). For $B \to \pi(\rho)$ transitions we use form factors calculated in the relativistic constituent quark model, with numerical input from the lattice QCD at large q^2 [74]. For the $D_s \to D$ and $K \to \pi$ form factors we use results of [75, 76] where the approach combining heavy quark and chiral symmetries was used.

3.3.2 Hadronic amplitudes

For three-body decays of B meson to pseudoscalars P, P_1 and P_2 we provide below the kinematically simplified expression for the factorized matrix element of the $\mathcal{O}_3$ operator, contributing in the frameworks of SM, MSSM, and Z'

$$\begin{aligned}\left\langle P_2(p_2)P_1(p_1)\,\middle|\,\bar{d}\gamma_\mu s\,\middle|\,0\right\rangle \left\langle P(p)\,\middle|\,\bar{d}\gamma^\mu b\,\middle|\,B^-(p_B)\right\rangle = \\ = (t-u)F_1^{P_2P_1}(s)F_1^{PB}(s) \\ + \frac{(m_{P_1}^2 - m_{P_2}^2)(m_B^2 - m_P^2)}{s}\left[F_1^{P_2P_1}(s)F_1^{PB}(s) - F_0^{P_2P_1}(s)F_0^{PB}(s)\right].\end{aligned} \tag{3.32}$$

We introduced Mandelstam variables $s = (p_B - p)^2$, $t = (p_B - p_1)^2$, and $u = (p_B - p_2)^2$. Crossing symmetry relates the transition $0 \to P_1P_2$ to the $P_1 \to P_2$, whose form factors are known. The above expression (3.32) also holds for contribution of operators $\tilde{\mathcal{O}}_3$, $\mathcal{O}_1$, and $\tilde{\mathcal{O}}_1$ to the $B \to PP_1P_2$ amplitude, as only the vector parts of currents have the correct parity. Explicit parameterization of form factors F_1 and F_0 are shown in Appendix A.3.

For the matrix elements of (pseudo)scalar operators $\mathcal{O}_4$ and $\tilde{\mathcal{O}}_4$ in the $\not{R}_p$MSSM framework one can use equation of motion for the quark fields

$$i\not{D}q = m_q q, \quad D_\mu = \partial_\mu - igG_\mu \tag{3.33}$$

to express the operators as divergences of (axial) vector currents

$$\bar{q}_i q_j = \frac{i\partial_\mu(\bar{q}_i\gamma^\mu q_j)}{m_{q_j} - m_{q_i}}, \tag{3.34a}$$

$$\bar{q}_i\gamma^5 q_j = -\frac{i\partial_\mu(\bar{q}_i\gamma^\mu\gamma^5 q_j)}{m_{q_j} + m_{q_i}}. \tag{3.34b}$$

Using (3.34) we write down matrix element expressed in terms of scalar form factor $F_0(q^2)$

$$\left\langle P_2(p_2)P_1(p_1)\,\middle|\,\bar{d}s\,\middle|\,0\right\rangle \left\langle P(p)\,\middle|\,\bar{d}b\,\middle|\,B^-(p_B)\right\rangle = \frac{(m^2_{P_1} - m^2_{P_2})(m^2_B - m^2_P)}{(m_b - m_d)(m_s - m_d)} F_0^{P_2P_1}(s)F_0^{PB}(s). \tag{3.35}$$

Again due to parity conservation, pseudoscalar components of operators $\mathcal{O}_4$ and $\tilde{\mathcal{O}}_4$ are irrelevant for the matrix element of $B \to PP_1P_2$. In the Z' model we also encounter contributions of the operators $\mathcal{O}_2$ and $\tilde{\mathcal{O}}_2$, whose color structure is Fierz rearranged to $\mathcal{O}_4$ and $\tilde{\mathcal{O}}_4$ and then (3.35) applies as well.

In two-body decays to vector meson V and pseudoscalar meson P in the final state we sum over the polarizations of V. The sum in our case reduces to

$$\sum_{\epsilon_V} |\epsilon_V^*(p_V)\cdot p_B|^2 = \frac{\lambda(m_B^2, m_V^2, m_P^2)}{4m_V^2}, \tag{3.36}$$

where ϵ_V is the polarization vector of V and λ is defined as $\lambda(x,y,z) = (x+y+z)^2 - 4(xy+yz+zx)$.

For decay to two vector mesons we use the helicity amplitudes formalism as described in [77]. Unpolarized decay width is expressed as sum of the three helicity widths

$$\Gamma = \frac{|\mathbf{p}_1|}{8\pi m_B^2}\left(|H_0|^2 + |H_{+1}|^2 + |H_{-1}|^2\right), \tag{3.37}$$

where $\mathbf{p}_1$ is momentum of the vector meson in B meson rest frame and helicity amplitudes are expressed as

$$H_{\pm1} = a \pm \frac{\sqrt{\lambda(m_B^2, m_1^2, m_2^2)}}{2m_1m_2}c, \tag{3.38a}$$

$$H_0 = -\frac{m^2 - m_1^2 - m_2^2}{2m_1m_2}a - \frac{\lambda(m_B^2, m_1^2, m_2^2)}{4m_1^2m_2^2}b. \tag{3.38b}$$

Vector meson masses are denoted $m_{1,2}$, while definition of the constants a, b and c is in terms of general Lorentz decomposition of the amplitude

$$H_\lambda = \epsilon_{1\mu}^*(\lambda)\epsilon_{2\nu}^*(\lambda)\left(ag^{\mu\nu} + \frac{b}{m_1m_2}p_B^\mu p_B^\nu + \frac{ic}{m_1m_2}\epsilon^{\mu\nu\alpha\beta}p_{1\alpha}p_{2\beta}\right), \tag{3.39}$$

where $\epsilon_{1,2}$ and $p_{1,2}$ are the respective vector mesons' polarizations and momenta.

3.3.3 Hadronic decay widths

$B^- \to \pi^-\pi^- K^+$

Hadronic matrix element entering in the amplitude for $B^- \to \pi^-\pi^- K^+$ in SM (MSSM) is readily given by (3.32) after identifying $P = \pi^-$, $P_1 = K^+$, $P_2 = \pi^-$ and using appropriate form factors whose explicit form can be found in Appendix A.3. Expression (3.35) is used instead for $\not{R}_p$MSSM, while for the Z' model the amplitude consists of both contributions (3.32) and (3.35).

The two final state pions are indistinguishable and the crossed term with interchange $u \leftrightarrow s$ is to be present in the amplitude. After phase space integration the hadronic decay widths can be written in a compact form with only Wilson coefficients on the matching scale Λ left in symbolic form:

$$\Gamma^{(\mathrm{MS})\mathrm{SM}}_{\pi\pi K} = \left|C_3^{(\mathrm{MS})\mathrm{SM}}\right|^2 \times 2.0 \times 10^{-3}\ \mathrm{GeV}^5, \tag{3.40}$$

$$\Gamma^{\not{R}_p}_{\pi\pi K} = \left|C_4^{\not{R}_p} + \tilde{C}_4^{\not{R}_p}\right|^2 \times 8.9 \times 10^{-3}\ \mathrm{GeV}^5, \tag{3.41}$$

$$\begin{aligned}\Gamma^{Z'}_{\pi\pi K} = &\left|C_1^{Z'} + \tilde{C}_1^{Z'}\right|^2 \times 3.5 \times 10^{-3}\ \mathrm{GeV}^5 \\ &+ \left|C_3^{Z'} + \tilde{C}_3^{Z'}\right|^2 \times 1.3 \times 10^{-3}\ \mathrm{GeV}^5 \\ &+ \mathrm{Re}\left[\left(C_1^{Z'} + \tilde{C}_1^{Z'}\right)\left(C_3^{Z'} + \tilde{C}_3^{Z'}\right)^*\right] \times 3.2 \times 10^{-3}\ \mathrm{GeV}^5.\end{aligned} \tag{3.42}$$

$B^- \to \pi^- D^- D_s^+$

In calculation of the $B^- \to \pi^- D^- D_s^+$ decay rate again we use (3.32) and (3.35), now with $P = \pi^-$, $P_1 = D_s^+$ and $P_2 = D^-$. Numerically this yields

$$\Gamma^{(\mathrm{MS})\mathrm{SM}}_{\pi D D_s} = \left|C_3^{(\mathrm{MS})\mathrm{SM}}\right|^2 \times 8.7 \times 10^{-9}\ \mathrm{GeV}^5, \tag{3.43}$$

$$\Gamma^{\not{R}_p}_{\pi D D_s} = \left|C_4^{\not{R}_p} + \tilde{C}_4^{\not{R}_p}\right|^2 \times 8.2 \times 10^{-5}\ \mathrm{GeV}^5, \tag{3.44}$$

$$\begin{aligned}\Gamma^{Z'}_{\pi D D_s} = &\left|C_1^{Z'} + \tilde{C}_1^{Z'}\right|^2 \times 1.6 \times 10^{-5}\ \mathrm{GeV}^5 \\ &+ \left|C_3^{Z'} + \tilde{C}_3^{Z'}\right|^2 \times 5.7 \times 10^{-9}\ \mathrm{GeV}^5 \\ &+ \mathrm{Re}\left[\left(C_1^{Z'} + \tilde{C}_1^{Z'}\right)\left(C_3^{Z'} + \tilde{C}_3^{Z'}\right)^*\right] \times 5.9 \times 10^{-7}\ \mathrm{GeV}^5.\end{aligned} \tag{3.45}$$

This mode turns out less favourable than $B^- \to \pi^-\pi^- K^+$ due to phase space suppression.

$B^- \to \pi^- K^0$

In [57] this decay was addressed as the mode with the wrong kaon mode, being highly suppressed in the SM compared to the decay with $\bar{K}^0$ in the final state. The operators $\mathcal{O}_{1,3}$ and $\tilde{\mathcal{O}}_{1,3}$ that are present in SM, MSSM, and Z' model have the

following contribution:

$$\begin{aligned}&\left\langle K^0(p_K)\,\middle|\,\bar{d}\gamma_\mu\gamma^5 s\,\middle|\,0\right\rangle\left\langle \pi^-(p_\pi)\,\middle|\,\bar{d}\gamma^\mu b\,\middle|\,B^-(p_B)\right\rangle\\&\quad= i(m_B^2-m_\pi^2)f_K F_0^{\pi B}(m_K^2).\end{aligned}\tag{3.46}$$

In the $\not{R}_p$MSSM and also in the Z' framework, operator $\mathcal{O}_2$ is first Fierz transformed to $\mathcal{O}_4$ and $\tilde{\mathcal{O}}_4$, which then result in

$$\begin{aligned}&\left\langle K^0(p_K)\,\middle|\,\bar{d}\gamma^5 s\,\middle|\,0\right\rangle\left\langle \pi^-(p_\pi)\,\middle|\,\bar{d}b\,\middle|\,B^-(p_B)\right\rangle\\&\quad= \frac{im_K^2(m_B^2-m_\pi^2)}{(m_b-m_d)(m_s+m_d)}f_K F_0^{\pi B}(m_K^2).\end{aligned}\tag{3.47}$$

However, in $\not{R}_p$MSSM and Z' models, the two chirally flipped contributions to the amplitude have opposite signs, resulting in a slightly different combination of Wilson coefficients compared to the $B^- \to \pi^-\pi^- K^+$ decay width

$$\Gamma_{\pi K}^{(\mathrm{MS})\mathrm{SM}} = \left|C_3^{(\mathrm{MS})\mathrm{SM}}\right|^2 \times 3.9\times 10^{-4}\ \mathrm{GeV}^5,\tag{3.48}$$

$$\Gamma_{\pi K}^{\not{R}_p} = \left|C_4^{\not{R}_p} - \tilde{C}_4^{\not{R}_p}\right|^2 \times 5.0\times 10^{-4}\ \mathrm{GeV}^5,\tag{3.49}$$

$$\begin{aligned}\Gamma_{\pi K}^{Z'} = &\left|C_1^{Z'} - \tilde{C}_1^{Z'}\right|^2 \times 6.8\times 10^{-5}\ \mathrm{GeV}^5\\&+\left|C_3^{Z'} - \tilde{C}_3^{Z'}\right|^2 \times 2.6\times 10^{-4}\ \mathrm{GeV}^5\\&-\mathrm{Re}\left[\left(C_1^{Z'} - \tilde{C}_1^{Z'}\right)\left(C_3^{Z'} - \tilde{C}_3^{Z'}\right)^*\right]\times 2.7\times 10^{-4}\ \mathrm{GeV}^5.\end{aligned}\tag{3.50}$$

$B^- \to \rho^- K^0$

Using the form factors parameterization (2.32) of the pseudoscalar to vector meson transition we derive the following two factorized matrix elements of axial-vector and pseudoscalar operators:

$$\begin{aligned}&\left\langle K^0(p_K)\,\middle|\,\bar{d}\gamma_\mu\gamma^5 s\,\middle|\,0\right\rangle\left\langle \rho^-(\epsilon_\rho,p_\rho)\,\middle|\,\bar{d}\gamma^\mu\gamma^5 b\,\middle|\,B^-(p_B)\right\rangle\\&\quad= -2m_\rho f_K A_0^{\rho B}(m_K^2)\epsilon_\rho^*\cdot p_B,\end{aligned}\tag{3.51}$$

$$\begin{aligned}&\left\langle K^0(p_K)\,\middle|\,\bar{d}\gamma^5 s\,\middle|\,0\right\rangle\left\langle \rho^-(\epsilon_\rho,p_\rho)\,\middle|\,\bar{d}\gamma^5 b\,\middle|\,B^-(p_B)\right\rangle\\&\quad= \frac{2m_\rho m_K^2}{(m_b+m_d)(m_s+m_d)}f_K A_0^{\rho B}(m_K^2)\epsilon_\rho^*\cdot p_B.\end{aligned}\tag{3.52}$$

Finally, we sum over polarizations of the ρ meson using (3.36), and the unpolarized decay rates read

$$\Gamma_{\rho K}^{(\mathrm{MS})\mathrm{SM}} = \left|C_3^{(\mathrm{MS})\mathrm{SM}}\right|^2 \times 3.9\times 10^{-4}\ \mathrm{GeV}^5,\tag{3.53}$$

$$\Gamma_{\rho K}^{\not{R}_p} = \left|C_4^{\not{R}_p} + \tilde{C}_4^{\not{R}_p}\right|^2 \times 5.0\times 10^{-4}\ \mathrm{GeV}^5,\tag{3.54}$$

$$\begin{aligned}\Gamma_{\rho K}^{Z'} = &\left|C_1^{Z'} + \tilde{C}_1^{Z'}\right|^2 \times 7.5\times 10^{-4}\ \mathrm{GeV}^5\\&+\left|C_3^{Z'} + \tilde{C}_3^{Z'}\right|^2 \times 2.6\times 10^{-4}\ \mathrm{GeV}^5\\&-\mathrm{Re}\left[\left(C_1^{Z'} + \tilde{C}_1^{Z'}\right)\left(C_3^{Z'} + \tilde{C}_3^{Z'}\right)^*\right]\times 8.8\times 10^{-4}\ \mathrm{GeV}^5.\end{aligned}\tag{3.55}$$

$B^- \to \pi^- K^{*0}$

Factorized matrix element here is a product of vector meson K^{0*} creation amplitude (2.29b) and $B^- \to \pi^-$ transition amplitude. Operators with vector currents result in

$$\left\langle K^{*0}(\epsilon_K, p_K) \,\middle|\, \bar{d}\gamma_\mu s \,\middle|\, 0 \right\rangle \left\langle \pi^-(p_\pi) \,\middle|\, \bar{d}\gamma^\mu b \,\middle|\, B^-(p_B) \right\rangle = 2 g_{K^*} F_1^{\pi B}(m_{K^*}^2) \epsilon_K^* \cdot p_B, \tag{3.56}$$

while the density operators $\mathcal{O}_4$ and $\tilde{\mathcal{O}}_4$ do not contribute as a result of (3.34) and (2.29b). Thus the $\not{R}_p$MSSM model does not contribute to this channel in the naive factorization approximation.

$$\Gamma_{\pi K^*}^{(\mathrm{MS})\mathrm{SM}} = \left| C_3^{(\mathrm{MS})\mathrm{SM}} \right|^2 \times 7.4 \times 10^{-4}\ \mathrm{GeV}^5, \tag{3.57}$$

$$\begin{aligned} \Gamma_{\pi K^*}^{Z'} = & \left| C_1^{Z'} + \tilde{C}_1^{Z'} \right|^2 \times 5.9 \times 10^{-4}\ \mathrm{GeV}^5 \\ & + \left| C_3^{Z'} + \tilde{C}_3^{Z'} \right|^2 \times 4.8 \times 10^{-4}\ \mathrm{GeV}^5 \\ & + \mathrm{Re}\left[\left(C_1^{Z'} + \tilde{C}_1^{Z'} \right) \left(C_3^{Z'} + \tilde{C}_3^{Z'} \right)^* \right] \times 1.1 \times 10^{-3}\ \mathrm{GeV}^5. \end{aligned} \tag{3.58}$$

$B^- \to \rho^- K^{*0}$

Like in the previous case, this channel does not receive factorizable contributions in the $\not{R}_p$MSSM framework. In SM, MSSM, and Z' we calculate unpolarized hadronic amplitudes of the operators $\mathcal{O}_{1,3}$ and $\tilde{\mathcal{O}}_{1,3}$ by utilizing the helicity amplitudes formalism. With form factor decomposition (2.29b), (2.32) we express the polarized amplitude as in (3.39) and identify constants a, b and c:

$$a = -\frac{i}{4}(m_B + m_\rho) g_{K^*} A_1^{\rho B}(m_{K^*}^2)(C - \tilde{C}), \tag{3.59a}$$

$$b = \frac{i}{2} \frac{m_{K^*} m_\rho}{m_B + m_\rho} g_{K^*} A_2^{\rho B}(m_{K^*}^2)(C - \tilde{C}), \tag{3.59b}$$

$$c = -\frac{i}{2} \frac{m_{K^*} m_\rho}{m_B + m_\rho} g_{K^*} V^{\rho B}(m_{K^*}^2)(C + \tilde{C}). \tag{3.59c}$$

C and $\tilde{C}$ are combinations of the Wilson coefficients present in a considered model. We have

$$C = C_3^{(\mathrm{MS})\mathrm{SM}}, \qquad \tilde{C} = 0 \tag{3.60}$$

in the SM and MSSM and

$$C = [f_{QCD}(m_{Z'})]^{-1/8} C_1^{Z'} + [f_{QCD}(m_{Z'})]^{-1/4} C_3^{Z'}, \tag{3.61}$$

$$\tilde{C} = [f_{QCD}(m_{Z'})]^{-1/8} \tilde{C}_1^{Z'} + [f_{QCD}(m_{Z'})]^{-1/4} \tilde{C}_3^{Z'} \tag{3.62}$$

in the Z' model. Decay rates are then

$$\Gamma_{\rho K^*}^{(\mathrm{MS})\mathrm{SM}} = \left| C_3^{(\mathrm{MS})\mathrm{SM}} \right|^2 \times 9.2 \times 10^{-4}\ \mathrm{GeV}^5, \tag{3.63}$$

$$\begin{aligned}
\Gamma_{\rho K^*}^{Z'} = & \left| C_1^{Z'} + \tilde{C}_1^{Z'} \right|^2 \times 2.8 \times 10^{-5}\ \mathrm{GeV}^5 \\
& + \left| C_1^{Z'} - \tilde{C}_1^{Z'} \right|^2 \times 7.2 \times 10^{-4}\ \mathrm{GeV}^5 \\
& + \left| C_3^{Z'} + \tilde{C}_3^{Z'} \right|^2 \times 2.3 \times 10^{-5}\ \mathrm{GeV}^5 \\
& + \left| C_3^{Z'} - \tilde{C}_3^{Z'} \right|^2 \times 5.8 \times 10^{-4}\ \mathrm{GeV}^5 \\
& + \mathrm{Re}\left[\left(C_1^{Z'} + \tilde{C}_1^{Z'} \right) \left(C_3^{Z'} + \tilde{C}_3^{Z'} \right)^* \right] \times 5.0 \times 10^{-5}\ \mathrm{GeV}^5 \\
& + \mathrm{Re}\left[\left(C_1^{Z'} - \tilde{C}_1^{Z'} \right) \left(C_3^{Z'} - \tilde{C}_3^{Z'} \right)^* \right] \times 1.3 \times 10^{-3}\ \mathrm{GeV}^5.
\end{aligned} \tag{3.64}$$

3.4 Constraints on the short distance parameters

We have investigated the $b \to dd\bar{s}$ transition within the SM, MSSM without and with $\not{R}_p$ terms and within a model with an extra Z' gauge boson. The SM contribution leads to extremely small branching ratio for this transition.

Roughly one order of magnitude increase in the MSSM compared to the SM predictions is still too insignificant for any experimental search. The supersymmetry with $\not{R}_p$ terms, however, might give significant contributions and a possibility to exclude down the parameter space even further. The Z' model exhibits its structure through interplay of different types of effective interactions and might also give opportunity to constrain its relevant parameters.

In the $b \to dd\bar{s}$ decay a particular combination of the model parameters appear which can be constrained using the $B^- \to \pi^-\pi^-K^+$ decay mode. In our calculation we have relied on the naïve factorization approximation, which is sufficient to obtain correct gross features of new physics effects. One might think that the nonfactorizable contributions might induce large additional uncertainties, but we do not expect them to change the order of magnitude of our predictions. Additional uncertainties might originate in the poor knowledge of the input parameters such as form factors. However, we do not expect these to exceed 30%.

Using the most stringent experimental bound for the $\mathcal{B}(B^- \to \pi^-\pi^-K^+) < 9.5 \times 10^{-7}$ [49] and normalizing the masses of sneutrinos to a common mass scale of 100 GeV we derive bounds on the $\not{R}_p$MSSM terms given in (3.21)

$$\left| \sum_{n=1}^{3} \left(\frac{100\ \mathrm{GeV}}{m_{\tilde{\nu}_n}} \right)^2 \left(\lambda'_{n31}\lambda'^*_{n12} + \lambda'_{n21}\lambda'^*_{n13} \right) \right| < 6.6 \times 10^{-5}. \tag{3.65}$$

Complementary bounds coming from measurements of K–$\bar{K}$ and B–$\bar{B}$ mixings have

been established in [78]

$$\left|\mathrm{Re}\left[\sum_{n=1}^{3}\left(\frac{100\ \mathrm{GeV}}{m_{\tilde{\nu}_n}}\right)^2\lambda'_{n31}\lambda'^{*}_{n12}\right]\right| < 2.6\times10^{-6}, \tag{3.66a}$$

$$\left|\mathrm{Im}\left[\sum_{n=1}^{3}\left(\frac{100\ \mathrm{GeV}}{m_{\tilde{\nu}_n}}\right)^2\lambda'_{n31}\lambda'^{*}_{n12}\right]\right| < 2.9\times10^{-8}, \tag{3.66b}$$

$$\left|\mathrm{Re}\left[\sum_{n=1}^{3}\left(\frac{100\ \mathrm{GeV}}{m_{\tilde{\nu}_n}}\right)^2\lambda'_{n21}\lambda'^{*}_{n13}\right]\right| < 2.9\times10^{-4}. \tag{3.66c}$$

From (3.66a) and (3.66b) it becomes apparent that the $\lambda'_{n31}\lambda'^{*}_{n12}$ term is negligible in (3.65), and the bound becomes simpler

$$\left|\sum_{n=1}^{3}\left(\frac{100\ \mathrm{GeV}}{m_{\tilde{\nu}_n}}\right)^2\lambda'_{n21}\lambda'^{*}_{n13}\right| < 6.6\times10^{-5}, \tag{3.67}$$

now being more restrictive than the bound (3.66c), obtained from B–$\bar{B}$ mixing alone.

Assuming that new physics arises due to an extra Z' gauge boson we derive bounds on the parameters given in (3.27). We neglect interference between Wilson coefficients, namely the third term in (3.42). Experimental bound of this simplified expression now confines $\left(|C_1^{Z'}+\tilde{C}_1^{Z'}|, |C_3^{Z'}+\tilde{C}_3^{Z'}|\right)$ to lie within an ellipse with semiminor and semimajor axes as upper limits

$$y\left|B_{12}^{d_L}\,B_{13}^{d_R}+B_{12}^{d_R}\,B_{13}^{d_L}\right| < 3.2\times10^{-4}, \tag{3.68a}$$

$$y\left|B_{12}^{d_L}\,B_{13}^{d_L}+B_{12}^{d_R}\,B_{13}^{d_R}\right| < 5.2\times10^{-4}. \tag{3.68b}$$

Complementary bounds of the same couplings originate from neutral meson mass-splittings and CP violation in kaon system and have been derived [70]

$$y\left|\mathrm{Re}\left[(B_{12}^{d_{R,L}})^2\right]\right| < 10^{-8}, \tag{3.69a}$$

$$y\left|\mathrm{Re}\left[(B_{13}^{d_{R,L}})^2\right]\right| < 6\times10^{-8}, \tag{3.69b}$$

$$y\left|\mathrm{Im}\left[(B_{12}^{d_{R,L}})^2\right]\right| < 8\times10^{-11}. \tag{3.69c}$$

The above bounds are stronger than our (3.68). Nevertheless, the bounds (3.65) and (3.68) are interesting since they offer an independent way of constraining the particular combination of the parameters, which are not constrained by the B_d^0–$\bar{B}_d^0$, B_s^0–$\bar{B}_s^0$, K^0–$\bar{K}^0$ oscillations, or by $B^-\to K^-K^-\pi^+$ decay rate (c.f. [79]).

Using these inputs we predict the branching ratios for the various possible two-body decay modes and the $B^-\to\pi^-D^-D_s^+$ decay. We apply the bound (3.65) on expressions for hadronic decay widths $\Gamma^{\not{R}_p}_{B^-\to X}$ from the previous section and find the experimental sensitivity to $\not{R}_p$MSSM couplings of the given channel. The procedure is straightforward except for the $B^-\to\pi^-K^0$ and $B^-\to\rho^-K^{*0}$ decay channels. In those we have to assume as in [51, 52] that interference term $C_4^{RPV}\tilde{C}_4^{RPV*}$ is negligible, which leads to the approximation $|C_4^{RPV}-\tilde{C}_4^{RPV}|\simeq|C_4^{RPV}+\tilde{C}_4^{RPV}|$.

In the case of the Z' model there are contributions from Wilson coefficients "1" ($C_1^{Z'}$ and $\tilde{C}_1^{Z'}$) and "3" ($C_3^{Z'}$ and $\tilde{C}_3^{Z'}$). We have already neglected the interference terms between "1" and "3" in (3.42) to find bounds (3.68) and we assume that these terms are small for all considered decay modes. Using (3.68) we can now predict branching ratios for decay modes $B^- \to \pi^- D^- D_s^+$, $B^- \to \rho^- K^0$, and $B^- \to \pi^- K^{*0}$. The remaining two decay widths $B^- \to \pi^- K^0$ and $B^- \to \rho^- K^{*0}$ can be approached after we neglect interference terms $C_1^{Z'} \tilde{C}_1^{Z'*}$ and $C_3^{Z'} \tilde{C}_3^{Z'*}$. The results are summarized in Table 3.2.

Decay channel	SM	MSSM	$\not{R}_p$MSSM	Z'
$B^- \to \pi^-\pi^- K^+$	1×10^{-15}	1×10^{-14}	constraint	constraint
$B^- \to \pi^- D^- D_s^+$	6×10^{-21}	6×10^{-20}	9×10^{-9}	4×10^{-9}
$B^- \to \pi^- K^0$	3×10^{-16}	3×10^{-15}	5×10^{-8}	2×10^{-7}
$B^- \to \rho^- K^0$	3×10^{-16}	3×10^{-15}	5×10^{-8}	4×10^{-7}
$B^- \to \pi^- K^{*0}$	5×10^{-16}	5×10^{-15}	—	5×10^{-7}
$B^- \to \rho^- K^{*0}$	6×10^{-16}	6×10^{-15}	—	6×10^{-7}

Table 3.2: The branching ratios for the $\Delta S = -1$ decays of the B^- meson calculated within SM, MSSM, $\not{R}_p$MSSM, and Z' models. The experimental upper bound for the $\mathcal{B}(B^- \to \pi^-\pi^- K^+) < 9.5 \times 10^{-7}$ has been used as an input parameter to fix the unknown combinations of the $\not{R}_p$MSSM terms (IV column) and the model with an additional Z' boson (V column).

The SM gives negligible contributions. The MSSM increases them by one order of magnitude, which is still insufficient for the current and foreseen experimental searches. Using constraints for the particular combination of the $\not{R}_p$MSSM parameters present in the $B^- \to \pi^-\pi^- K^+$ decay we obtain the largest possible branching ratios for the two-body decays of $B^- \to \rho^- K^0$ and $B^- \to \pi^- K^0$, while for the $B^- \to \pi^- K^{*0}$ and $B^- \to \rho^- K^{*0}$ the RPV contribution is suppressed by the vanishing of factorizable contributions. However, these two decay channels are most likely to be observed in the model with an additional Z' boson, if we assume that interference terms are negligible.

Since in the experimental measurements only K_S or K_L are detected and not K^0 or $\bar{K}^0$, it might be difficult to observe new physics in the $B^- \to \pi^- K^0$ decay mode. Namely, the branching ratio $\mathcal{B}(B^- \to \pi^- \bar{K}_0) = (23.1 \pm 1.0) \times 10^{-6}$ [80] is two orders of magnitude higher than our upper bound for the $\mathcal{B}(B^- \to \pi^- K^0)$ making the extraction of new physics from this decay mode almost impossible. Therefore, the two-body decay modes with K^{*0} in the final state seem to be better candidates for the experimental searches of new physics in the $b \to dd\bar{s}$ transitions.

Chapter 4

Neutral currents in charm and $D \to P\ell^+\ell^-$

Charm mesons are the only low energy window into flavour changing currents (FCNCs) involving up-type quarks. There are essentially two distinct up-type quark FCNC processes in the SM at low energy. One of them is the decay $c \to u\gamma$, which can be either on-shell or virtual, and other the neutral meson mixing $c\bar{u} \leftrightarrow \bar{c}u$. This is to be contrasted with wealth of experimental information on FCNCs in the down-type quark sector. Top quark physics will bring in additional input but already a handful of charm observables is worth studying as new possibilities opened up with the recent measurement of D^0–$\bar{D}^0$ oscillations.

The mixing was reported by Belle, BaBar, and CDF collaborations [11–15]. Combining the measured quantities [80] resulted in determination of mass splitting between the two CP-eigenstates Δm_D as well as $\Delta\Gamma_D$

$$x \equiv \frac{\Delta m_D}{\bar{\Gamma}_D} = (0.98 \pm 0.25) \times 10^{-2}, \tag{4.1a}$$

$$y \equiv \frac{\Delta\Gamma_D}{2\bar{\Gamma}_D} = (0.83 \pm 0.16) \times 10^{-2}. \tag{4.1b}$$

These results immediately stimulated many studies (c.f. [81–86]). In light of the long distance dominated SM prediction for x and y, ranging from 10^{-5}–10^{-2} [87–90], the measured values of x and y are not in favour of NP effects. However, they give additional constraints on physics beyond the SM as observed in [82, 83]. On the other hand, also the study of rare D meson decays is not considered very informative in current searches of physics beyond the SM [91–98], as it is expected from B physics. Namely, most of the charm meson FCNC processes are dominated by virtual d and s quarks, signaling strong presence of long distance (LD) resonant contributions, which dominate over genuine short distance (SD) effects [91–99]. In light of new data on charm meson mixing we will study rare decays $D \to \pi\ell^+\ell^-$ and $D_s \to K\ell^+\ell^-$, where $\ell = e, \mu$, and provide updated constraints of R_p-violating MSSM and a model with scalar leptoquark.

4.1 Charm decays and resonances

Conspiracy of CKM elements and quark masses makes FCNC charm decays very susceptible for presence of low energy QCD dynamics. Up to $\sim \lambda^2$ Cabibbo order, the third generation of quarks does not mix with the first two and in CP-conserving processes hadronic states of the first two generations saturate the decays widths. As for the genuine short distance contribution, the GIM mechanism and smallness of the down-type quark masses renders the radiative $c \to u\gamma$ decay width strongly suppressed at the leading order in the SM [91, 95]. The QCD effects enhance it up to the order of 10^{-8} [100], however the overall decay width is saturated with the long-distance resonant contributions. We will show that when one includes into consideration the possible effects of MSSM with non-universal soft breaking terms on $c \to u\gamma$ [101, 102], the enhancement relative to the SM value is a factor 10, still too small to give any observable effects in $D \to V\gamma$ decays (V is a light vector meson). The dominant long-distance (LD) contributions in the $D \to V\gamma$ decays give the branching ratios of the order $\mathcal{B} \sim 10^{-6}$ [91, 95], which makes the search for new physics effects impossible in $D \to V\gamma$.

Another possibility to search for the effects of new physics in the charm sector is offered in the studies of $D \to P\ell^+\ell^-$ or $D \to V\ell^+\ell^-$ exclusive decays which might be result of the $c \to u\ell^+\ell^-$ transition [84, 92, 93, 96, 97, 99]. Within the SM inclusion of renormalization group improved QCD corrections of $c \to u\ell^+\ell^-$ gave an additional significant suppression leading to the inclusive rates $\Gamma(c \to ue^+e^-)/\Gamma_{D^0} = 2.4 \times 10^{-10}$ and $\Gamma(c \to u\mu^+\mu^-)/\Gamma_{D^0} = 0.5 \times 10^{-10}$ [103]. These transitions are largely driven by a virtual photon at low dilepton mass $q^2 \equiv (p_+ + p_-)^2$, while the total rate for $D \to X\ell^+\ell^-$ is saturated by the LD resonant contributions at dilepton invariant masses $q^2 = m_\rho^2, m_\omega^2, m_\phi^2$ [92, 97]. NP could possibly modify the dilepton invariant mass spectra below ρ or above ϕ resonant peaks. In the q^2 spectrum of $D \to \pi\ell^+\ell^-$ decay there is a broad kinematical region of dilepton invariant mass above the ϕ resonance which presents a unique possibility to study $c \to u\ell^+\ell^-$ [97]. In order to compare effects of NP and the SM we have to estimate size of the resonant contributions. We will also extend our analysis on FCNC decays to the charm-strange mesons $D_s \to K\mu^+\mu^-$, whose upper bounds are currently much weaker than for the corresponding D decays.

There are intensive experimental efforts by CLEO [104, 105] experiment and Fermilab collaborations [106, 107] to improve the upper limits on the rates for $D \to X\ell^+\ell^-$ decays. Two events in the channel $D^+ \to \pi^+e^+e^-$ with q^2 close to m_ϕ^2 have already been observed by CLEO [104]. Currently the upper bounds are

$$\mathcal{B}(D^+ \to \pi^+e^+e^-) < 7.4 \times 10^{-6} \qquad [108], \tag{4.2a}$$

$$\mathcal{B}(D^+ \to \pi^+\mu^+\mu^-) < 3.9 \times 10^{-6} \qquad [109]. \tag{4.2b}$$

Other rare D meson decays are more difficult to access experimentally, but with the plans to make more experimental studies in rare charm decays at CLEO-c, Tevatron and charm physics sections of the forthcoming LHCb and Belle 2 experiments makes the study of rare D decays more attractive.

4.2 New physics scenarios

4.2.1 Additional up-type quark singlet

Some models of new physics contain an extra up-type heavy quark singlet [110, 111] inducing FCNCs driven by Z boson exchange in the up-type quark sector [94, 112–115], while the neutral current for the down-type quarks is the same as in SM. The most stringent bound on parameters of these models comes from the measured x of D^0–$\bar{D}^0$ mixing as given in (4.1). In our calculation, we analyze how these bounds on the FCNC vertex cuZ affect the $D \to P\ell^+\ell^-$ decays. A particular version of the model with tree-level up-quark FCNC transitions is the Littlest Higgs model [116]. In this case the magnitude of the relevant $c \to uZ$ coupling is further constrained by the large scale $f \geq \mathcal{O}(1\ \text{TeV})$. The smallness implies that the effect of this particular model on $c \to u\ell^+\ell^-$ decay and relevant rare D decays is insignificant [94]. Similar effect can be produced in the model with an extra Z' gauge boson, which couples as $c \to uZ'$, and was shown to produce weaker constraints in $D^0 \to \ell^+\ell^-$ than in D^0–$\bar{D}^0$ mixing [117].

4.2.2 Supersymmetry

The leading contribution to $c \to u\gamma$ in MSSM with conserved R_p-parity comes from one-loop diagram with gluino and squarks in the loop [92, 97, 102]. Using the new bound on the mass insertion parameters within MSSM [81, 82] from the D^0–$\bar{D}^0$ oscillations constraints (4.1) and constraints from the MSSM vacuum neutrality we will argue there are no good prospects for using $D \to V\gamma$ as probe of MSSM. Same holds for the tree-level photon exchange which enhances the short distance $c \to u\ell^+\ell^-$ spectrum at small q^2. Bounds on the mass insertion parameters make the abovementioned enhancement in $D \to P\ell^+\ell^-$ decay negligible [92, 93].

On the other hand, among popular models of NP the supersymmetric extension of the SM including the R_p-parity violation ($\not{R}_p$MSSM) is still not constrained as other NP models. As noticed in [92, 103] one can test some combinations of the R_p-parity violating contributions in $D^+ \to \pi^+\ell^+\ell^-$ decays. We place new constraints on the relevant parameters and demonstrate the effects of $\not{R}_p$MSSM in the $D_s^+ \to K^+\ell^+\ell^-$ decays which might be interesting for the future experimental studies.

4.2.3 Weak singlet leptoquark

Leptoquark states are expected to exist in various extensions of SM. They were first introduced in the early grand unification theories (GUTs) in the seventies [1,2]. Scalar leptoquarks are expected to exist at TeV scale in extended technicolor models as well as in models of quark and lepton compositeness. Squarks in supersymmetric models with R_p violation may also have leptoquark-type Yukawa couplings. Usually, they are present due to some symmetry between leptons to quarks in the fundamental theory and consequently their interactions may trigger lepton and baryon number violation which might lead to proton decay. Recently, leptoquarks were revived in search of resolution of the so-called f_{D_s} puzzle [118].

Namely, the measured decay widths of $D_s \to \mu\nu, \tau\nu$ have been with moderate significance $> 2\sigma$ larger than the prediction in terms of G_F, V_{cs}, and f_{D_s}:

$$\Gamma^{SM}_{D_s\to\tau\nu} = \frac{G_F^2 m_\tau^2 \left|V_{cs}\right|^2 f_{D_s}^2 m_{D_s}}{8\pi}\left[1-\left(\frac{m_\tau}{m_{D_s}}\right)^2\right]^2 . \tag{4.3}$$

It was first pointed out in [118] that scalar leptoquark exchange could, in contrast to other mechanisms such as s-channel charged Higgs exchange, add positively to the SM decay width of $D_s \to \ell\nu$. Several studies have been done [119–122] but in the meantime the f_{D_s} puzzle has lost its significance [123, 124] Either way, weak singlet scalar leptoquark can also contribute to the effective operators mediating $c \to u\ell^+\ell^-$. In [119] this state was part of the 45-dimensional representation of the $SU(5)$ group, which contains also other scalars states which might be light and contribute notably in low energy phenomena or top quark physics [125].

4.3 $c \to u\gamma$

Given the recent observation of D^0–$\bar{D}^0$ mixing, we evaluate the possible effect of MSSM on $c \to u\gamma$, taking into account the D^0–$\bar{D}^0$ mixing parameters (4.1). Since MSSM with universal soft-breaking terms is known to have negligible effect [102], we consider the case of non-universal soft-breaking terms. We take into account only the gluino exchange diagrams through $(\delta^u_{12})_{LR}$ and $(\delta^u_{12})_{RL}$, since the remaining mass insertions cannot have sizable effect as shown in [101, 102]. The maximal value of $(\delta^u_{12})_{LR,RL}$ insertions has been constrained by saturating parameter x with the gluino exchange mechanism in [82]. Their results corresponding to a value $x = (0.79\pm0.34)\times10^{-2}$ are shown in second column of Table 4.1. Another constraint is obtained by requiring of minima of MSSM scalar potential not to break electric charge or colour and they are bounded from above $(\delta^u_{12})_{LR,RL} \leq \sqrt{3}m_c/m_{\tilde{q}}$ [126], with values given in third column of Table 4.1. The second constraint is obviously stronger for $m_{\tilde{q}} \geq 350$ GeV, while Δm_D gives more stringent constraint for lighter squarks. Using $(\delta^u_{12})_{LR,RL} \leq \sqrt{3}\ m_c/m_{\tilde{q}}$, $m_{\tilde{q}} = m_{\tilde{g}} = 350$ GeV, $m_c = 1.25$ GeV and expressions from [102] we get the upper bound

$$\Gamma(c \to u\gamma)/\Gamma_{D^0} \leq 8 \times 10^{-7}, \tag{4.4}$$

which is one order of magnitude larger than the SM prediction $\Gamma(c \to u\gamma)/\Gamma_{D^0} = 2.5\times10^{-8}$ [100]. However, this possible MSSM enhancement by 1 order of magnitude

$m_{\tilde{q}} = m_{\tilde{g}}$	$\max\left\|(\delta^u_{12})_{LR,RL}\right\|$ from Δm_D	$\max\left\|(\delta^u_{12})_{LR,RL}\right\|$ from stability bound
350 GeV	0.007	0.006
500 GeV	0.01	0.004
1000 GeV	0.02	0.002

Table 4.1: Upper bounds on mass insertions $\left|(\delta^u_{12})_{LR,RL}\right|$ from measured Δm_D and stability bound [126].

would not affect the rate of the $D \to V\gamma$ decays, which are completely dominated by LD contributions with $\mathcal{B} \sim 10^{-6}$ [91–93, 95, 99]. The only theoretically sound observable probing the $c \to u\gamma$ remains the $B_c \to B_u^*\gamma$ decay, where LD contributions are strongly suppressed and thus comparable in size with SD contributions [127].

4.4 $D \to P\ell^+\ell^-$ decays: short distance amplitudes

4.4.1 SM

The $c \to u\ell^+\ell^-$ transition is induced at one loop level in the SM. We will use the effective theory description where W boson, t and b quark degrees of freedom are already integrated out. Here we will follow the procedure taken in [103]. Starting at the weak scale $\mu_W \simeq m_W$ we have

$$\mathcal{L}_{\text{eff}} = -\frac{4G_F}{\sqrt{2}}\left[\lambda_d \sum_{i=1,2} C_i(\mu_W)(Q_i^d - Q_i^b) + \lambda_s \sum_{i=1,2} C_i(\mu_W)(Q_i^s - Q_i^b)\right], \tag{4.5}$$

with standard current-current operators

$$Q_1^q = (\bar{u}_L^\alpha \gamma^\mu q_L^\beta)\,(\bar{q}_L^\beta \gamma_\mu c_L^\alpha), \tag{4.6a}$$
$$Q_2^q = (\bar{u}_L \gamma^\mu q_L)\,(\bar{q}_L \gamma_\mu c_L), \tag{4.6b}$$

where we have denoted CKM mixing factors $\lambda_i = V_{ci}^* V_{ui}$. The direct quark-lepton operators

$$Q_9 = \frac{e^2}{(4\pi)^2}(\bar{u}_L \gamma^\mu c_L)\,(\bar{\ell}\gamma_\mu \ell) \tag{4.7a}$$
$$Q_{10} = \frac{e^2}{(4\pi)^2}(\bar{u}_L \gamma^\mu c_L)\,(\bar{\ell}\gamma_\mu \gamma_5 \ell) \tag{4.7b}$$

are not present in SM and neither are the standard QCD penguin operators $Q_{3\ldots6}$ (c.f. [128]). Operators Q_9 and $Q_{3\ldots6}$ are not present as a consequence of CKM unitarity since at the matching scale m_W we sum over all down-type quarks which are considered massless and GIM cancellation is exact.Operator Q_{10} is negligible in the SM and does not mix with other operators [103]. The electromagnetic dipole contribution

$$Q_7 = \frac{e m_c}{(4\pi)^2}(\bar{u}_L \sigma^{\mu\nu} c_R)\, F_{\mu\nu} \tag{4.8}$$

is further suppressed by α and thus neglected in (4.10). Matching of the Wilson coefficients at the weak scale is performed at NLO in QCD [128]

$$C_1(m_W) = \frac{11}{2}\frac{\alpha_s(m_W)}{4\pi}, \tag{4.9a}$$
$$C_2(m_W) = 1 - \frac{11}{6}\frac{\alpha_s(m_W)}{4\pi}. \tag{4.9b}$$

The scale dependent Wilson coefficients $C_{1,2}(\mu)$ are then run down to the b quark threshold using the 2×2 anomalous dimension matrix given in [128]. At μ_b the

5-flavour effective theory is matched onto the 4-flavour theory, which generates the penguin operators (see Appendix A of [103]). Evolution of the Wilson coefficients $C_{1,2}^{d,s}$ and $C_{3\ldots6,9}$ down to hadronic scale μ_c is performed using the 7×7 anomalous dimension matrix (see [128], eqs. (6.25), (6.26) for $C_{1\ldots6}$, and (8.11), (8.12) for C_9). Finally, the effective Lagrangian at the charm scale μ_c is then [103]

$$\mathcal{L}_{\text{eff}}^{\text{SM}} = -\frac{4G_F}{\sqrt{2}} \left[\lambda_d \sum_{i=1,2} C_i(\mu_c) Q_i^d + \lambda_s \sum_{i=1,2} C_i(\mu_c) Q_i^s - \lambda_b \sum_{i=3,\ldots,10} C_i(\mu_c) Q_i \right], \tag{4.10}$$

The term in (4.10) containing QCD penguins $Q_{3\ldots6}$, dipole operators $Q_{7,8}$, and operators with (axial)vector lepton current $Q_{9,10}$ are in SM rendered negligible due to strong Cabibbo suppression $\lambda_b \simeq \lambda^5$. The dominant contribution comes from the two loop diagrams on Figure 4.1 with Q_2 insertion and additional virtual gluon [100]. The amplitude of the free quark decay $c \to u\ell^+\ell^-$ in SM can be parameterized by

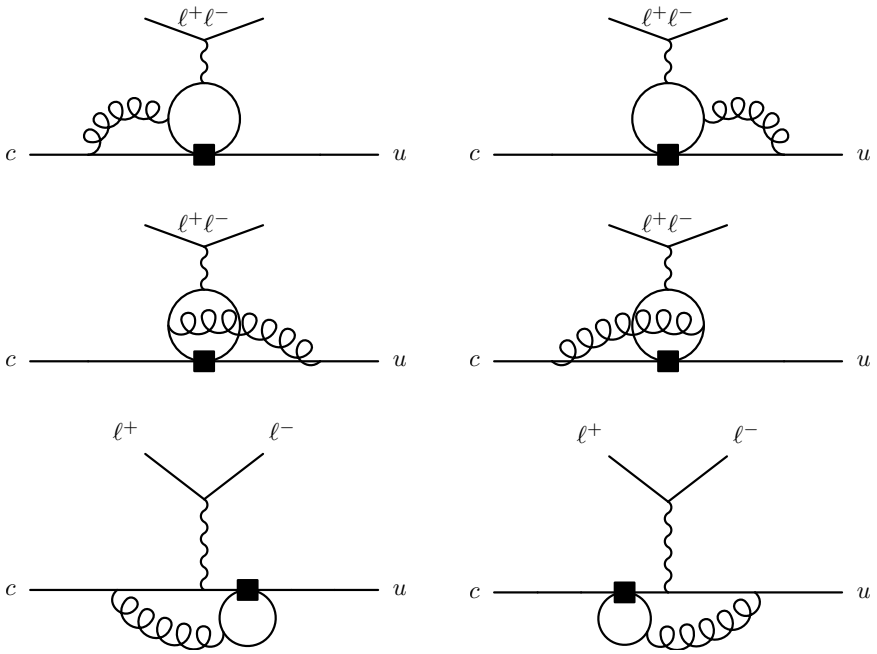

Figure 4.1: Dominantly contributing diagrams to $c \to u\ell^+\ell^-$ in SM. Box vertex denotes the Q_2 insertion.

the electromagnetic dipole operator Q_7 (4.8) which is generated by the insertions of Q_2 operator (Fig. 4.1). We take for the effective coefficient $\hat{C}_7^{\text{eff}}$ [100, 103]

$$\hat{C}_7^{\text{eff}} = \lambda_s(0.007 + 0.020i)(1 \pm 0.2). \tag{4.11}$$

4.4.2 Models with additional up-type quark singlet

The class of models with an extra up-like quark singlet (EQS) induce FCNCs at tree level [94, 110]

$$\mathcal{L}_{\text{EQS}} = \frac{g}{\cos\theta_W} Z_\mu (J_{W^3}^\mu - \sin^2\theta_W J_{\text{EM}}^\mu). \tag{4.12}$$

Electromagnetic current is denoted J^μ_{EM}, while the weak neutral current contains the singlet quark T

$$J^\mu_{W^3} = \bar{Q}_{iL}\gamma^\mu \frac{\tau_3}{2}\Omega_{ij}Q_{jL} = \frac{1}{2}\bar{u}_{iL}\gamma^\mu\Omega_{ij}u_{jL} - \frac{1}{2}\bar{d}_{iL}\gamma^\mu d_{iL}. \tag{4.13}$$

There is mixing among up-type quarks present in (4.13) [116], where $u_{1\ldots4}$ and $d_{1\ldots3}$ are the quark mass eigenstates. Using the convention where we assign the physical flavour rotations to up-type quark sector, the CKM matrix is generalized to 4×4 unitary matrix

$$T^U_L = \begin{pmatrix} V_{ud} & V_{us} & V_{ub} & \Theta_u \\ V_{cd} & V_{cs} & V_{cb} & \Theta_c \\ V_{td} & V_{ts} & V_{tb} & \Theta_t \\ V_{Td} & V_{Ts} & V_{Tb} & \Theta_T \end{pmatrix}, \tag{4.14}$$

which causes tree-level FCNCs in the interaction term $J^\mu_{W^3}Z_\mu$ in the up-type sector. The mixing matrix of the up-type quarks Ω contains the elements of the last column of matrix T^U_L

$$\Omega = \begin{pmatrix} 1-|\Theta_u|^2 & -\Theta_u\Theta_c^* & -\Theta_u\Theta_t^* & -\Theta_u\Theta_T^* \\ -\Theta_c\Theta_u^* & 1-|\Theta_c|^2 & -\Theta_c\Theta_t^* & -\Theta_c\Theta_T^* \\ -\Theta_t\Theta_u^* & -\Theta_t\Theta_c^* & 1-|\Theta_t|^2 & -\Theta_t\Theta_T^* \\ -\Theta_T\Theta_u^* & -\Theta_T\Theta_c^* & -\Theta_T\Theta_t^* & 1-|\Theta_T|^2 \end{pmatrix}. \tag{4.15}$$

The unitarity of the extended CKM matrix then implies that off-diagonal elements of Ω could be non-zero, e.g. $\Omega_{uc} \equiv -\Theta_u\Theta_c^* = V_{ud}V_{cd}^* + V_{us}V_{cs}^* + V_{ub}V_{cb}^* \neq 0$. The effects are encoded in Wilson coefficients C_9 and C_{10}. Relative to the negligible SM values, they are modified by the presence of an extra up-like quark:

$$V_{ub}V_{cb}^*\delta C_9 = \frac{4\pi}{\alpha}\Omega_{uc}(4\sin^2\theta_W - 1), \tag{4.16a}$$

$$V_{ub}V_{cb}^*\delta C_{10} = \frac{4\pi}{\alpha}\Omega_{uc}\,. \tag{4.16b}$$

The element Ω_{uc} of the up-type quark mixing matrix is constrained by the measurements of D^0–$\bar{D}^0$ mixing (4.1). Using expression $\Delta m_D = 2\times10^{-7}\,|\Omega_{uc}|^2$ GeV derived in [116], we find

$$\Omega_{uc} < 2.8\times10^{-4}\,. \tag{4.17}$$

4.4.3 MSSM

The leading contribution to $c\to u\ell^+\ell^-$ in MSSM with conserved R_p-parity comes from the gluino exchange diagram via virtual photon and could enhance $c\to u\ell^+\ell^-$ at small q^2. However, this enhancement is sizable only in vector decay channels, e.g. $D\to\rho\ell^+\ell^-$ [92], whereas gauge invariance cancels the $1/q^2$ behaviour as the decay to $D\to P\gamma$ with on-shell photon is forbidden. To clarify this, consider the amplitude for $D(p)\to P(p')\gamma^*(q,\epsilon)$ with virtual photon

$$\mathcal{A}_{D\to P\gamma^*} \sim A(q^2)\left[q^2(p+p')^\mu - (m_D^2 - m_P^2)q^\mu\right]\epsilon^*_\mu, \tag{4.18}$$

which, as written is gauge invariant and vanishes in the limit $q^2 \to 0$. Scalar function $A(q^2)$ summarizes hadronic form factors and is analytic at $q^2 = 0$. Replacing the photon polarization with propagator and coupling it to a lepton pair gives

$$\mathcal{A}_{D\to P\gamma^*\to P\ell\ell} \sim A(q^2)\left[q^2(p+p')^\mu - (m_D^2 - m_P^2)q^\mu\right]\frac{1}{q^2}\bar{u}(p_-)\gamma_\mu v(p_+) \tag{4.19}$$

$$\sim A(q^2)\bar{u}(p_-)(\not{p} + \not{p}')v(p_+), \tag{4.20}$$

where the term proportional to q^μ dropped out and the remaining term cancelled the $1/q^2$ enhancement. Consequently, penguin diagrams with gluino exchanges in MSSM can not produce interesting signatures in $D \to P\ell^+\ell^-$ and we will not pursue them any further.

4.4.4 $\not{R}_p$ violating MSSM

In MSSM with broken R_p-parity ($\not{R}_p$MSSM), the $c \to u\ell^+\ell^-$ process is mediated by the tree-level exchange of down squarks [92] (see the discussion about aspects of $\not{R}_p$MSSM in Section 3.2.3). The relevant trilinear interaction terms are contained in the superpotential [67]

$$\mathcal{L}_{\not{R}_p} \ni \lambda'_{ijk}\tilde{d}^*_{kR}\overline{(l_{iL})^c}u_{jL} + \text{H.c.}. \tag{4.21}$$

Integrating out the squarks leads to the effective four-fermion interaction

$$\mathcal{L}_{\text{eff}} = \sum_{k=1}^{3}\frac{\tilde{\lambda}'_{i2k}\tilde{\lambda}'^*_{i1k}}{2m^2_{\tilde{d}_{kR}}}(\bar{u}_L\gamma^\mu c_L)(\bar{\ell}_{iL}\gamma_\mu\ell_{iL}), \tag{4.22}$$

Note that down squark is a leptoquark with SM quantum numbers $(3, 1, -1/3)$ whose effects in a more general setting will be studied in the next section. The CKM-rotated couplings between the L, Q, and D supermultiplets in the superpotential are denoted [92]

$$\tilde{\lambda}'_{ijk} = \lambda'_{irs}\mathcal{U}^L_{rj}\mathcal{D}^{*R}_{sk}, \tag{4.23}$$

where $\mathcal{U}^L$ and $\mathcal{D}^R$ matrices transform the up-type left-handed quarks and down-type right-handed squarks from mass to weak basis, respectively. In the effective theory framework (4.10), the tree-level squark exchanges contribute in Wilson coefficients $C_{9,10}$ [103]

$$V^*_{cb}V_{ub}\delta C_9 = -V^*_{cb}V_{ub}\delta C_{10} = \frac{\sin^2\theta_W}{2\alpha^2}\sum_{k=1}^{3}\left(\frac{m_W}{m_{\tilde{d}_{kR}}}\right)^2\tilde{\lambda}'_{i2k}\tilde{\lambda}'^*_{i1k}, \tag{4.24}$$

where $i = 1$ (2) is relevant for the e^+e^- ($\mu^+\mu^-$) mode. The $\tilde{\lambda}'_{12k}$ and $\tilde{\lambda}'_{11k}$ have been constrained from tests of charged current universality and neutrinoless double β-decay searches [103, 129]

$$\tilde{\lambda}'_{11k} < 0.021\frac{m_{\tilde{d}}}{100\text{ GeV}}, \tag{4.25a}$$

$$\tilde{\lambda}'_{12k} < 0.043\frac{m_{\tilde{d}}}{100\text{ GeV}}. \tag{4.25b}$$

Taking into account (4.25a) we determine the maximum value of $\delta C^e_{9,10}$ to be

$$|V^*_{cb}V_{ub}\delta C^e_{9,10}| < 4. \tag{4.26}$$

Value of $\sum_k \tilde{\lambda}'_{22k}\tilde{\lambda}'_{21k}$ can be inferred from the experimental upper limit $\mathcal{B}(D^+ \to \pi^+\mu^+\mu^-) < 3.9 \times 10^{-6}$ [109]. The latter experimental bound is almost saturated with LD amplitude. Analysis is undertaken where we include in the amplitude both long distance SM and short distance $\not{R}_p$MSSM contributions in order to constrain the $\tilde{\lambda}'_{2xx}/m_{\tilde{d}}$ couplings.

4.4.5 Scalar leptoquark $(3, 1, -1/3)$

Interactions of the scalar Δ particle in the $(3, 1, -1/3)$ representation of the SM gauge group with SM fermions are

$$\mathcal{L}_\Delta = Y_L^{ij}\overline{Q^c_i}i\tau_2\Delta^* L_j + Y_R^{ij}\overline{u^c_{Ri}}\Delta^* e_{Rj} \tag{4.27}$$

Here we have restricted ourselves to the dimension-4 interactions. Doublets Q and L denote left-handed leptons and quarks in the mass basis, and we assigned the physical flavour rotations in the quark sector to down-type quarks

$$Q_i = \begin{pmatrix} u_i \\ V^{ij}d_j \end{pmatrix}, \tag{4.28}$$

where V is the CKM matrix. $Y_{L,R}$ are arbitrary matrices with i, j denoting generation indices, whereas $\psi^c \equiv C\bar{\psi}^T$ [1]. Omitted colour indices are contracted between quark and Δ fields, both of which are the fundamental (anti)triplets of $SU(3)_c$. Note that both Y_L and Y_R couple Δ to up-type quarks and charged leptons. Their contribution to the effective Lagrangian for the $c \to u\ell^+\ell^-$ decay is

$$V_{ub}V^*_{cb}\delta C_9 = -V_{ub}V^*_{cb}\delta C_{10} = \frac{\sin^2\theta_W}{2\alpha^2}\frac{m_W^2}{m_\Delta^2}Y_L^{2i}Y_L^{1i*}, \tag{4.29a}$$

$$V_{ub}V^*_{cb}\delta \tilde{C}_9 = V_{ub}V^*_{cb}\delta \tilde{C}_{10} = \frac{\sin^2\theta_W}{2\alpha^2}\frac{m_W^2}{m_\Delta^2}Y_R^{2i}Y_R^{1i*}, \tag{4.29b}$$

where $\tilde{C}_{9,10}$ are Wilson coefficients of the chirality flipped operators

$$\tilde{Q}_9 = (\bar{u}_R\gamma^\mu c_R)\,(\bar{\ell}\gamma_\mu\ell), \tag{4.30a}$$

$$\tilde{Q}_{10} = (\bar{u}_R\gamma^\mu c_R)\,(\bar{\ell}\gamma_\mu\gamma_5\ell). \tag{4.30b}$$

Comparison of (8.28) and (4.24) suggests that the $\not{R}_p$MSSM model can be embedded into the LQ model if one sets $Y_L^{2i}Y_L^{1i*}/m_\Delta^2 \to \sum_k \tilde{\lambda}'_{i2k}\tilde{\lambda}'^*_{i1k}/m^2_{\tilde{d}_{kR}}$. As the right-handed down-type squarks $\tilde{d}_{kR}$ have the quantum numbers of Δ they act as leptoquarks with exclusively left-handed couplings. In addition to $Q_{9,10}$ and $\tilde{Q}_{9,10}$, Δ exchange induces scalar (S) and tensor (T) operators

$$\begin{aligned}\mathcal{L}^{ST}_{\text{eff}} =& \frac{Y_L^{2i}Y_R^{1i*}}{2m_\Delta^2}\left[-(\bar{u}_R c_L)\,(\bar{\ell}_R\ell_L) + (\bar{u}\sigma^{\mu\nu}c)\,(\bar{\ell}_R\sigma_{\mu\nu}\ell_L)\right] \\ &+ \frac{Y_R^{2i}Y_L^{1i*}}{2m_\Delta^2}\left[-(\bar{u}_L c_R)\,(\bar{\ell}_L\ell_R) + (\bar{u}\sigma^{\mu\nu}c)\,(\bar{\ell}_L\sigma_{\mu\nu}\ell_R)\right].\end{aligned} \tag{4.31}$$

[1] For charge conjugation matrix we take $C = i\gamma^2\gamma^0$.

Their contribution is small because new upper bounds [130] of leptonic branching fractions

$$\mathcal{B}(D^0 \to e^+e^-) < 7.9 \times 10^{-8}, \tag{4.32a}$$

$$\mathcal{B}(D^0 \to \mu^+\mu^-) < 1.4 \times 10^{-7}, \tag{4.32b}$$

put strong constraints on the mixed helicity products of couplings $Y_R^{2i}Y_L^{1i*}$, $Y_L^{2i}Y_R^{1i*}$. Namely, saturating the above branching fractions with pure Δ exchange

$$\Gamma^{\Delta}_{D^0\to\ell^+\ell^-} = \frac{f_D^2 m_{D_0}^5}{256\pi m_c^2} \frac{|Y_L^{2i}Y_R^{1i}|^2 + |Y_R^{2i}Y_L^{1i}|^2}{m_\Delta^4}, \tag{4.33}$$

where we use $f_D = 206$ MeV [131], $m_c = 1.25$ GeV, and $m_\ell = 0$, to find bounds

$$\frac{|Y_{L(R)}^{21}Y_{R(L)}^{11}|}{(m_\Delta/100\text{ GeV})^2} < 1.2 \times 10^{-4}, \tag{4.34a}$$

$$\frac{|Y_{L(R)}^{22}Y_{R(L)}^{12}|}{(m_\Delta/100\text{ GeV})^2} < 1.6 \times 10^{-4}, \tag{4.34b}$$

which apply for the couplings to electrons (4.34a) and muons (4.34b). SM contribution is of the order 10^{-13} [92] and thus negligible with respect to the bounds (4.32). Clearly the products of the same helicity couplings Y_RY_R or Y_LY_L contribute to $D^0 \to \ell^+\ell^-$ width with helicity suppression factor m_ℓ^2. Thus $\mathcal{B}(D^0 \to \ell^+\ell^-)$ is not a good probe of those coupling combinations.

On the other side, in the $D^+ \to \pi^+\ell^+\ell^-$ all terms of (8.28) and (4.31) contribute. Differential decay width can be written in a quite compact way

$$\begin{aligned}\frac{\mathrm{d}^2\Gamma_{D^+\to\pi^+\ell^+\ell^-}}{\mathrm{d}q^2\,\mathrm{d}t} = \frac{1}{(16\pi m_D)^3 m_\Delta^4}\Bigg[&\left(\left|Y_L^{2i}Y_L^{1i}\right|^2 + |Y_R^{2i}Y_R^{1i}|^2\right) F_+^2(q^2)(q^2-m_D^2)^2 \\ &+ \left(|Y_L^{2i}Y_R^{1i}|^2 + |Y_R^{2i}Y_L^{1i}|^2\right)\left(s(q^2)(m_D^2 - m_\pi^2 - q^2 - 2t) + \frac{m_D^2}{m_c}F_0(q^2)\right)^2 q^2\Bigg].\end{aligned} \tag{4.35}$$

We have set $m_\ell = 0$ and introduced $t = (p' + p_+)^2$. For matrix elements of scalar operators the QCD equations of motion (3.33) are used (3.34). Note that the decay spectrum is independent of possible phases contained in Y matrices. We will in the following set to zero products of type $Y_{L(R)}Y_{R(L)}$ as they are too strongly constrained by leptonic decay branching fractions (4.34).

4.4.6 $D_{(s)} \to \pi\,(K)$ form factors

Evaluating the matrix elements of operators $Q_{7,9,10}$ requires the knowledge of vector and tensor form factors of $D \to P$ transition:

$$\begin{aligned}\left\langle P(p')\,\middle|\,\bar{u}\gamma^\mu(1-\gamma_5)c\,\middle|\,D(p)\right\rangle =& F_+(q^2)\left[(p+p')^\mu - \frac{m_D^2 - m_P^2}{q^2}q^\mu\right] \\ &+ F_0(q^2)\frac{m_D^2 - m_P^2}{q^2}q^\mu,\end{aligned} \tag{4.36}$$

$$\left\langle P(p')\,\middle|\,\bar{u}\sigma^{\mu\nu}(1\pm\gamma_5)c\,\middle|\,D(p)\right\rangle = is(q^2)\left[(p+p')^\mu q^\nu - q^\mu(p+p')^\nu \pm i\epsilon^{\mu\nu\alpha\beta}(p+p')_\alpha q_\beta\right], \tag{4.37}$$

where P denotes π^+ (K^+) in the case of D^+ (D_s^+) decay. Momentum transfer $q = p - p'$ equals momentum of the lepton pair. For the F_+ form factor we use the double pole parameterization [132] of the analysis performed in the heavy meson chiral perturbation theory [133]

$$F_+(q^2) = \frac{F_+(0)}{(1 - q^2/m_{D^*}^2)(1 - aq^2/m_{D^*}^2)}, \tag{4.38}$$

with values $F_+(0) = 0.54$ (0.62) for the $D \to \pi$ ($D_s \to K$) transitions, whereas we fix $a = 0.58$ for both cases [133]. The latter parameter was determined also in the experimental analyses of $D \to P\ell\nu$ decays with the result $a = 0.52(10)$ (c.f. [134] and references therein). Lattice simulation, on the other hand provided $a = 0.44(4)$ [135]. We approximate the tensor form factor $s(q^2)$ by $F_+(q^2)/m_D$ which is valid in the limit of heavy c quark and zero recoil limit [136]. Finally, expression for the SD amplitude of $c \to u\ell^+\ell^-$ decay is

$$\begin{aligned}\mathcal{A}_{\rm SD} = -i\frac{4\pi\alpha G_F}{\sqrt{2}}\lambda_b \Bigg[&\frac{C_{10}^{\rm eff}}{16\pi^2}\bar{u}(p_-)\not{p}\gamma_5 v(p_+) + \\ &+ \left(\frac{C_7^{\rm eff}}{2\pi^2}\frac{m_c}{m_D} + \frac{C_9^{\rm eff}}{16\pi^2}\right)\bar{u}(p_-)\not{p}v(p_+)\Bigg] F_+(q^2).\end{aligned} \tag{4.39}$$

Momenta p, p_+ and p_- belong to the decaying D (D_s) meson and the leptons in the final state, respectively. We neglect the lepton masses in our further study.

4.5 Long distance contributions in $D \to P\ell^+\ell^-$

The dominant short distance part of the SM amplitude is generated by the operator Q_2 and the light quark loops accompanied by the virtual gluon. In addition to SD, poles in momentum transfer q^2 may appear due to bound (quasi)stable states of QCD, whose properties are governed by nonperturbative QCD. The background they produce is crucial for isolating short distance physics in semileptonic decays $D \to P\ell^+\ell^-$. Following procedure described in [94] we model the LD contributions with vector resonances V of appropriate quantum numbers. D meson first weakly decays to P and a neutral vector meson V, followed by decay of $V \to \ell^+\ell^-$. Weak nonleptonic decay is controlled by the $Q_{1,2}$ operators of (4.10), which are, after Fierz transforming the operator with color non-singlet currents Q_1

$$\begin{aligned}\mathcal{L}_{\rm nonlep} = -\frac{G_F}{\sqrt{2}}\sum_{q=d,s} V_{uq}V_{cq}^* \,[&a_1\bar{u}\gamma^\mu(1-\gamma_5)q\,\bar{q}\gamma_\mu(1-\gamma_5)c \\ &+a_2\bar{u}\gamma^\mu(1-\gamma_5)c\,\bar{q}\gamma_\mu(1-\gamma_5)q]\end{aligned} \tag{4.40}$$

The effective Wilson coefficients of naïve factorization on the scale $m_c = 1.25$ GeV are [73, 103]

$$a_1 = 1.26 \pm 0.10, \quad a_2 = -0.49 \pm 0.15. \tag{4.41}$$

The flavour structure of (4.40) allows intermediate resonance V to be either ρ, ω or ϕ. Since branching fractions of separate stages in the cascade are well measured,

we shall not use a factorization approximation (4.40,4.41) but will instead make use of currently available experimental data. Resonant decay spectrum must contain a pole due to intermediate resonance [137, 138]

$$\frac{\mathrm{d}\Gamma}{\mathrm{d}q^2}(D \to KV \to K\ell^+\ell^-) = \frac{1}{\pi}\Gamma_{D\to PV}(q^2)\frac{\sqrt{q^2}}{(m_V^2 - q^2)^2 + m_V^2\Gamma_V^2}\Gamma_{V\to\ell^+\ell^-}(q^2). \tag{4.42}$$

Here $\Gamma_{D\to KV}(q^2)$ and $\Gamma_{V\to\ell^+\ell^-}$ would be decay rates if mass of V were $\sqrt{q^2}$ and these rates are known experimentally at $q^2 = m_V^2$. Since the resonances $V = \rho, \omega, \phi$ are relatively narrow ($\Gamma_V \ll m_V$) the narrow width (NW) approximation holds

$$\mathcal{B}\left[D \to PV \to P\ell^-\ell^+\right] \simeq \mathcal{B}\left[D \to PV\right] \times \mathcal{B}\left[V \to \ell^-\ell^+\right]. \tag{4.43}$$

The Breit-Wigner resonant amplitude that reproduces the above behaviour (4.43) is then

$$\mathcal{A}^{\mathrm{LD}}\left[D \to KV \to K\ell^-\ell^+\right] = e^{i\phi_V}\frac{a_V}{q^2 - m_V^2 + im_V\Gamma_V}\,\bar{u}(p_-)\not{p}\,v(p_+). \tag{4.44}$$

In the NW approximation the a_V coefficient dependence on q^2 is irrelevant and we assume a_V to be free parameters. We included phase ϕ_V explicitly, so that individual a_V are positive. Equivalent description of the long distance amplitude was used in [92, 103] where they instead included it in the C_9^{eff} coefficient.

4.5.1 $D^+ \to \pi^+\ell^+\ell^-$

Right-hand side of (4.43) are measured experimental branching fractions (Table 4.2) which in turn fix the parameters a_V of (4.44). Decay mode $D^+ \to \pi^+\omega$ has not been

decay channel	$D^+ \to \pi^+\rho$	$D^+ \to \pi^+\omega$	$D^+ \to \pi^+\phi$
$\mathcal{B}\,[10^{-3}]$	0.82 ± 0.15	< 0.34	5.53 ± 0.24

Table 4.2: Branching ratios of decays of D^+ meson to the intermediate resonant states [28].

decay channel	$\rho \to e^+e^-$	$\omega \to e^+e^-$	$\phi \to e^+e^-$
$\mathcal{B}\,[10^{-5}]$	4.7	7.3	30

Table 4.3: Branching ratios of vector resonances decays to lepton pairs [28].

measured yet, but we can relate a_ω and its phase to the well measured contribution of the ρ resonance relying on the underlying nonleptonic weak Lagrangian (4.40) as in [94]. Relative phases and magnitudes of the resonances can be derived by considering the flavour structure of nonleptonic weak Lagrangian (4.40) and electromagnetic coupling of V resonance to photon. The flavour structure of the resonances then determines relative sizes and phases of resonant amplitudes. Detailed analysis has already been done in [94], where the relative phases of ρ and ω contributions were found to be opposite in sign, while for the ratio of their magnitudes it was

found $a_\omega/a_\rho = 1/3$. Also the phases of ρ and ϕ are opposite. Thus we get for the final LD amplitude

$$\mathcal{A}^{\mathrm{LD}} = \left[a_\rho \left[\mathrm{BW}(q^2,\rho) - \frac{1}{3}\mathrm{BW}(q^2,\omega)\right] - a_\phi\,\mathrm{BW}(q^2,\phi)\right] \bar{u}(p_-)\not{p}\,v(p_+), \qquad (4.45)$$

with individual contributions $a_\rho = (2.6 \pm 0.2) \times 10^{-9}$ and $a_\phi = (4.0 \pm 0.2) \times 10^{-9}$, where uncertainties are estimated from the experimental ones. We have defined

$$\mathrm{BW}(q^2, V) \equiv (q^2 - m_V^2 + i m_V \Gamma_V)^{-1}. \qquad (4.46)$$

4.5.2 $D_s^+ \to K^+\ell^-\ell^+$

In this case only the branching ratio of $D_s^+ \to K^+\rho$ is known (see Table 4.4). Contributions of ρ and ω are related like in the case of D^+ meson, namely $a_\omega/a_\rho =$

decay channel	$D_s^+ \to K^+\rho$	$D_s^+ \to K^+\omega$	$D_s^+ \to K^+\phi$
$\mathcal{B}\,[10^{-3}]$	2.7 ± 0.5	—	< 0.28

Table 4.4: Branching ratios of D_s^+ meson to the intermediate resonant state [28].

1/3 with relative minus sign between the two amplitudes. In the same way as for the D decays, we determine $a_\rho = 7.1 \times 10^{-9}$. However, we cannot determine the a_ϕ in the same manner due to unknown width of $D_s \to K\phi$. Consequently, the total LD amplitude for resonant decay $D_s \to VK \to K\ell^+\ell^-$ is a sum of two terms:

$$\mathcal{A}^{\mathrm{LD}} = a_\rho \left[\mathrm{BW}, (q^2,\rho) - \frac{1}{3}\mathrm{BW}(q^2,\omega)\right] \bar{u}(p_-)\not{p}\,v(p_+) + \mathcal{A}_\phi^{\mathrm{LD}}. \qquad (4.47)$$

Last term of above amplitude can be calculated in the factorization approximation using the nonleptonic weak Lagrangian (4.40), which determines the width of $D_s \to K\phi$. Both a_1 and a_2 parts of (4.40) can generate the flavour quantum numbers of ϕ and K^+. The a_1 part connects initial D_s^+ state to ϕ through a charged current $(\bar{s}c)_{V-A}$, while the $(\bar{u}s)_{V-A}$ creates the K^+ out of vacuum. Neutral currents, namely the a_2 part, act in the following way: $D_s^+ \to K^+$ and $0 \to \phi$. Subsequent decay $\phi \to \ell^+\ell^-$ is measured (Table 4.3). The resulting ϕ contribution to the LD amplitude in the factorization approximation is

$$\begin{aligned}\mathcal{A}_\phi^{\mathrm{LD}} = i\frac{4\pi\sqrt{2}}{3} G_F V_{us} V_{cs}^* \alpha \frac{g_\phi}{q^2(q^2 - m_\phi^2 + i m_\phi \Gamma_\phi)} \\ \times \left[a_1 m_\phi f_K A_0(m_K^2) + a_2 g_\phi f_+(q^2)\right] \bar{u}(p_-)\not{p} v(p_+). \end{aligned} \qquad (4.48)$$

where g_ϕ is a ϕ decay constant, defined as

$$\langle 0 \,|\, \bar{s}\gamma^\mu s \,|\, \phi(q,\epsilon)\rangle = g_\phi \epsilon^\mu, \qquad g_\phi = 0.233\ \mathrm{GeV}^2. \qquad (4.49)$$

Value of g_ϕ is determined from $\Gamma_{\phi\to e^+e^-}$

$$\Gamma_{\phi\to e^+e^-} = \frac{4\pi g_\phi^2 \alpha^2}{27 m_\phi^3}, \qquad (4.50)$$

the value of which is taken from [28]. Transition $D_s^+ \to \phi$ is parametrized by the form factor A_0 (see Section 2.3.1) whose shape we take from [139].

4.6 Decay spectra and widths of $D_{(s)} \to \pi(K)\ell^+\ell^-$

From the point of view of resonances it is by far most convenient to show spectra in variable q^2, where one can isolate the resonance dominated region. Using the combined approach described in the previous section, where we account for the SD and resonant LD dynamics, we now show the impact of SD physics on decay spectra with respect to LD resonant background. Since the SD contribution of SM and MSSM is completely overshadowed by LD, we will only estimate the experimental prospects for discovering or constraining EQS and $\not{R}_p$MSSM models. Current constraints on EQS model coming from the D^0–$\bar{D}^0$ mixing already indicate only minor role in the total decay width. On the other hand, the contribution of $\not{R}_p$MSSM model is still allowed by existing constraints to show up in the nonresonant part of the decay spectrum. When deriving the upper bounds for the underlying parameters of $\not{R}_p$MSSM model we always vary free phases in the Lagrangian as to achieve the most conservative constraint.

4.6.1 $D^+ \to \pi^+\ell^+\ell^-$

decay	experiment	res.	EQS	res.+$\not{R}_p$MSSM/LQ
$D^+ \to \pi^+e^+e^-$	$< 7.4 \times 10^{-6}$	1.7×10^{-6}	$< 1.3 \times 10^{-9}$	$< 4.2 \times 10^{-6}$
$D^+ \to \pi^+\mu^+\mu^-$	$< 3.9 \times 10^{-6}$	1.7×10^{-6}	$< 1.6 \times 10^{-9}$	constraint on λ'

Table 4.5: Comparison of experimental branching fractions with predictions for branching fractions of $D^+ \to \pi^+\ell^+\ell^-$ decay. In the last three columns, separate predictions of resonant amplitude, short distance EQS amplitude, and the total amplitude in the $\not{R}_pMSSM$ or LQ case, are given.

Branching fractions are listed in Table 4.5. Clearly, the EQS model is already too stringently constrained from D^0–$\bar{D}^0$ mixing and measuring the $D \to P\ell^+\ell^-$ cannot bring any further information with current experimental sensitivities (Figure 4.2).

On the other hand, relevant couplings for the electron final states in the $\not{R}_p$MSSM are already constrained (4.25a) and moderately increase the branching ratio almost to the upper experimental bound. Deviation from the LD amplitude is pronounced in the nonresonant region, either at $q^2 < m_\rho^2$ or $q^2 > m_\phi^2$ (Figure 4.3). However, the most promising mode is the channel with muons. The LD contribution (1.7×10^{-6}) is at par with the experimental upper bound 3.9×10^{-6} and should be combined together with the SD part to derive constraints on the Wilson coefficients. The bound we obtained by saturating the experimental bound entirely with $\not{R}_p$MSSM contributions was $|V_{cb}^* V_{ub} C_{9,10}^\mu| < 18$, whereas more stringent bound resulted after we included resonant amplitude in the analysis:

$$|V_{cb}^* V_{ub} C_{9,10}^\mu| < 14. \tag{4.51}$$

The latter bound is the most conservative with respect to the unknown phase of λ' couplings. Although the inclusion of the LD term does not make substantial difference in resulting bound, it should be included as the experiment will eventually measure a signal with branching fraction of the order 1.7×10^{-6}. All the branching

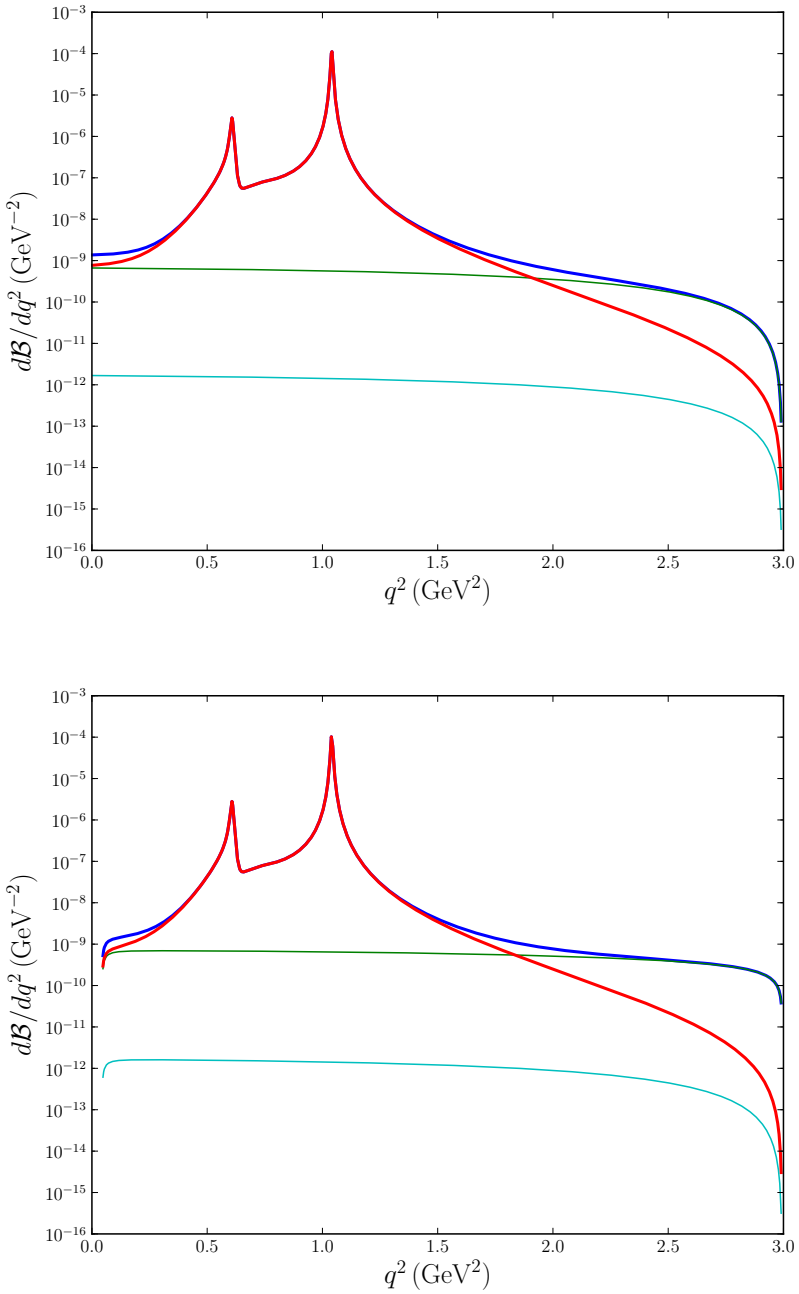

Figure 4.2: Distributions of the branching fractions in the EQS model for the decay channels $D^+ \to \pi^+ e^+ e^-$ (top) and $D^+ \to \pi^+ \mu^+ \mu^-$ (bottom). Blue line represents the combined resonant and EQS contribution, with EQS mixing matrix element Ω_{uc} constrained from D^0–$\bar{D}^0$ mixing (4.17). Red, green, and light blue lines show individual contributions of resonances, short distance EQS, and short distance SM, respectively.

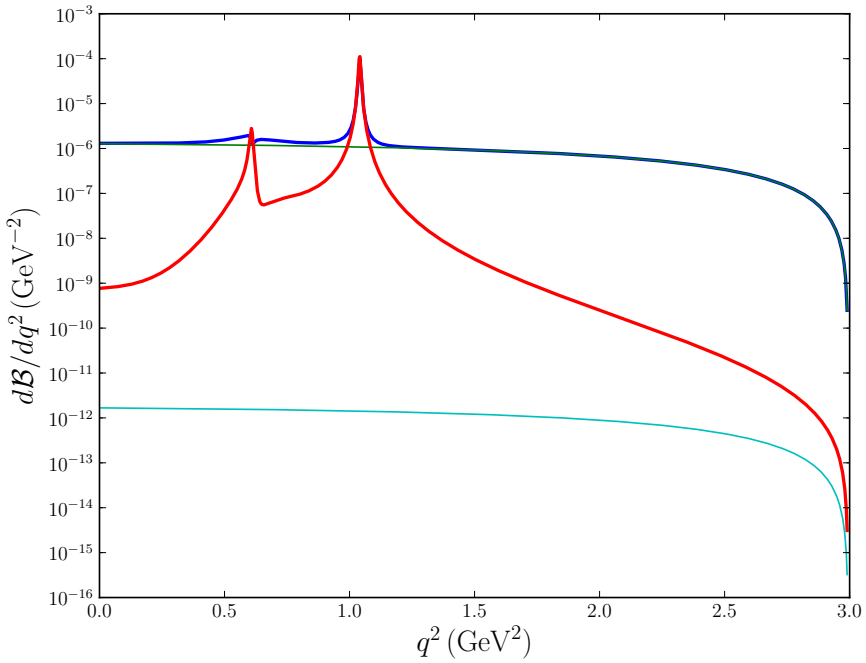

Figure 4.3: Distributions of branching fractions in the $\not{R}_p$MSSM model for the decay mode $D^+ \to \pi^+ e^+ e^-$. Blue line represents total contributions of resonances and $\not{R}_p$MSSM with parameters $\lambda'_{12k}/m_{\tilde{d}}$, $\lambda'_{11k}/m_{\tilde{d}}$ constrained from charged current universality and neutrinoless double β-decay (4.25a). Red, light blue, and green lines show separate contributions of resonances, SM short distance amplitude, and $\not{R}_p$MSSM, respectively.

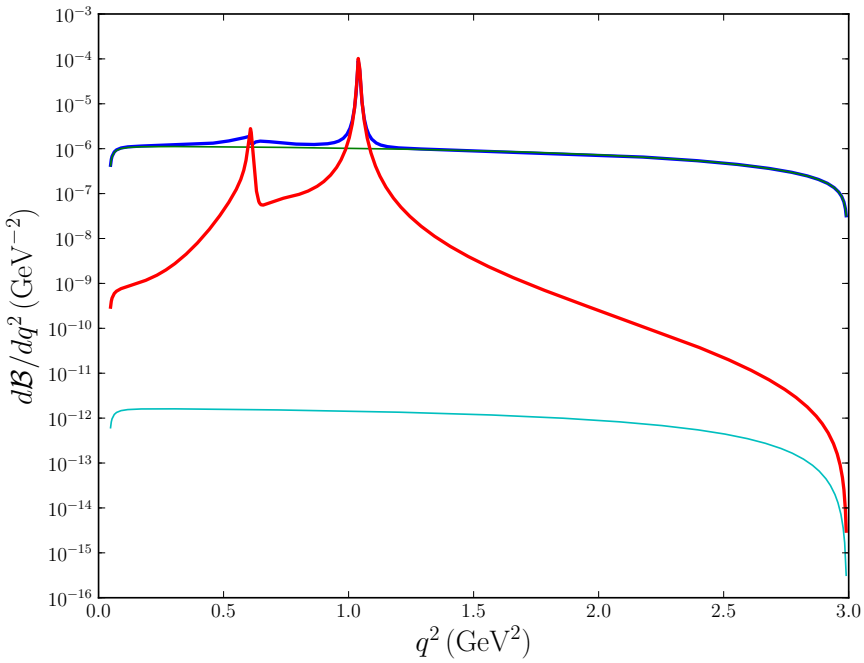

Figure 4.4: Distributions of the branching fractions in the $\not{R}_p$MSSM model for the decay mode $D^+ \to \pi^+\mu^+\mu^-$. Blue line represents total contributions of resonances and $\not{R}_p$MSSM with parameters $\lambda'_{22k}/m_{\tilde{d}}$, $\lambda'_{21k}/m_{\tilde{d}}$ adjusted as to saturate the experimental upper bound (4.2b). Red, light blue, and green lines show separate contributions of resonances, SM short distance, and $\not{R}_p$MSSM contributions, respectively.

ratios within the $\not{R}_p$MSSM model with muons in the final state (Tables 4.5, 4.6) and their kinematical distributions (Fig. 4.4,4.7) are calculated using the bound (4.51).

In the singlet leptoquark framework the couplings $Y^{2i}_{L,R}$ and $Y^{1i}_{L,R}$, with i denoting the lepton flavour, result in various terms, contributing to $D^+ \to \pi^+\ell^+\ell^-$. In the leading order, we only consider the resonant amplitude and its interference with the LQ amplitude, while dropping the LQ amplitude squared. The decay spectrum of intereference terms is

$$\frac{\mathrm{d}\Gamma^{\mathrm{LQinterf.}}_{D\to\pi\ell^+\ell^-}}{\mathrm{d}q^2} = \frac{1}{3(8\pi)^3 m_D^3}\left[((m_D+m_\pi)^2-q^2)((m_D-m_\pi)^2-q^2)\right]^{3/2} \times \Im\left[X_{\mathrm{res.}}(q^2)\frac{Y^{2i}_L Y^{1i*}_L + Y^{2i}_R Y^{1i*}_R}{m^2_\Delta}\right] \tag{4.52}$$

where a resonant shape was introduced

$$X_{\mathrm{res.}} = \left[a_\rho\left[\mathrm{BW}(q^2,\rho) - \frac{1}{3}\mathrm{BW}(q^2,\omega)\right] - a_\phi\,\mathrm{BW}(q^2,\phi)\right]. \tag{4.53}$$

Spectrum (4.52) depends only on sum of the products of couplings of the same chirality, namely $Y_L Y_L^*$ or $Y_R Y_R^*$. However, when trying to impose a limit on this particular combination by requiring $0 < \mathcal{B}(Y) < \mathcal{B}_{\mathrm{experiment}}$, where $\mathcal{B}(Y)$ denotes the branching fraction without the LQ amplitude squared, we find no limit on $|Y^{2i}_L Y^{1i*}_L + Y^{2i}_R Y^{1i*}_R|$. So it happens that there exist a special direction in complex plane of parameters, where a large cancellation of phases takes place between LQ couplings and the resonant amplitudes. The allowed region is shown on Figures 4.5 with blue triangles. It is clear however, that in regions where the LQ couplings get large, one should also include the LQ amplitude squared

$$\frac{\mathrm{d}\Gamma^{\mathrm{LQ}}_{D\to\pi\ell^+\ell^-}}{\mathrm{d}q^2} = \frac{1}{(16\pi m_D)^3}\left(\left|\frac{Y^{2i}_L Y^{1i}_L}{m^2_\Delta}\right|^2 + \left|\frac{Y^{2i}_R Y^{1i}_R}{m^2_\Delta}\right|^2\right) \times F_+^2(q^2)(m_D^2-q^2)^2\left[((m_D+m_\pi)^2-q^2)((m_D-m_\pi)^2-q^2)\right]^{1/2}. \tag{4.54}$$

We have not included the terms with mixed chirality $Y_{L(R)}Y_{R(L)}$ due to very strong constraints (4.34). Note the parabolic shape of (4.54) which admits no cancellations between $Y^{2i}_L Y^{1i}_L$ and $Y^{2i}_R Y^{1i}_R$ and therefore the flat direction (blue triangles on Figure 4.5) will not be allowed anymore. Instead we get a bounded region of allowed couplings shown with red circles on Figure 4.5. Derived bounds are complementary to those coming from $\mathcal{B}(D^0 \to \ell^+\ell^-)$ (4.34)

$$\frac{\left|Y^{21}_{L(R)}Y^{11*}_{L(R)}\right|}{(m_\Delta/100\ \mathrm{GeV})^2} < 1.6\times10^{-3}, \tag{4.55a}$$

$$\frac{\left|Y^{22}_{L(R)}Y^{12*}_{L(R)}\right|}{(m_\Delta/100\ \mathrm{GeV})^2} < 1.0\times10^{-3} \tag{4.55b}$$

4.6.2 $D_s^+ \to K^+\ell^+\ell^-$

Current experimental bounds of $D_s^+ \to K^+\ell^+\ell^-$ cannot compete with the bounds from D^0–$\bar{D}^0$ (4.17) mixing, charged current universality, neutrinoless double β-decay

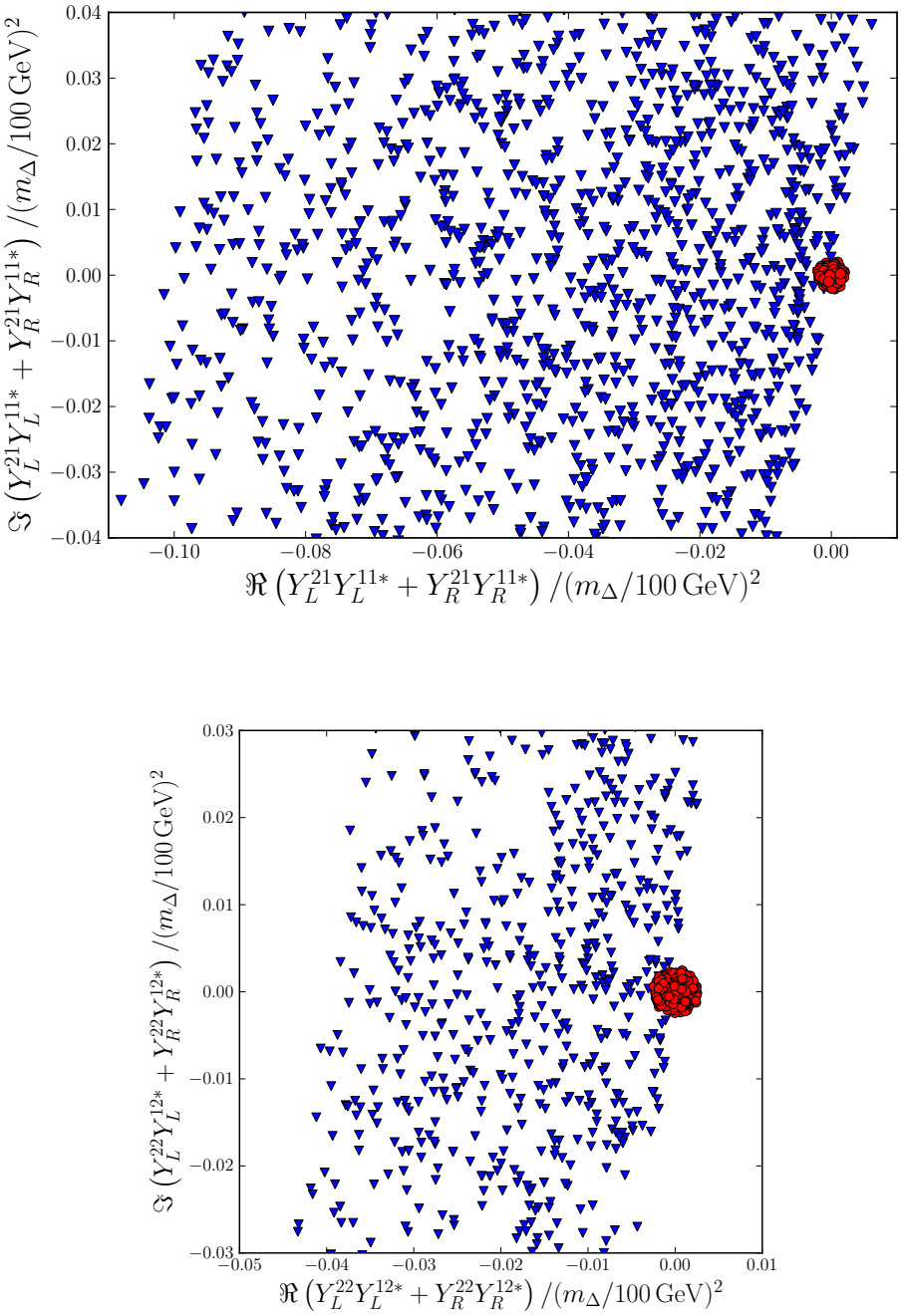

Figure 4.5: Allowed region for couplings of the singlet leptoquark scenario, where, (i) only the interference term was considered (blue triangles), or, (ii) entire leptoquark contributions taken into account (red circles), for the semileptonic decays to electrons (above) and muons (below).

(4.25a), or $D^+ \to \pi^+\mu^+\mu^-$ decay (4.51) and we use all those processes as input to decay process $D_s \to K\ell^+\ell^-$. The branching fractions contributions are summarized in Table 4.6. Again, the EQS model has negligible effect (Figure 4.6). $\not{R}_p$MSSM has notable effect, especially in the $\mu^+\mu^-$ mode, where it increases branching ratio by an order of magnitude (Figure 4.7). In this case, $\not{R}_p$MSSM contributions overshadows the LD contribution throughout the phase space, except in the close vicinity of the resonant peaks.

decay	experiment	res.	EQS	res. + $\not{R}_p$MSSM/LQ
$D_s^+ \to K^+e^+e^-$	$< 1.6 \times 10^{-3}$	6.0×10^{-7}	$< 3.4 \times 10^{-10}$	$< 1.9 \times 10^{-6}$
$D_s^+ \to K^+\mu^+\mu^-$	$< 2.6 \times 10^{-5}$	6.0×10^{-7}	$< 3.8 \times 10^{-10}$	$< 1.8 \times 10^{-6}$

Table 4.6: Comparison of experimental branching fractions with predictions for branching fractions of $D_s^+ \to K^+\ell^+\ell^-$ decay. In the last three columns, separate predictions for the resonant amplitude, short distance EQS amplitude, and total resonant amplitude including the $\not{R}_p$MSSM or LQ contributions, are given.

4.7 Summary

Recently measured D^0–$\bar{D}^0$ mass difference constrains the value of tree-level flavour changing neutral coupling $c \to uZ$, which is present in the models with an additional singlet up-type quark. We have studied the impact of this coupling on rare $D^+ \to \pi^+\ell^+\ell^-$ and $D_s^+ \to K^+\ell^+\ell^-$ decays, where its effects are accompanied by the long distance contributions. Long distance contributions in $D_s^+ \to K^+\ell^+\ell^-$ have been assessed following the same phenomenologically inspired model as it has been done previously in the case of $D^+ \to \pi^+\ell^+\ell^-$. The constraint coming from D^0–$\bar{D}^0$ mixing render the effects of additional singlet up-type quark to be too small to be seen in dilepton invariant mass spectra of either decay mode. In a previous study [94] forward-backward asymmetry in $D^0 \to \rho^0\ell^+\ell^-$ was considered and very small effect was found. New constraint reduces that asymmetry even more, making it insignificant for the experimental searches.

Present constraints on mass insertions in MSSM with conserved R_p-parity still allow for increase of $c \to u\gamma$ rate by one order of magnitude. For this reason MSSM could significantly increase $c \to u\ell^+\ell^-$ rate at small lepton invariant mass q^2. However, this MSSM enhancement is not drastic in D decays, since $D \to V\gamma$ and $D \to V\ell^+\ell^-$ have large long distance contributions in the small q^2 region, while $D \to P\ell^+\ell^-$ rate is multiplied by factor of q^2 owing to gauge invariance.

The remaining possibility to search for new physics in rare D decays is offered by the MSSM models which contain R_p-parity violating terms or in a more general model with scalar weak singlet leptoquark. We have found new bounds on the combinations of these parameters in $D^+ \to \pi^+\ell^+\ell^-$ by including the long distance effects. Using current upper bound on the width of $D^+ \to \pi^+\mu^+\mu^-$ decay we derive

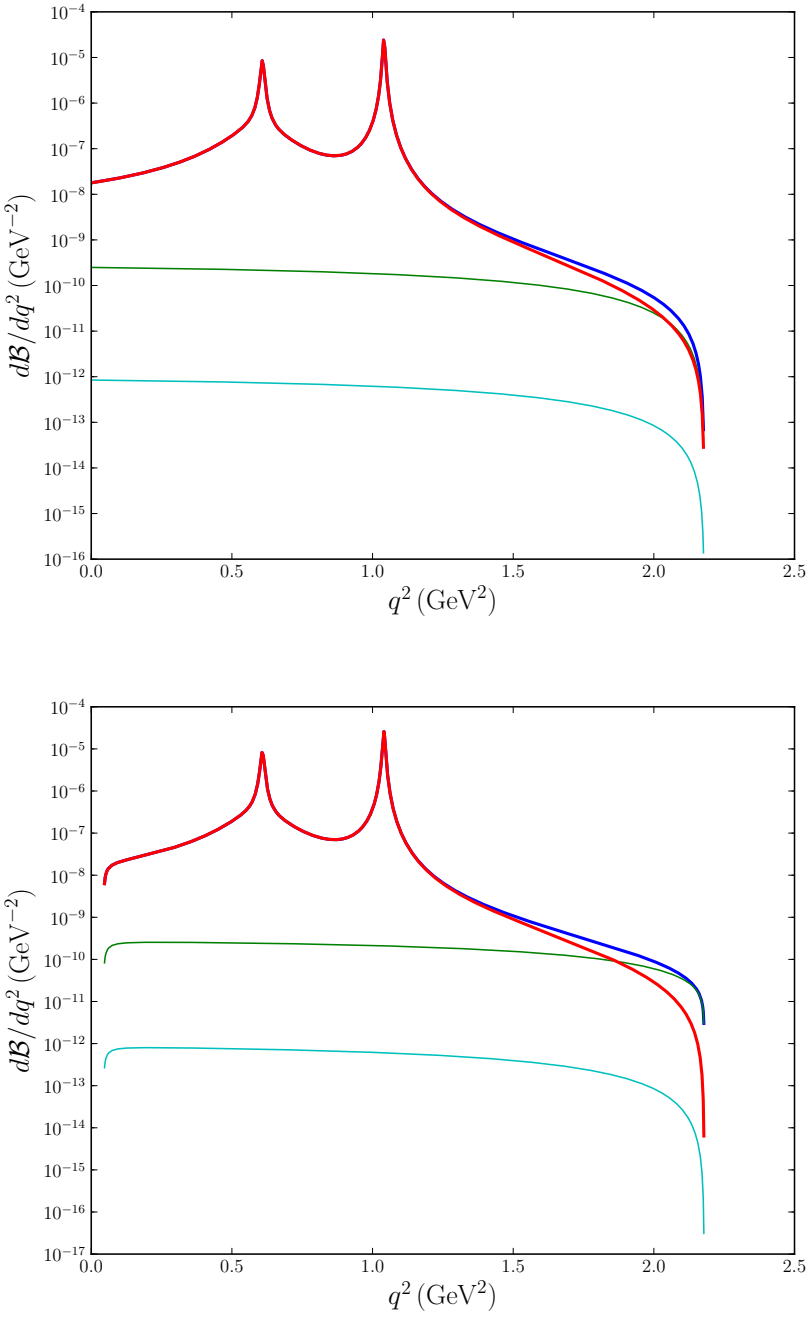

Figure 4.6: Distributions of branching ratios in the EQS model for the decay modes $D_s^+ \to K^+e^+e^-$ (top) and $D_s^+ \to K^+\mu^+\mu^-$ (bottom). Blue line represents the combined LD and SD contributions. Red line represents the resonant contributions, whereas green and light blue lines are the pure short distance spectra of EQS model and the SM.

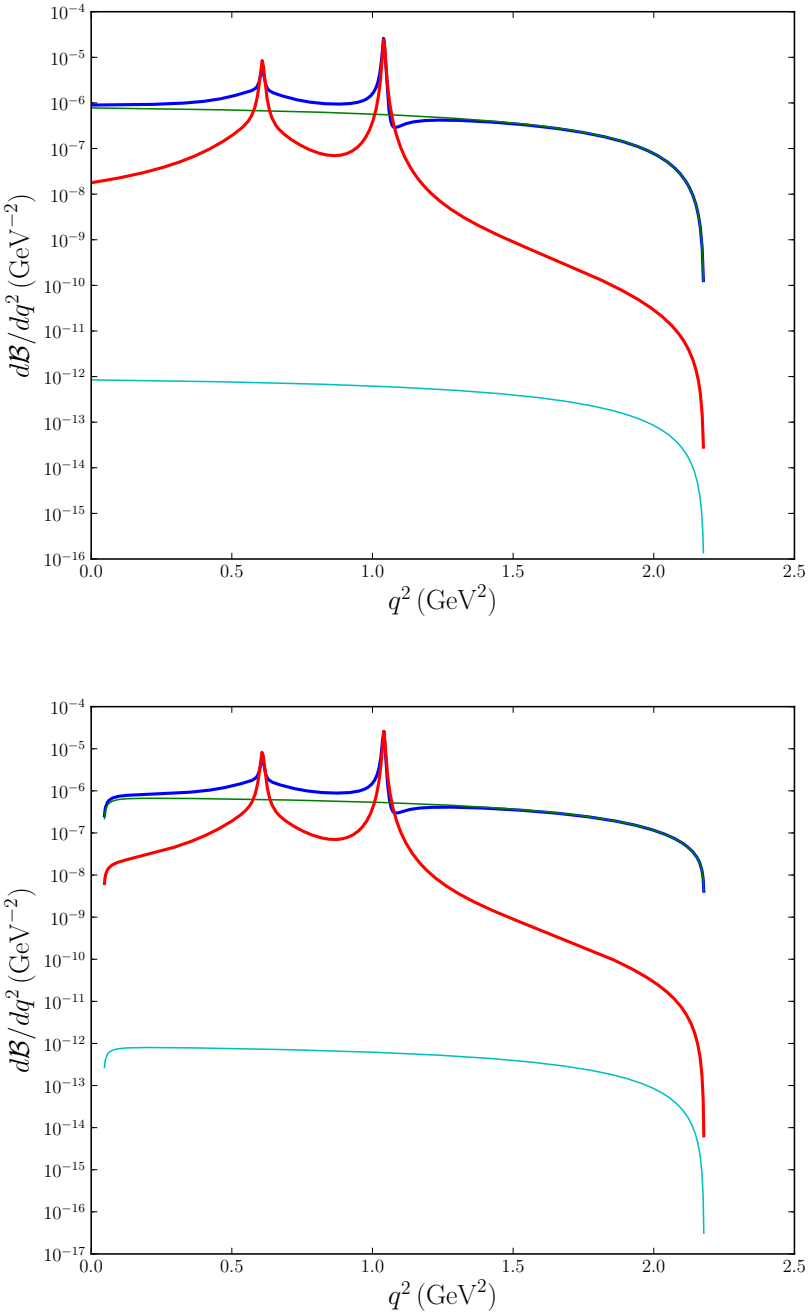

Figure 4.7: Distributions of the branching ratios in the $\not{R}_p$MSSM model for the decay modes $D_s^+ \to K^+e^+e^-$ (top) and $D_s^+ \to K^+\mu^+\mu^-$ (bottom). Blue line represents combined LD and SD contributions. Red line represent the resonant contributions, whereas green and light blue lines are the pure SD spectra of the EQS model and the SM.

limits for the couplings of a weak singlet leptoquark model

$$\frac{\left|Y^{21}_{L(R)}Y^{11*}_{L(R)}\right|}{(m_\Delta/100\ \text{GeV})^2} < 1.6\times 10^{-3}, \tag{4.56a}$$

$$\frac{\left|Y^{22}_{L(R)}Y^{12*}_{L(R)}\right|}{(m_\Delta/100\ \text{GeV})^2} < 1.0\times 10^{-3}. \tag{4.56b}$$

Second bound applies also for the R_p-violating MSSM, namely

$$\sum_{k=1}^{3}\frac{\left|\tilde{\lambda}'_{22k}\tilde{\lambda}'^{*}_{21k}\right|}{(m_{\tilde{d}_{kR}}/100\ \text{GeV})^2} < 1.0\times 10^{-3}. \tag{4.57}$$

Since at Belle 2 there are plans to investigate rare D decays [140] we have used upper bounds (4.56b), (4.57), and calculated the dilepton invariant mass spectrum for the decay $D_s^+ \to K^+\ell^+\ell^-$. This bound still gives small increase of the dilepton invariant mass distribution for the larger invariant dilepton mass, making it attractive for the planned experimental studies.

Chapter 5

Dalitz plot analysis of the $B \to K\eta\gamma$ decays

An interesting proposal has been made by the authors of [141] on the possible effects of new physics in $B \to P_1 P_2 \gamma$ decays. Namely, in these decays new physics might affect the polarization of outgoing photons. As it is known, in the SM photon emitted in $b \to s\gamma$ is dominantly left-handed [142, 143]. Since most of experiments only have access to photon momentum and energy one has to rely on an indirect method of measuring photon polarization. Suitable observable is the time-dependent CP asymmetry of neutral B decays to a CP-eigenstate f and a photon:

$$\frac{\Gamma(\bar{B}(t) \to f\gamma) - \Gamma(B(t) \to f\gamma)}{\Gamma(\bar{B}(t) \to f\gamma) + \Gamma(B(t) \to f\gamma)} = S_{f\gamma} \sin(\Delta m t) - C_{f\gamma} \cos(\Delta m t). \tag{5.1}$$

Mixing induced parameter $S_{f\gamma}$ has been studied in radiative decays of neutral B decays to $K^*\gamma$ [142], $B \to PP\gamma$ [141, 144], and also $B \to PV\gamma$ [145], where P and V are a light pseudoscalar and vector meson. For three-body decay $\bar{B}^0 \to K_S \pi^0 \gamma$ the authors in [144] used Soft Collinear Effective Theory (SCET) in the region with soft pion. They used the Breit-Wigner ansatz for the resonant channel via intermediate $K^*\gamma$ and concluded that right-handed photons are mainly due to the resonance and related interference effects.

In this chapter we focus on the decay width spectrum of $B \to K\eta\gamma$ in kinematical region with the hard photon carrying energy of the order $\sim m_B/2$ and one soft pseudoscalar whose energy is of the order Λ_{QCD}. Obviously, the remaining light meson is necessarily hard under these circumstances. These restrictions will allow us to simplify considerably evaluation of hadronic matrix elements. Emission of soft pseudoscalar off a heavy B meson line is driven by the leading order heavy meson chiral perturbation theory, whereas we use heavy quark symmetry and large energy effective theory for transition of heavy state transition to light energetic meson. We predict differential decay widths in these regions. This decay channel has been already observed by Belle and BaBar experiments [146–148], with the branching fractions [148]

$$\mathcal{B}(B^0 \to K^0\eta\gamma) = (7.1^{+2.1}_{-2.0} \pm 0.4) \times 10^{-6}, \tag{5.2a}$$

$$\mathcal{B}(B^+ \to K^+\eta\gamma) = (7.7 \pm 1.0 \pm 0.4) \times 10^{-6}. \tag{5.2b}$$

Quoted errors are statistical and systematic, respectively.

On the list of excited strange mesons, compiled by the Particle Data Group [28], one finds only two strange resonances with spin 2 and 3 which potentially contribute to the $\bar{B}^0 \to \bar{K}^0\eta\gamma$ decays in the low to intermediate region of low K and η invariant mass $M_{K\eta}$. Their effects are not so important, as for the $K_2^*(1430)$, the product $\mathcal{B}(B \to K_2^*(1430)\gamma) \times \mathcal{B}(K_2^*(1430) \to K\eta) \sim 10^{-6}$ is one order of magnitude below branching fractions (5.2) and we can neglect it in the first approximation. Similar contribution from $K_3^*(1780)$ is 10^{-8} which is completely negligible. Smallness of resonant contributions has been confirmed by Belle experiment [146]. On the other hand, spectra of BaBar [148] show some excess of events in the 1.4 GeV $< M_{K\eta} <$ 1.8 GeV region, but due to large error bars one cannot draw any conclusion. Following this features we do not include any resonant contributions in our approach.

5.1 Framework

The $b \to s\gamma$ is induced by the $\Delta B = 1$ effective Hamiltonian [128]

$$\mathcal{L}_{\text{eff}} = -\frac{G_F}{\sqrt{2}} V_{ts}^* V_{tb} \left[\sum_{i=1}^{6} C_i Q_i + C_7 Q_7 + C_8 Q_8 \right] \tag{5.3}$$

The most important contribution in SM is due to electroweak penguin operator Q_7 which couples tensor current between b and s quarks to the electromagnetic tensor

$$Q_7 = \frac{e}{8\pi^2} \left[m_b \bar{s}\sigma_{\mu\nu}(1+\gamma_5)b + m_s \bar{s}\sigma_{\mu\nu}(1-\gamma_5)b \right] F^{\mu\nu}. \tag{5.4}$$

Final state photons coming from the above operator are dominantly left-handed, with right-handed ones being suppressed by m_s/m_b on the amplitude level. Keeping only Q_7, this suppression is evident also in the asymmetry (5.1), however, it was shown that in multibody decays $Q_2^c = (\bar{s}\gamma_\mu(1-\gamma_5)c)(\bar{c}\gamma^\mu(1-\gamma_5)b)$ can induce charm-loop mediated $b \to s\gamma g$, with equal rates for γ_L and γ_R, and lift the suppression to $\sim 10\%$ [143]. For our purpose of calculating decay width we can neglect the m_s-proportional term of (5.4) as well as the Q_2^c effects, keeping only left-(right-)handed photons from the decay of b ($\bar{b}$) quark.

In decay of B meson to three light particles, at least two final state particles will have energy of the order $m_b/3$. We shall study kinematical region of soft η and energetic K, or vice-versa, whereas the photon will always be energetic ($E_\gamma \sim m_b/2$), as shown on Figure 5.1, where E_η and $K\eta$ invariant mass $M_{K\eta}$ are used as kinematical variables.

Feynman graphs in the leading order in $p_{\text{soft}}/\Lambda_\chi$, Λ_{QCD}/m_b are shown in Figure 5.2, where heavy meson emits a soft pseudoscalar and is excited to a vector state which subsequently decays weakly through Q_7 insertion to energetic photon and meson. We stress that those two diagrams are for two different final states, i.e. with different momentum configurations, and their sum has no physical interpretation. Each of them corresponds to precisely defined kinematical region where light meson, attached to heavy line has low momentum. This is unlike the decay $\bar{B} \to \bar{K}^0\pi^0\gamma$ [144], where one cannot apply effective description in the soft K region, due to lack of $s\bar{s}$ component in π^0.

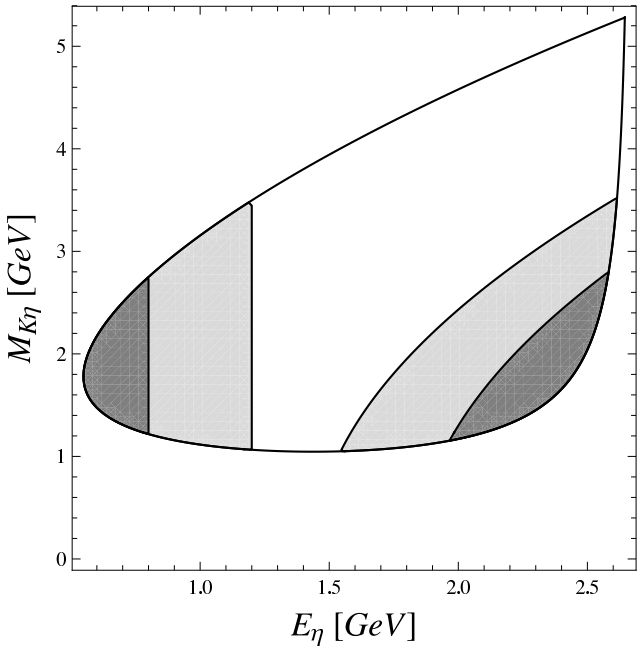

Figure 5.1: $\bar{B}^0 \to \bar{K}^0\eta\gamma$ phase space regions where soft pseudoscalars have energy below 1.2 GeV (0.8 GeV) in the light-gray (gray) region. Left corner corresponds to soft η and right one to soft K.

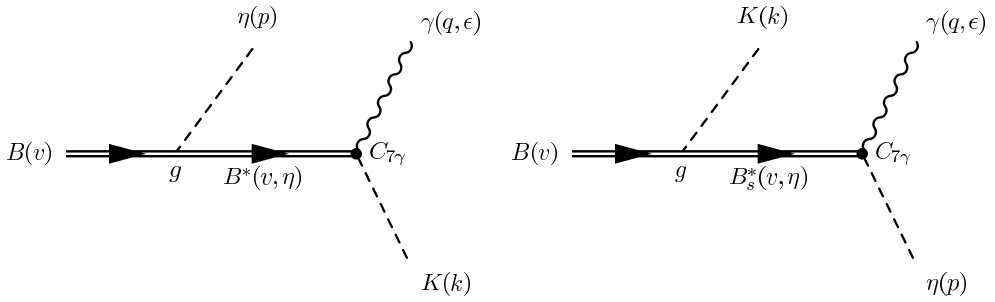

Figure 5.2: On the left-hand side, the leading contribution in the region of soft η. On the right-hand side K is soft. They govern the decay amplitude in the left and right region in Figure 5.1, respectively.

For strong emission of the soft pseudoscalar off the heavy-meson line, we utilize the low energy chiral Lagrangian combined with the heavy quark symmetry (see Section 2.3.3)

$$\mathcal{L}_{\text{strong}} = g \left\langle H_a(v)\mathcal{A}^\mu_{ab}\gamma_\mu\gamma_5\bar{H}_b(v)\right\rangle . \tag{5.5}$$

The low energy pion coupling to heavy pseudoscalar and vector has been calculated on the lattice with unquenched quarks [149] and its value is $g = 0.5 \pm 0.1$, in agreement with the value extracted in [150]. Contribution of the effective weak

vertex Q_7 in the left-hand graph of Figure 5.2 is

$$\begin{aligned}
&\frac{e}{8\pi^2} m_b \left\langle \bar{K}^0(k)\gamma(q,\epsilon) \,\middle|\, \bar{s}(0)\sigma^{\mu\nu}F_{\mu\nu}(0)(1+\gamma_5)b(0) \,\middle|\, B^*(\eta,p)\right\rangle \qquad (5.6)\\
&= \frac{e}{8\pi^2} m_b \left\langle \gamma(\epsilon,q) \,\middle|\, 2\partial_\mu A_\nu \,\middle|\, 0\right\rangle \times \left\langle \bar{K}^0(k) \,\middle|\, \bar{s}\sigma^{\mu\nu}(1+\gamma_5)b \,\middle|\, B^*(\eta,p)\right\rangle \\
&= \frac{iem_b}{4\pi^2} q_\mu \epsilon^*_\nu \left\langle \bar{K}^0(k) \,\middle|\, \bar{s}\sigma^{\mu\nu}(1+\gamma_5)b \,\middle|\, B^*(\eta,p)\right\rangle ,
\end{aligned}$$

where η and ϵ are the respective polarizations of B^* meson and the photon. For soft $\bar{K}^0$ (right-hand graph of Figure 5.2), the above manipulations are performed on flavor rotated states $(B_s^*, \eta) \leftrightarrow (B^*, \bar{K}^0)$. Virtuality of intermediate B^* is zero up to $1/m_b$ corrections, so use of the heavy quark spin symmetry is justified up to hard spectator effects [151]. In this picture, we assume heavy-quark interacts with light degrees of freedom solely through soft gluon exchanges and thus we use only upper-components field h_v for the b-quark. This is similar to approaches in [151, 152].

5.2 Large energy limit of $B \to P$ form factor

In the following, we shall relate the $B^* \to \bar{K}^0$ tensor form-factors to the vector ones of $B \to \bar{K}^0$. We repeat the standard form factors

$$\left\langle \bar{K}^0(k) \,\middle|\, \bar{s}q_\mu\sigma^{\mu\nu} \,\middle|\, B^*(\eta,p_B)\right\rangle = 2T_1^{BK}(q^2)\epsilon^{\nu\mu\rho\sigma}p_{B,\mu}k_\rho\eta_\sigma, \qquad (5.7a)$$

$$\begin{aligned}
\left\langle \bar{K}^0(k) \,\middle|\, \bar{s}q_\mu\sigma^{\mu\nu}\gamma_5 b \,\middle|\, B^*(\eta,p_B)\right\rangle =& iT_2^{BK}(q^2)\left[(M^2-m_K^2)\eta - \eta\cdot q(p_B+k)\right]^\nu \qquad (5.7b)\\
&+ iT_3^{BK}(q^2)(\eta\cdot q)\left[q - \frac{q^2}{M^2-m_K^2}(p_B+k)\right]^\nu ,
\end{aligned}$$

$$\begin{aligned}
\left\langle \bar{K}^0(k) \,\middle|\, \bar{s}\gamma^\nu b \,\middle|\, B(p_B)\right\rangle =& F_+^{BK}(q^2)\left[p_B + k - \frac{M^2-m_K^2}{q^2}q\right]^\nu \qquad (5.7c)\\
&+ F_0^{BK}(q^2)\frac{M^2-m_K^2}{q^2}q^\nu ,
\end{aligned}$$

where M and m_K are the B and K meson masses, respectively, and $q = p_B - k$. Now we can use underlying heavy quark and large energy symmetries to constrain the number of independent form factors. Following [151], we express the matrix element between B and energetic $\bar{K}^0$ as Dirac-trace of their wave functions and the matrix Γ which is the Dirac structure of interaction

$$\left\langle \bar{K}^0(En_-) \,\middle|\, \bar{s}_n\Gamma h_v \,\middle|\, B^{(*)}(\eta, Mv)\right\rangle = \mathrm{Tr}\left[A(E)\overline{\mathcal{M}}_K\Gamma\mathcal{M}_B\right]. \qquad (5.8)$$

$E = \frac{M^2+m_K^2-q^2}{2M}$ is the energy of K and n_- is a light-cone vector almost parallel to the K momentum

$$k = En_- + k', \qquad n_-^2 = 0. \qquad (5.9)$$

Residual momentum k' is of the order Λ_{QCD}. s_n is the effective large-energy field of the s quark with factored out dependence on large energy

$$s_n(x) = e^{iEn_-\cdot x}\frac{\not{n}_-\not{n}_+}{4}s(x), \qquad (5.10)$$

and $n_+ = 2v - n_-$. Long distance physics is parameterized by function $A(E)$, which does not depend on Γ, since Hamiltonians of heavy quark effective theory and large energy effective theory commute with quark spin operators. The most general parameterization of $A(E)$ is then in terms of the four energy-dependent functions [151]:

$$A(E) = a_1(E) + a_2(E)\not{v} + a_3(E)\not{n}_- + a_4(E)\not{n}_-\not{v}. \tag{5.11}$$

For wave functions of mesons we use Dirac structures transforming as fermionic bilinears under the Lorentz transformations

$$\overline{\mathcal{M}}_K = -\gamma_5\frac{\not{n}_-\not{n}_+}{4}, \qquad \mathcal{M}_B = \frac{1+\not{v}}{2}\begin{cases} \not{\eta} & ; \quad B = B^*(\eta, Mv) \\ (-\gamma_5) & ; \quad B = B(Mv) \end{cases}. \tag{5.12}$$

Evaluating the traces on the right-hand side of (5.8), one can connect form factors with functions $a_1(E), \ldots, a_4(E)$ and find at $q^2 = 0$ the symmetry relation

$$T_1^{BK}(0) = T_2^{BK}(0) = T_3^{BK}(0) = F_+^{BK}(0). \tag{5.13}$$

Consequently, matrix element of Q_7 for $B^* \to \bar{K}^0$ transition

$$\begin{aligned}\left\langle \bar{K}^0(k) \,\middle|\, \bar{s}q_\mu\sigma^{\mu\nu}(1+\gamma_5)h_v \,\middle|\, B^*(v,\eta)\right\rangle = F_+^{BK}(0)\Big[&2M\epsilon^{\nu\mu\rho\sigma}v_\mu k_\rho\eta_\sigma \\ &+ iM^2\eta^\nu - i\eta\cdot q(Mv+k)^\nu\Big]\end{aligned} \tag{5.14}$$

is proportional to $F_+^{BK}(0)$, the value of which has been determined with the light-cone sum rules approach [153]

$$F_+^{BK}(0) = 0.33 \pm 0.04. \tag{5.15}$$

5.3 Hard photon spectra

The diagram on the left-hand side in Figure 5.2, representing the soft η region is then

$$\begin{aligned}\mathcal{A}_{\eta\text{ soft}} =& -iG_F V_{ts}^* V_{tb} C_7(m_b)\frac{em_b}{8\pi^2}F_+^{BK}(0)\frac{g}{f}\left(\frac{\cos\theta}{\sqrt{6}} - \frac{\sin\theta}{\sqrt{3}}\right) \\ &\times \frac{(p_\sigma - v\cdot p\, v_\sigma)}{v\cdot p}\left[2M\epsilon^{\nu\lambda\rho\sigma}v_\lambda k_\rho + iM^2 g^{\sigma\nu} - i(Mv-k)^\sigma(Mv+k)^\nu\right]\epsilon_\nu^*,\end{aligned} \tag{5.16}$$

where $\theta = -15.4^\circ$ is the $\eta_8 - \eta_1$ mixing angle [154] and $f = 93$ MeV is the pion decay constant. Wilson coefficient C_7 on scale of the b quark is $C_7(\mu = 5\text{ GeV}) = -0.30$ [128]. Electromagnetic gauge invariance is found to be valid in the limit of small E_η.

The right-hand side diagram of Figure 5.2 with soft $\bar{K}^0$ represents the amplitude of similar form

$$\begin{aligned}\mathcal{A}_{K\text{ soft}} =& iG_F V_{ts}^* V_{tb} C_7(m_b)\frac{em_b}{8\pi^2}F_+^{BK}(0)\frac{g}{f}\frac{\sqrt{2}\cos\theta + \sin\theta}{\sqrt{3}} \\ &\times \frac{(k_\sigma - v\cdot k\, v_\sigma)}{v\cdot k}\left[2M\epsilon^{\nu\lambda\rho\sigma}v_\lambda p_\rho + iM^2 g^{\sigma\nu} - i(Mv-p)^\sigma(Mv+p)^\nu\right]\epsilon_\nu^*,\end{aligned} \tag{5.17}$$

In comparison to the soft η amplitude (5.16), the soft K amplitude (5.17) has interchanged momenta $p \leftrightarrow k$ and $\eta_8 - \eta_1$ mixing factors now originate from $B_s^*\eta\gamma$ vertex, where we rely on flavor $SU(3)$ symmetry to estimate form factor $F_+^{B_s\eta}$.

To find the amplitude for η' in the final state, one only has to modify $\eta_8 - \eta_1$ mixing coefficients in the amplitudes (5.16), (5.17) and find for soft η'

$$\begin{aligned}\mathcal{A}'_{\eta' \text{ soft}} = &- iG_F V_{ts}^* V_{tb} C_7(m_b) \frac{em_b}{8\pi^2} F_+^{BK}(0) \frac{g}{f} \left(\frac{\sin\theta}{\sqrt{6}} + \frac{\cos\theta}{\sqrt{3}} \right) \\ &\times \frac{(p_\sigma - v\cdot p\, v_\sigma)}{v\cdot p} \left[2M\epsilon^{\nu\lambda\rho\sigma} v_\lambda k_\rho + iM^2 g^{\sigma\nu} - i(Mv-k)^\sigma (Mv+k)^\nu \right] \epsilon_\nu^*. \end{aligned} \tag{5.18}$$

Momentum of η' is here denoted by p. Amplitude for soft K and energetic η' is

$$\begin{aligned}\mathcal{A}'_{K \text{ soft}} = &- iG_F V_{ts}^* V_{tb} C_7(m_b) \frac{em_b}{8\pi^2} F_+^{BK}(0) \frac{g}{f} \frac{\cos\theta - \sqrt{2}\sin\theta}{\sqrt{3}} \\ &\times \frac{(k_\sigma - v\cdot k\, v_\sigma)}{v\cdot k} \left[2M\epsilon^{\nu\lambda\rho\sigma} v_\lambda p_\rho + iM^2 g^{\sigma\nu} - i(Mv-p)^\sigma (Mv+p)^\nu \right] \epsilon_\nu^*. \end{aligned} \tag{5.19}$$

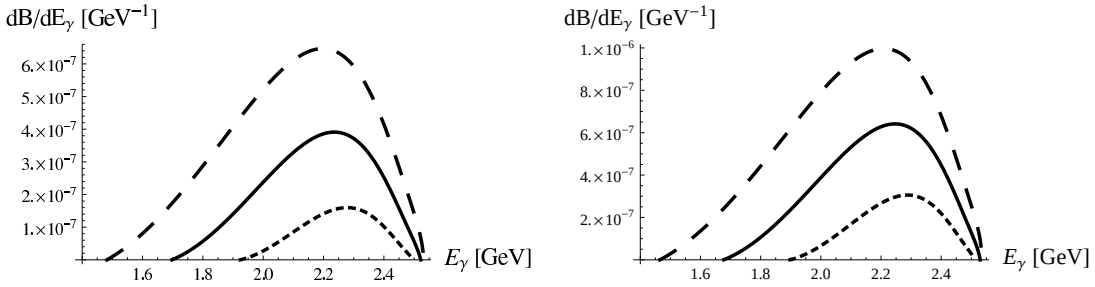

Figure 5.3: $\bar{B}^0 \to \bar{K}^0\eta\gamma$ spectra. Left: Photon spectrum in the region of $E_\eta < 0.8$ GeV (short dashes), $E_\eta < 1.0$ GeV (solid line), and $E_\eta < 1.2$ GeV (long dashes). Right: same for soft K, $E_K < 0.8, 1.0, 1.2$ GeV.

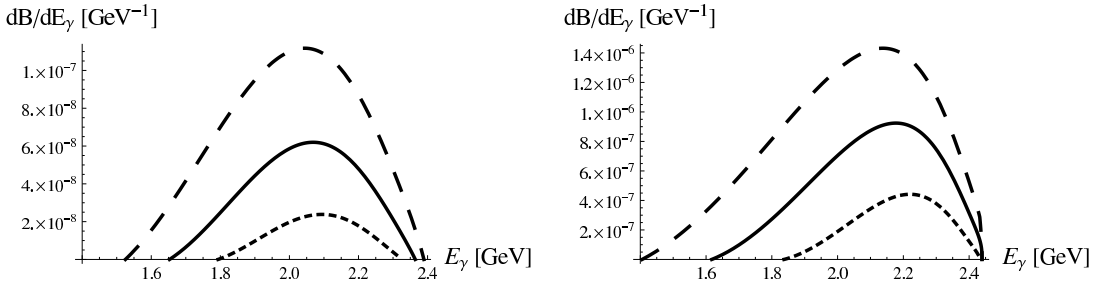

Figure 5.4: $\bar{B}^0 \to \bar{K}^0\eta'\gamma$ spectra. Left: Photon spectrum in the region of $E_{\eta'} < 1.1$ GeV (short dashes), $E_{\eta'} < 1.2$ GeV (solid line), and $E_{\eta'} < 1.3$ GeV (long dashes). Right: same for soft K, $E_K < 0.8, 1.0, 1.2$ GeV.

5.4 Summary

We have investigated photon spectra of the $B \to \eta(\eta')K\gamma$ decays in the region of Dalitz plot with energetic photon and one soft meson. We applied the combined heavy quark, large energy, and chiral symmetries. Use of this approach is justified owing to the fact that in the considered regions of Dalitz plot kinematical configuration allows simultaneous expansion in soft momentum, $1/m_b$, and $1/E_{\rm hard}$. In the approach we proposed only the nonresonant production is taken into account, neglecting in particular the resonant $B \to K^*\gamma \to K\eta\gamma$ decay. Since η and η' are isosinglets we do not expect any significant final state effects.

Partial branching ratio integrated over both regions in Figure 5.1 with upper bound on soft meson energies set to 1.2 GeV accounts for about 10 % of the $\bar{B}^0 \to \bar{K}^0\eta\gamma$ branching ratio (5.2a). Thus, with increasing statistics, these two corners of phase space could be studied more thoroughly and bring in complementary information on the magnitude of C_7.

Chapter 6

Radiative background of $B \to D\ell\nu$ decays

Many efforts have been devoted to experimentally check validity of the Cabibbo-Kobayashi-Maskawa (CKM) mechanism which predicts that all quark flavor observables agree with the unitary CKM matrix which connects all CP-violating processes. If one is to confirm the CKM mixing then either measuring sides or the angles of the unitarity triangle the apex $(\bar{\rho}, \bar{\eta})$ should come out unique. The value of V_{cb} determines lengths of the two sides adjacent to the apex, among them also the side opposite to the angle β which is precisely measured. CP-violating parameter ϵ_K of K–$\bar{K}$ mixing is one of the most important experimental inputs of the unitarity triangle analyses and is also extremely sensitive to the value of $|V_{cb}|$. Full expression can be found in [155], here we isolate the dependence on CKM values and nonperturbative physics, which contribute largest uncertainties:

$$|\epsilon_K| \propto \hat{B}_K \eta A^2 \lambda^6. \tag{6.1}$$

Scale invariant bag-parameter of matrix element of $\Delta S = 2$ matrix element between K^0 and $\bar{K}^0$ states has been denoted $\hat{B}_K$, while η, A, and λ are the CKM parameters in the Wolfenstein parameterization (2.10). Letting $A = V_{cb}/\lambda^2$, we find

$$|\epsilon_K| \propto \hat{B}_K \eta |V_{cb}|^2 \lambda^2. \tag{6.2}$$

Cabibbo angle $\lambda = 0.226 \pm 0.001$ [28] is known with good precision. Bag parameter $\hat{B}_K$ has been computed on the lattice and in the last years unquenched results with relatively small errors have become available. Recent average of results amounts to [156]

$$\hat{B}_K = 0.731(7)(35), \tag{6.3}$$

where the numbers in brackets represent the respective statistical and systematic errors. A 5% percent error of the bag parameter is becoming less important than the error of $|V_{cb}|^2$, whose current values, determined by the inclusive and the exclusive methods disagree

$$|V_{cb}| = (38.6 \pm 1.2) \times 10^{-3}, \text{ exclusive } B \to D\ell\nu \text{ and } B \to D^*\ell\nu \text{ [157]}, \tag{6.4a}$$

$$|V_{cb}| = (41.5 \pm 0.4 \pm 0.6) \times 10^{-3}, \text{ inclusive } B \to X_c\ell\nu \text{ and } B \to X_s\gamma \text{ [80]}. \tag{6.4b}$$

Values from exclusive analyses are consistently below the inclusive analyses. Precision of the inclusive method is better but in future flavor experiments one expects to approach precision of about 1% even for the exclusive method.

6.1 Extraction of V_{cb} in $B \to D\ell\nu$

The problem with extraction of the V_{cb} value using measured spectra and decay widths of a exclusive process are the ever pertaining hadronic dynamics. Effects and uncertainties of these are encoded in the form factors, which are to this day the main source of theoretical uncertainty. Spectrum of $B \to D\ell\nu$ semileptonic decay to a light lepton is conventionally expressed with $\mathcal{G}(w)$ form factor, where $w = v \cdot v'$ is the product of the two mesons' velocities

$$\frac{d\Gamma}{dw}(B \to D\ell\nu) = \frac{G_F^2 |V_{cb}|^2}{48\pi^3} m_D^3 (m_B + m_D)^2 (w^2 - 1)^{3/2} \mathcal{G}^2(w). \tag{6.5}$$

For the heavy $\to$ heavy transition $B \to D$ mediated by the (axial-)vector weak currents, starting point is the heavy quark symmetry (HQS) at the point where B and D velocities are equal and the light degrees of freedom dynamics is described by the Isgur-Wise [16] function. Then one has to invoke HQS breaking corrections in powers of α_s and especially $\Lambda_{\mathrm{QCD}}/m_Q$ ($Q = c, b$) to account for the relatively light c-quark. The HQS supplemented by the breaking terms provides a reliable theoretical prediction for the form factors at the zero-recoil, a kinematical point with maximum momentum transfer squared between the heavy mesons $t_{\max} = (m_B - m_D)^2$.

However, phase space vanishes at zero-recoil point and the decay spectrum is correspondingly small. Experimentalists measure the bulk of semileptonic events in the region away from the zero-recoil limit, where no theoretical predictions based on HQS are available. The usual procedure in this case is to fit the data to a physically viable shape of the form factor and extrapolate the measured spectrum to obtain the value of $V_{cb}\mathcal{G}(w = 1)$. Commonly used parametrization is the one of Neubert, Lellouch, and Caprini [158] (CLN) which resides on the analytical properties of the current correlators and HQS. On the other hand, lattice QCD simulations have provided in the last years quenched values of the form factor $\mathcal{G}(w)$ at several points away from the zero-recoil thus establishing direct contact with experimental data [159–161]. In future also unquenched results will be at hand for the heavy-to-heavy form factors, computed at several w [162].

In this chapter we will study the possible background of $B \to D\ell\nu$ decay due to radiative events, which are not recognized by the experiment. The control over systematics is very important if we are to reconcile the inclusive and exclusive values of V_{cb}. Furthermore, the exclusive decay $B \to D$ is determined by two hadronic form factors that are accessible to lattice QCD and have now been computed at several values of q^2. In our case the dominant contribution to radiative events with soft photons will turn out to be the D^{0*} resonance which decays to D^0 and a photon, and is always very soft in the B meson rest frame.

6.2 Amplitude decomposition

Radiative process $b \to cl\nu\gamma$ is induced by the effective weak Lagrangian accompanied by the electromagnetic interaction.

$$\mathcal{L}_{\text{eff}} = -\frac{G_F V_{cb}}{\sqrt{2}} H_\mu L^\mu, \tag{6.6a}$$

$$\mathcal{L}_{\text{QED}} = eB^\mu(x) J_\mu. \tag{6.6b}$$

We use B^μ for the electromagnetic field, whereas weak currents H_μ, L_μ and electromagnetic current J_μ are defined as

$$H_\mu = \bar{c}\gamma_\mu(1-\gamma_5)b \equiv V_\mu - A_\mu, \tag{6.7a}$$

$$L_\mu = \bar{\ell}\gamma_\mu(1-\gamma_5)\nu, \tag{6.7b}$$

$$J_\mu = -\bar{\ell}\gamma_\mu\ell + 2/3\bar{u}\gamma_\mu u - 1/3\bar{d}\gamma_\mu d + 2/3\bar{c}\gamma_\mu c - 1/3\bar{s}\gamma_\mu s - 1/3\bar{b}\gamma_\mu b. \tag{6.7c}$$

Leading order S-matrix element for $B(p) \to D(p')\ell(p_\ell)\nu(k)\gamma(\epsilon, q)$ is

$$\begin{aligned}
\langle Dl\nu\gamma \,|\, S \,|\, B\rangle &= \left\langle Dl\nu\gamma \left| -\int d^4x\, d^4y\, T\left[\mathcal{L}_{\text{eff}}(x)\mathcal{L}_{\text{QED}}(y)\right] \right| B \right\rangle \\
=&(2\pi)^4\delta^4(\Sigma_i p_i)\frac{eG_F V_{cb}}{\sqrt{2}}\epsilon^{*\mu}\Bigg[\langle D \,|\, H^\nu(0) \,|\, B\rangle \int d^4y\, e^{iq\cdot y}\, \langle l\nu \,|\, T\left[J_\mu(y)L_\nu(0)\right] \,|\, 0\rangle \\
&+ \langle l\nu \,|\, L^\nu(0) \,|\, 0\rangle \int d^4y\, e^{iq\cdot y}\, \langle D \,|\, T\left[J_\mu(y)H_\nu(0)\right] \,|\, B\rangle \Bigg].
\end{aligned} \tag{6.8}$$

T in the above expression denotes the time-ordering operator. The resulting invariant amplitude is

$$\begin{aligned}
&\mathcal{A}(B(p) \to D(p')\ell(p_l)\bar{\nu}(k)\gamma(\epsilon, q)) = \\
=&\frac{eG_F V_{cb}}{\sqrt{2}}\epsilon^{*\mu}\,\bar{u}(p_l)\Big[-\frac{F_\nu(t)}{2p_l\cdot q}\gamma_\mu(\not{p}_l + \not{q} + m_l) + V_{\mu\nu} - A_{\mu\nu}\Big]\gamma^\nu(1-\gamma_5)v(k).
\end{aligned} \tag{6.9}$$

First term in brackets is the amplitude for photon emission from the lepton leg, and is proportional to the vector form factors of $B \to D$ transition:

$$F_\nu(t) \equiv i\left\langle D(p') \left| H_\nu^{(\dagger)}(0) \right| B(p)\right\rangle, \qquad t = (p-p')^2. \tag{6.10}$$

The last two terms in bracket of (6.9) correspond to photon coupled to the heavy line (Figure 6.1), and is given in terms of vector and axial hadronic correlators

$$V_{\mu\nu} \equiv \int d^4y\, e^{iq\cdot y}\left\langle D(p') \,\middle|\, T\left[J_\mu(y)V_\nu(0)\right] \,\middle|\, B(p)\right\rangle, \tag{6.11a}$$

$$A_{\mu\nu} \equiv \int d^4y\, e^{iq\cdot y}\left\langle D(p') \,\middle|\, T\left[J_\mu(y)A_\nu(0)\right] \,\middle|\, B(p)\right\rangle. \tag{6.11b}$$

Gauge invariance of the amplitude (6.9) (i.e. vanishing of the amplitude after we have replaced ϵ by q) is guaranteed by the nontrivial Ward identities for $V_{\mu\nu}$ and $A_{\mu\nu}$ (see Section B.1):

$$q^\mu V_{\mu\nu} = (Q_D - Q_B)F_\nu(t) = F_\nu(t), \tag{6.12a}$$

$$q^\mu A_{\mu\nu} = 0, \tag{6.12b}$$

where $Q_{D,B}$ denote electric charges of mesons. Correlator of vector current $V_{\mu\nu}$ can be decomposed into inner bremsstrahlung (IB) and structure dependent (SD) parts according to

$$-iV_{\mu\nu} = V^{\mathrm{IB}}_{\mu\nu} + V^{\mathrm{SD}}_{\mu\nu}, \qquad q^\mu V^{\mathrm{SD}}_{\mu\nu} \equiv 0. \tag{6.13}$$

$V_{\mu\nu}$ and $A_{\mu\nu}$ depend on momenta of respective momenta of B, D, and γ: p, p', and q. Their most general Lorentz covariant parameterization, consistent with Ward identities (6.12) is in terms of eight scalar functions of momenta $V_{1\ldots4}$, $A_{1\ldots4}$

$$V^{\mathrm{IB}}_{\mu\nu} = \frac{p_\mu}{p\cdot q} F_\nu(t), \tag{6.14a}$$

$$\begin{aligned} V^{\mathrm{SD}}_{\mu\nu} =& V_1\left(p'_\mu q_\nu - p'\cdot q\, g_{\mu\nu}\right) + V_2\left(p_\mu q_\nu - p\cdot q\, g_{\mu\nu}\right) \\ &+ \left(p\cdot q\, p'_\mu - p'\cdot q\, p_\mu\right)\left(V_3\, p_\nu + V_4\, p'_\nu\right), \end{aligned} \tag{6.14b}$$

$$A_{\mu\nu} = A_1\epsilon_{\mu\nu\alpha\beta}\, p^\alpha q^\beta + A_2\epsilon_{\mu\nu\alpha\beta}\, p'^\alpha q^\beta + \left(A_3 p_\nu + A_4 p'_\nu\right)\, \epsilon_{\mu\alpha\beta\gamma}\, p^\alpha q^\beta p'^\gamma. \tag{6.14c}$$

Note that one has a freedom in splitting the vector current correlator $V_{\mu\nu}$ to SD and IB parts, namely one can freely move gauge invariant parts from one to another. Explicit choice of $V^{\mathrm{IB}}_{\mu\nu}$ clearly defines what is included in $V^{\mathrm{SD}}_{\mu\nu}$. Adding a term $q_\nu\epsilon_{\mu\alpha\beta\gamma}p^\alpha q^\beta p'^\gamma$ to the axial correlator $A_{\mu\nu}$ might seemed legitimate but then the Schouten's identity

$$\sum_{(\mu\alpha\beta\gamma\nu)} \epsilon_{\mu\alpha\beta\gamma} q_\nu = 0, \qquad (\mu\alpha\beta\gamma\nu) \text{ cyclical permutations} \tag{6.15}$$

would render this term redundant, since it can be absorbed by the parameterization (6.14c).

6.2.1 Single particle poles in $V_{\mu\nu}$ and $A_{\mu\nu}$

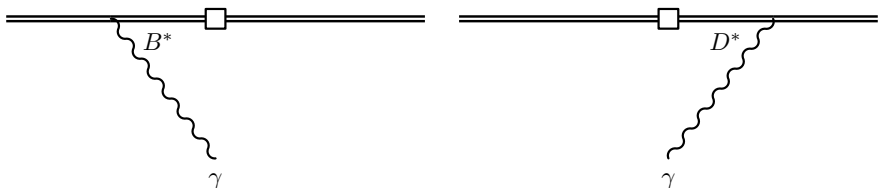

Figure 6.1: Possible one particle intermediate states' contributions.

Inserting the sum over all possible intermediate states into correlators (6.11) exposes the pole structure connected to all possible single particle states. Excited B and D states generate poles in variables $(p-q)^2$ and $(p'+q)^2$ invariant masses, respectively (left and right Feynman graphs of Figure 6.1).

$$\begin{aligned} V^{\mathrm{poles}}_{\mu\nu} = \sum_n \int d^4y\, e^{iq\cdot y} \int \frac{d^3p_n}{(2\pi)^3 2E_n} \\ \Big[\Theta(y_0)\left\langle D(p')\,\middle|\, J_\mu(0)\,\middle|\, D^*_n(\mathbf{p}_n)\right\rangle \left\langle D^*_n(\mathbf{p}_n)\,\middle|\, V_\nu(0)\,\middle|\, B(p)\right\rangle e^{-i(p_n-p')\cdot y} \\ +\Theta(-y_0)\left\langle D(p')\,\middle|\, V_\nu(0)\,\middle|\, B^*_n(\mathbf{p}_n)\right\rangle \left\langle B^*_n(\mathbf{p}_n)\,\middle|\, J_\mu(0)\,\middle|\, B(p)\right\rangle e^{-i(p-p_n)\cdot y}\Big]. \end{aligned} \tag{6.16}$$

Sum runs over all beauty (B_n^*) and charm (D_n^*) flavoured states. Of the B_n^* intermediate states, only B^- introduces a pole in the physical region when photon is soft ($E_\gamma \to 0$). This pole contribution precisely matches the $V_{\mu\nu}^{\mathrm{IB}}$. Amplitude for bremsstrahlung off the lepton leg is also singular at $E_\gamma = 0$. Consequently, the two amplitudes together are gauge invariant (as can be seen by comparing Ward identities (6.12) and the amplitude (6.9)) and they comprise the well-known soft divergence of quantum electrodynamics. According to Bloch-Nordsieck theorem [163] it cancels against one-loop virtual correction on the level of decay width.

SD amplitude is divergence free at $E_\gamma \to 0$, however, additional poles appear at finite E_γ due to D_n^* states, and since the outgoing photon is assumed to be soft, only the lowest excited states should contribute dominantly. Here we will consider only the first excited state D^* and argue in the end why contribution of higher states is not substantial. Close to the D^* pole $V_{\mu\nu}^{\mathrm{SD}}$ takes the following form

$$\frac{i\,\langle D(p')\,|\,J_\mu\,|\,D^*(\mathbf{p}'+\mathbf{q})\rangle\,\langle D^*(\mathbf{p}'+\mathbf{q})\,|\,V_\nu\,|\,B(p)\rangle}{(p'+q)^2 - m_{D^*}^2 + i m_{D^*}\Gamma_{D^*}}, \tag{6.17}$$

where we accounted for the finite width of the D^* via the Breit-Wigner ansatz. $A_{\mu\nu}$ also has the same pole structure, only with axial current A_ν in place of V_ν.

6.3 Hadronic parameters of $B \to D^*$ and $D^* \to D\gamma$ transitions

$D^{0*} \to D^0\gamma$

This decay is governed by the magnetic-dipole transition

$$\left\langle D^0(p')\gamma(k,\eta)\,\middle|\,D^{0*}(p,\epsilon)\right\rangle = e g_{D^{0*}D^0\gamma}\epsilon'^{\mu\nu\alpha\beta}\eta_\mu\epsilon_\nu p_\alpha p'_\beta, \tag{6.18}$$

whose value $g_{D^{0*}D^0\gamma} = 2.0 \pm 0.6\ \mathrm{GeV}^{-1}$ was computed on the lattice [164] along with the strong coupling constant $g_{D^*D\pi} = 20 \pm 2$. We combine the lattice results with the measured ratio [28]

$$R_{\pi/\gamma} \equiv \frac{\Gamma(D^{0*} \to D^0\pi^0)}{\Gamma(D^{0*} \to D^0\gamma)} = 1.74 \pm 0.13 \tag{6.19}$$

to find a tighter constraint: $1.8 < g_{D^{0*}D^0\gamma} < 2.5$ (see Figure 6.2). Knowledge of $g_{D^{0*}D^0\gamma}$ allows us to predict the decay width of D^{0*} meson from the measured branching fraction $\mathcal{B}(D^{0*} \to D^0\gamma) = 0.381 \pm 0.029$ [28]:

$$53\ \mathrm{keV} < \Gamma_{D^{0*}} < 108\ \mathrm{keV}. \tag{6.20}$$

This is much lower than the current experimental upper bound $\Gamma_{D^{0*}} < 2.1$ MeV [28].

$B^- \to D^{0*}$

Vector and axial-vector form factors of $B \to D^{0*}$ (see Section 2.3.1) have been computed using the quenched lattice simulation [165] at several values of $w = (t - m_B^2 - m_{D^*}^2)/(2m_B m_{D^*})$. We perform the chi-squared fit on their stated values and errors using the CLN shapes of the form factors [158].

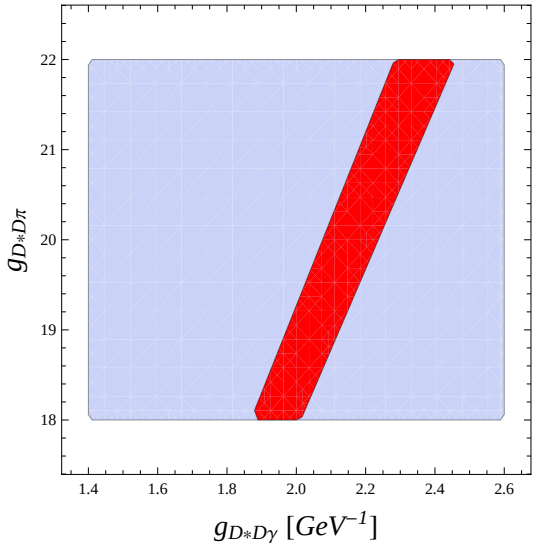

Figure 6.2: Blue region represents the lattice allowed values of $g_{D^{0*}D^0\pi}$ and $g_{D^{0*}D^0\gamma}$, and red region is allowed by the measurement of $R_{\pi/\gamma}$.

The resulting contribution of the D^* resonance to structure dependent functions $A_{1\ldots4}$, $V_{1\ldots4}$ (6.14a) are expressed in terms of form factors V^{BD^*}, $a^{BD^*}_{0,1,2}$ (we use lowercase a for the form factors (2.32) to avoid ambiguity with functions $A_{1\ldots4}$ used in decomposition of $A_{\mu\nu}$). Their explicit expressions are stated in the Section B.2.

6.4 Irreducible background to $B^- \to D^0\ell\nu$ channel from $D^{0*} \to D^0\gamma$

The resonant decay chain $B \to D^*\ell\nu$ followed by $D^* \to D\gamma$ forms an irreducible background to $B \to D\ell\nu$ if the experiment overlooks the final state soft photons whose energy is $E_\gamma = 137$ MeV in the center-of-mass frame of D^*. Depending on the experimental ability to discern events accompanied by the photon from ordinary semileptonic events, a number of fake events are included in the sample of semileptonic events.

The available experimental data [28] is sufficient to estimate the importance of $B^- \to D^{0*}\ell\nu$ pollution in $B^- \to D^0\ell\nu$. Using the narrow width approximation gives for the branching fraction of resonant $B^- \to D^0\gamma\ell\nu$ a value of $(2.2 \pm 0.2)\%$, which is of the same size as non-radiative decay [28]. This clearly poses a serious problem since the major part of the photons are quite soft due to small mass splitting between D^{0*} and D^0.

We show the photon spectrum, calculated using the framework defined in Sections 6.2 and 6.3, on Figure 6.3. The 137 MeV photon in the D^{0*} rest frame is boosted to energies up to ≈ 350 MeV in the B meson rest frame. Figure 6.4 shows the ratio of radiative events recognized as $B^- \to D^0\ell\nu$ to the total sum of radiative and semileptonic events.

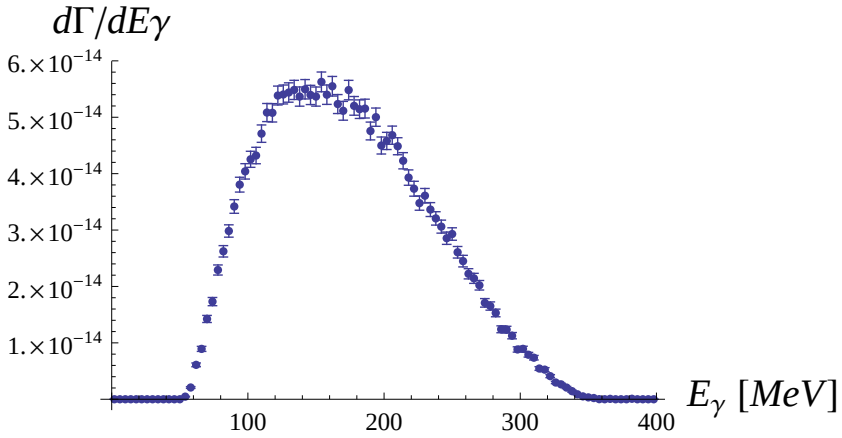

Figure 6.3: Spectrum of resonant $B \to D^{0*}\ell\nu \to D^0\gamma\ell\nu$.

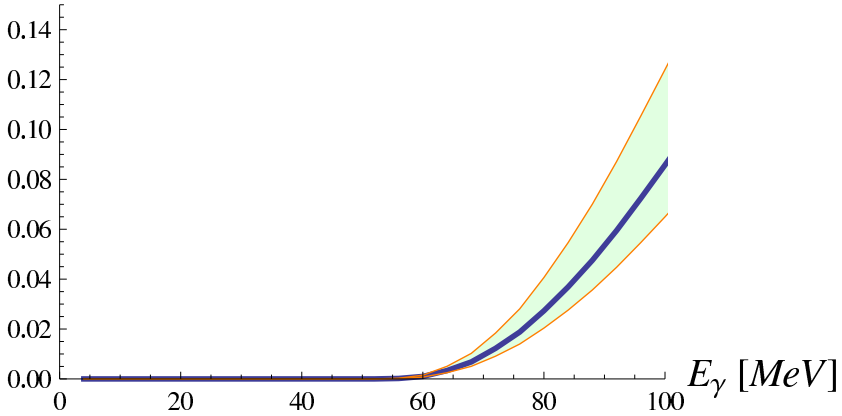

Figure 6.4: Fraction of misidentified events in the sample depending on the photon energy resolution of the analysis. The uncertainty corresponds to the range allowed for the Γ_{D^*}.

6.5 Summary

Precision of V_{cb} determined by measuring an exclusive $b \to c$ decay channel is important in reconciling a discrepancy between inclusive and exclusive methods of V_{cb} extraction.

Unitarity triangle analyses rely heavily on the CP-violating parameter of K–$\bar{K}$ mixing ϵ_K, and largest uncertainties are stemming from errors of the bag parameter $\hat{B}_K$ and the value of V_{cb}. Advances in unquenched lattice calculations have provided a value of bag parameter with a good precision of $\sim 5\%$. Thus, experimental value of $|V_{cb}|$ is becoming a dominant source of errors in using ϵ_K as an experimental input to unitarity triangle analyses.

Since $B^- \to D^0\ell\nu$ channel is expected to be measured also at future Belle 2 experiment we have analysed the background radiative events $B^- \to D^0\ell\nu\gamma$. We have found the dominant contribution due to D^{0*} resonance, decaying into $D^0\gamma$. We have shown spectrum (Figure 6.3) and the fraction of fake events in the experimental

sample (Figure 6.4). Due to small mass splitting 142 MeV between m_{D^0} and $m_{D^{0*}}$, all the photons are soft in the B meson rest frame. Higher excited charm states would necessarily produce more energetic photons, which experiment could detect, so those states have been of minor importance in our analysis. We have come to conclusion that for a required precision of V_{cb} of the one percent order, experiment should be sensitive to the photons of energy well below 100 MeV.

Chapter 7

Concluding remarks

The search for new physics in precision low-energy observables has been a long lasting aim of joint experimental and theoretical efforts. The physics programme of B-factories even exceeded the original goals and, together with input from other experiments, confirmed that a global fit of the standard model quark Yukawa sector shows no serious anomalies. The unitarity triangle analyses tested the Cabibbo-Kobayashi-Maskawa mixing mechanism at the $\sim 10\%$ level. The most precisely measured and theoretically unproblematic observables like CP-violation parameters in K–$\bar{K}$ mixing already push the scale of new physics up to $\sim$ 100–1000 TeV. It has become clear that new physics contributes to the quark flavour observables on the level of few percent or even smaller. It is thus crucial to have the standard model theoretical predictions under good control.

In first part of the thesis we have put emphasis on comparison between standard model and new physics signatures in rare decays. The standard model contributions in that context act as background of new physics signals. In Chapter 3 however, we studied a process $b \to dd\bar{s}$, occurring at a negligibly slow rate in the standard model. This allowed us to consider contributions of the new physics scenarios alone. We found that certain hadronic decay channels shall play a role in constraining a model of supersymmetry with broken R_p-parity and a model with additional Z' gauge boson, once the experiment is able to probe their branching fractions on the 10^{-7} level. Chapter 4 dealt with semileptonic charm decays $D \to P\ell^+\ell^-$, which are notorious for their poorly controlled long distance contributions. In this case we had to model the resonant background, whereas the short distance standard model contributions proved negligible. Same quark level transition $c \to u\ell^+\ell^-$ triggers the well constrained leptonic decays $D \to \ell^+\ell^-$, which give useful additional information in this case. We showed that experiment is on the verge of discovery of $D \to \pi\ell^+\ell^-$ and currently puts severe bounds on the R_p-parity violating supersymmetry and a more general singlet leptoquark model. All the abovementioned decays will be searched for in future at LHCb and the Belle 2 experiments and will provide useful exclusion bounds in parameter spaces of new physics models.

In the second part, namely in Chapters 5 and 6 we did not focus on any particular new physics model but instead devised methods of testing the standard model predictions themselves. For the $B \to K\eta\gamma$ decay we predicted in the standard model photonic spectra for the decay channels with η and η' in final state. These spectra will be recorded at the Belle 2 and LHCb experiments and will probe the chiral

nature as well as the scale of $b \to s\gamma$ coupling. In Chapter 6 we exposed the pitfall present in the exclusive determination of Cabibbo-Kobayashi-Maskawa element $|V_{cb}|$, a very important parameter in the unitarity triangle analyses. Namely, the discriminating power between $B \to D\ell\bar{\nu}\gamma$ and $B \to D\ell\bar{\nu}$ decays depends crucially on the lower cut on photon energy. For the case of $B^- \to D^0$ we identified the dominantly contributing resonance D^{0*} and estimated the number of misidentified radiative events depending on the photon cut. Results of these two chapters may prove to be valuable in progressively stringent tests of the standard model.

The quark flavour observables studied in the thesis constitute important aspect of new physics searches. The precision low-energy experiments, although affected by hadronic uncertainties, are best-suited to assess the new physics flavour properties. In forthcoming era of the Large Hadron Collider a fruitful interplay between the high p_T experiments at hadron colliders and precision flavour physics will further test the standard model and hopefully expose the principles behind it.

Appendix A

Technical aside on $b \to dd\bar{s}$ process

A.1 Matching and renormalization of composite operators

We choose to regularize the loop integrals in the effective theory using the naive dimensional regularization (NDR) and renormalize them by minimal subtraction scheme [166, 167] (MS). Using a mass-independent renormalization scheme like $\overline{MS}$ results in a well defined power expansion in $1/m_W^2$ of the amplitudes unlike mass-dependent schemes, where loop contributions of higher dimensional (dimension-8 and higher) composite operators is not suppressed.

When we choose to include virtual QCD corrections we work in the modified minimal subtraction scheme [166, 167] ($\overline{MS}$) to renormalize divergent loop integrals. However, in $\overline{MS}$ scheme also the QCD beta function is mass-independent and heavy particles do not decouple as the Appelquist-Carazzone theorem does not apply [168, 169]. This is why we have to decouple a heavy particle[1] with mass M "by hand", integrating it out on the scale $\mu \sim \Lambda$ [170]. At matching scale Λ we determine the Wilson coefficients, by imposing equality of 1-particle irreducible (1PI) Green functions calculated in the full theory and the 1PI Green functions (GF) calculated in the effective theory. Following [29] we demonstrate, how the matching and operator renormalization is calculated in LO in α_s and leading logarithm approximation. First we express GF in the effective theory as

$$-\frac{\sqrt{2}}{4G_F}\mathcal{A}_{\text{eff}} = \sum_i C_i(\Lambda)\,\langle Q_i(\Lambda)\rangle = \left\langle \vec{Q}^T(\Lambda)\right\rangle \vec{C}(\Lambda), \tag{A.1}$$

where $\left\langle \vec{Q}\right\rangle$ denotes the vector of GFs calculated with composite operator insertions (Fig. A.1). Assuming our basis of operators is complete under QCD renormalization, GFs can be expressed as combinations of tree-level GFs (i.e. calculated without QCD correction), denoted $\vec{S}$

$$\left\langle \vec{Q}(\Lambda)\right\rangle = \left(1 + \frac{\alpha_s}{4\pi} r^T\right)\vec{S}. \tag{A.2}$$

[1] Here qualification "heavy" should be understood as heavy with respect to typical momentum scale of the problem, namely $\mu_{\text{had}} \ll M$.

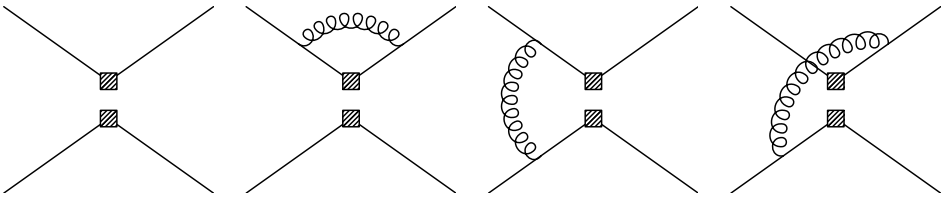

Figure A.1: 1PI Green function diagrams in the effective theory. Shaded squares represent currents in the effective 4-fermion vertex.

The corresponding full theory GF is (Fig. A.2) (keeping only leading terms in $1/m_W^2$):

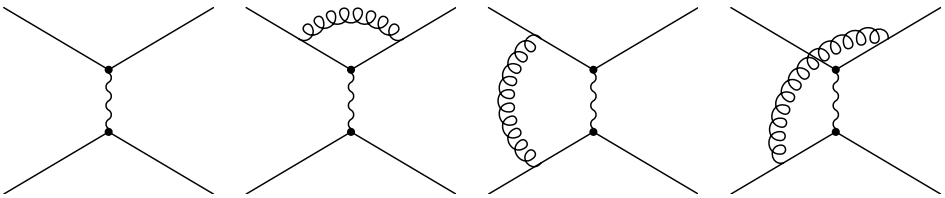

Figure A.2: 1PI Green function diagrams in the full theory. Dots are the weak currents.

$$-\frac{\sqrt{2}}{4G_F}\mathcal{A}_{\text{full}} = \vec{S}^T\left(\vec{A}^{(0)} + \frac{\alpha_s(\Lambda)}{4\pi}\vec{A}^{(1)}\right). \tag{A.3}$$

The above full amplitude as written (A.3) is finite after we have accounted for the external leg renormalization by adding factor $Z_q^{1/2}$ for each external fermion. In the leading order in α_s the quark field renormalization constant is

$$Z_q = 1 - \frac{\alpha_s}{4\pi}\frac{C_F}{\epsilon} + \mathcal{O}(\alpha_s^2), \qquad C_F = \frac{N^2-1}{2N} = \frac{4}{3}. \tag{A.4}$$

Also the effective theory result (A.3) is finite, but there a mere multiplicative factor Z_q^2 does not suffice to render the GF finite. That should come as no surprise since the effective theory is not renormalizable as is the case with full theory. Especially the UV behaviour is different in the two theories. One should treat Wilson coefficients C_i as ordinary coupling constants and proceed with usual renormalization procedure where also Wilson coefficients get renormalized. Equivalently we can consider renormalizing the composite operators as

$$\vec{Q}^{(0)} = Z\vec{Q}. \tag{A.5}$$

This renormalization is chosen to be done in the MS scheme, subtracting only the $1/\epsilon$ poles[2]. Once we have adopted the same scheme for renormalization of QCD divergences in both theories and having included composite operator in (A.2), we read off the Wilson coefficients at the matching scale Λ from equality of (A.1) and (A.3)

$$\vec{C}(\Lambda) = \vec{A}^{(0)} + \frac{\alpha_s(\Lambda)}{4\pi}(\vec{A}^{(1)} - r^T\vec{A}^{(0)}). \tag{A.6}$$

[2]We calculate the momentum loop diagrams in $D = 4 - 2\epsilon$ spacetime dimensions.

Our final goal are the values $\vec{C}(\mu_{\text{had}})$ and thus we could in principle set $\Lambda = \mu_{\text{had}}$ in (A.6). However, if the α_s-proportional terms in coefficients (A.6) contain large logarithms of scale separation $\ln \Lambda^2/M^2$ they would invalidate perturbative treatment for $\Lambda \ll M$ [29, 171]. Thus the matching calculation is valid only for $\Lambda \simeq M$.

The aforementioned large logarithms can be summed using the renormalization group improved theory, which amounts to performing a sequence of matching procedures with infinitesimal scale separations, allowing one to write the renormalization group equations (RGE) for a renormalized parameter. RG equations express the rate of change or "running" or "evolution" of a parameter as the renormalization scale μ is being changed. Renormalized Wilson coefficients' running is determined by the anomalous dimension matrix γ

$$\frac{d\vec{C}(\mu)}{d\ln\mu} = \gamma^T(g)\vec{C}(\mu), \tag{A.7}$$

where in the minimal subtraction scheme $\gamma(g)$ is μ-dependent only indirectly through $g(\mu)$. Same RG equation holds for the evolution matrix

$$\frac{dU(\mu,\Lambda)}{d\ln\mu} = \gamma^T(g)U(\mu,\Lambda), \qquad \vec{C}(\mu) \equiv U(\mu,\Lambda)\vec{C}(\Lambda). \tag{A.8}$$

Since γ is a function of g in MS scheme, it is more suitable to treat g as independent variable, namely

$$\frac{d}{dg}U(\mu(g),\Lambda) = \frac{\gamma^T(g)}{\beta(g)}U(\mu(g),\Lambda)), \tag{A.9}$$

where β is the standard beta-function of QCD

$$\frac{dg}{d\ln\mu} = \beta(g), \qquad \beta(g) = -\beta_0\frac{g^3}{(4\pi)^2} + \mathcal{O}(g^5), \tag{A.10}$$

$$\beta_0 = (33 - 2f)/3. \tag{A.11}$$

f is the number of dynamical quark flavours at scale μ. The solution to running $\alpha_s(\mu) = g^2/(4\pi)$ in leading order in α_s is

$$\alpha_s(\mu) = \frac{\alpha_s(m_Z)}{1 - \beta_0\frac{\alpha_s(m_Z)}{4\pi}\ln m_Z^2/\mu^2} = \frac{4\pi}{\beta_0 \ln \mu^2/\Lambda^2_{\text{QCD}}}. \tag{A.12}$$

Solution of (A.9) can be written iteratively resulting in

$$U(\mu,\Lambda) = T_g \exp\left[\int_{g(\Lambda)}^{g(\mu)} dg' \frac{\gamma^T(g')}{\beta(g')}\right]. \tag{A.13}$$

Operator T_g enforces products of matrices to be coupling-ordered, meaning that the matrix with largest g is placed leftmost, the one with second largest g is placed next to the leftmost and so on, if $g(\Lambda) < g(\mu)$. If however, $\mu > \Lambda$, then the ordering must be reversed. The anomalous dimension matrix γ is connected to the composite operator renormalization, in particular to coefficient Z_1 of the $1/\epsilon$ term of matrix Z (A.5)

$$\gamma(g) = -2g^2\frac{dZ_1(g)}{dg^2}. \tag{A.14}$$

A.1.1 Mixing of effective operators in $b \to dd\bar{s}$

Working in the leading logarithm approximation we can perform matching on scale Λ at order $\mathcal{O}(\alpha_s^0)$. To determine the anomalous dimension matrix of the operators (8.8) we have to calculate the insertions of operators $\mathcal{O}_{1\ldots3}$ into the 1PI Green function to first order in α_s.

$\mathcal{O}_1\mathcal{O}_2$ mixing

We have to evaluate the loop diagrams on Figure A.1 with insertions of $\mathcal{O}_1$ and $\mathcal{O}_2$

$$\left\langle \mathcal{O}_1^{(0)} \right\rangle = \left\langle \mathcal{O}_1^{(0)} \right\rangle_0 \left[1 + \frac{\alpha_s}{4\pi} \frac{2C_F - 1}{\epsilon}\right] + \left\langle \mathcal{O}_2^{(0)} \right\rangle_0 \frac{\alpha_s}{4\pi} \frac{3}{\epsilon}, \tag{A.15}$$

$$\left\langle \mathcal{O}_2^{(0)} \right\rangle = \left\langle \mathcal{O}_2^{(0)} \right\rangle_0 \frac{\alpha_s}{4\pi} \frac{3}{\epsilon}, \tag{A.16}$$

where $\langle \ldots \rangle_0$ denotes the tree-level insertion of operator, i.e. without QCD corrections. Evidently, the operator $\mathcal{O}_2$ does not mix into $\mathcal{O}_1$. Insertions of the renormalized operators $\mathcal{O}_{1,2}$ into the four point functions are finite and are expressed as

$$\begin{pmatrix} \langle \mathcal{O}_1 \rangle \\ \langle \mathcal{O}_2 \rangle \end{pmatrix} = Z_q^2 Z^{-1} \begin{pmatrix} \left\langle \mathcal{O}_1^{(0)} \right\rangle \\ \left\langle \mathcal{O}_2^{(0)} \right\rangle \end{pmatrix}. \tag{A.17}$$

Inserting the quark field renormalizations (A.4) and $C_F = 4/3$ we find for the composite operator renormalization matrix

$$Z = 1 + \frac{\alpha_s}{4\pi\epsilon} \begin{pmatrix} -1 & 3 \\ 0 & 8 \end{pmatrix}. \tag{A.18}$$

The anomalous dimension matrix is determined by the $1/\epsilon$ term in expansion of Z in powers of ϵ (see (A.14))

$$\gamma = \frac{\alpha_s}{2\pi} \begin{pmatrix} 1 & -3 \\ 0 & -8 \end{pmatrix}. \tag{A.19}$$

$\mathcal{O}_3$ renormalization

The $\mathcal{O}_3$ insertion into graphs of Figure A.1 also generates at $\mathcal{O}(\alpha_s)$ an operator with the colour nonsinglet currents, which is not present in our basis. However, owing to the presence of two d quark fields we can Fierz transform the abovementioned operator back to $\mathcal{O}_3$. Thus, $\mathcal{O}_3$ only mixes into itself and will be multiplicatively renormalized

$$\left\langle \mathcal{O}_3^{(0)} \right\rangle = \left(1 + \frac{\alpha_s}{4\pi} \frac{2C_F - 2}{\epsilon}\right) \left\langle \mathcal{O}_3^{(0)} \right\rangle_0. \tag{A.20}$$

After the quark field renormalization we find for the anomalous dimensions

$$Z = 1 - \frac{\alpha_s}{4\pi} \frac{2}{\epsilon}, \qquad \gamma = \frac{\alpha_s}{\pi}. \tag{A.21}$$

A.2 GIM mechanism in the $b \to dd\bar{s}$

Note that in (3.11) the two independent sums over quark flavors imply exact GIM cancellation of any term in $f(x_i, x_j)$ that does not depend on *both* x_i and x_j. Resulting freedom in choice of $f(x, y)$ is

$$f(x, y) \to f(x, y) + u(x) + v(y), \tag{A.22}$$

with arbitrary functions u and v. In (3.12) we fixed $u(x)$ and $v(y)$ by imposing the constraint $f(x, 0) = f(0, y) = 0$ to suppress the contribution of light quarks and retain relatively simple form. We could also forbid contributions at chosen value of x and y. For example, t quark would not explicitly contribute in the box diagram if we redefined $f(x, y)$ as

$$f(x, y) \to f(x, y) - f(x_t, y) - f(x, x_t) + f(x_t, x_t). \tag{A.23}$$

A.3 Parameterization of $B \to \pi$ form factors

For the $B^- \to \pi^-$ and $B^- \to \rho^-$ transitions we use form factors calculated in the relativistic constituent quark model with numerical input from lattice QCD at high q^2 [74].

A.3.1 $B \to \pi$ form factors

$$F_1^{\pi B}(q^2) = \frac{F_1^{\pi B}(0)}{(1 - q^2/m_{B^*}^2)[1 - \sigma_1 q^2/m_{B^*}^2]}, \quad F_1^{\pi B}(0) = 0.29, \quad \sigma_1 = 0.48, \tag{A.24a}$$

$$F_0^{\pi B}(q^2) = \frac{F_0^{\pi B}(0)}{1 - \sigma_1 q^2/m_{B^*}^2 + \sigma_2 q^4/m_{B^*}^4}, \quad F_0^{\pi B}(0) = 0.29, \quad \sigma_1 = 0.76, \, \sigma_2 = 0.28, \tag{A.24b}$$

A.3.2 $B \to \rho$ form factors

$$V^{\rho B}(q^2) = \frac{V^{\rho B}(0)}{(1 - q^2/m_{B^*}^2)[1 - \sigma_1 q^2/m_{B^*}^2]}, \quad V^{\rho B}(0) = 0.31, \quad \sigma_1 = 0.59, \tag{A.25a}$$

$$A_0^{\rho B}(q^2) = \frac{A_0^{\rho B}(0)}{(1 - q^2/m_B^2)[1 - \sigma_1 q^2/m_B^2]}, \quad A_0^{\rho B}(0) = 0.30, \quad \sigma_1 = 0.54, \tag{A.25b}$$

$$A_1^{\rho B}(q^2) = \frac{A_1^{\rho B}(0)}{1 - \sigma_1 q^2/m_{B^*}^2 + \sigma_2 q^4/m_{B^*}^4}, \quad A_1^{\rho B}(0) = 0.26, \quad \sigma_1 = 0.73, \, \sigma_2 = 0.10, \tag{A.25c}$$

$$A_2^{\rho B}(q^2) = \frac{A_2^{\rho B}(0)}{1 - \sigma_1 q^2/m_{B^*}^2 + \sigma_2 q^4/m_{B^*}^4}, \quad A_2^{\rho B}(0) = 0.24, \quad \sigma_1 = 1.40, \, \sigma_2 = 0.50. \tag{A.25d}$$

The transition form factors between heavy mesons $D_s^- \to D^-$ have been calculated in the chiral Lagrangian approach in [75]

$$F_1^{DD_s}(q^2) = 0, \tag{A.26a}$$

$$F_0^{DD_s}(q^2) = \frac{q^2}{m_{D_s}^2 - m_D^2} \frac{(g_\pi/4) f_{K(1430)} \sqrt{m_{D_s} m_D}}{q^2 - m_{K(1430)}^2 + i\sqrt{q^2}\Gamma_{K(1430)}}. \tag{A.26b}$$

A.3.3 $K \to \pi$ form factors

The same method has been used to obtain the $K^- \to \pi^-$ form factors [76]

$$F_1^{\pi K}(q^2) = \frac{2 g_{VK(892)} g_{K^*}}{q^2 - m_{K(892)}^2 + i\sqrt{q^2}\Gamma_{K(892)}(q^2)}, \tag{A.27a}$$

$$\begin{aligned} F_0^{\pi K}(q^2) =& \frac{2 g_{VK(892)} g_{K^*}(1 - q^2/m_{K(892)}^2)}{q^2 - m_{K(892)}^2 + i\sqrt{q^2}\Gamma_{K(892)}(q^2)} \\ &+ \frac{q^2}{m_K^2 - m_\pi^2} \frac{f_{K(1430)} g_{SK(1430)}}{q^2 - m_{K(1430)}^2 + i\sqrt{q^2}\Gamma_{K(1430)}(q^2)}. \end{aligned} \tag{A.27b}$$

Here the decay widths of resonances $K^*(892)$ and $K(1430)$ are taken to be energy dependent [76]

$$\begin{aligned} \Gamma_{K(892)}(q^2) =& \left(\frac{m_{K(892)}^2}{q^2} \right)^{5/2} \\ &\times \left(\frac{[q^2 - (m_K + m_\pi)^2][q^2 - (m_K - m_\pi)^2]}{[m_{K(892)}^2 - (m_K + m_\pi)^2][m_{K(892)}^2 - (m_K - m_\pi)^2]} \right)^{3/2} \Gamma_{K(892)}, \end{aligned} \tag{A.28a}$$

$$\begin{aligned} \Gamma_{K(1430)}(q^2) =& \left(\frac{m_{K(1430)}^2}{q^2} \right)^{3/2} \\ &\times \left(\frac{[q^2 - (m_K + m_\pi)^2][q^2 - (m_K - m_\pi)^2]}{[m_{K(1430)}^2 - (m_K + m_\pi)^2][m_{K(1430)}^2 - (m_K - m_\pi)^2]} \right)^{1/2} \Gamma_{K(1430)}. \end{aligned} \tag{A.28b}$$

Appendix B

Ward identity and amplitude expressions for $B^- \to D^0 \ell \bar{\nu} \gamma$

B.1 Ward identities

To derive the Ward identity of electromagnetic gauge invariance for $V_{\mu\nu}, A_{\mu\nu}$ of Chapter 6 we write out explicitly the time-ordering

$$\begin{aligned} & q^\mu V_{\mu\nu} \\ &= -i \int d^4y \, (\partial^\mu e^{iq\cdot y}) \, \langle D \,|\, T \left[J_\mu(y) V_\nu(0) \right] |\, B \rangle \\ &= i \int d^4y \, e^{iq\cdot y} \, \partial^\mu \left\langle D \,\middle|\, \Theta(y^0) J_\mu(y) V_\nu(0) + \Theta(-y^0) V_\nu(0) J_\mu(y) \,\middle|\, B \right\rangle \\ &= i \int d^3y \, e^{-i\mathbf{q}\cdot\mathbf{y}} \, \langle D \,|\, [J_0(\mathbf{y}), V_\nu(\mathbf{0})] \,|\, B \rangle \, . \end{aligned} \tag{B.1}$$

Using the canonical commutation relations shows [138, p. 444] that $[J_0(\mathbf{y}), F(\mathbf{x})] = -q_F F(\mathbf{x}) \delta(\mathbf{y} - \mathbf{x})$, where F is a local function of fields, present in the Lagrangian, and q_F is the sum of charges of all the fields in F. So we have

$$q^\mu V_{\mu\nu} = i \int d^3y \, e^{-i\mathbf{q}\cdot\mathbf{y}} (1/3 + 2/3) \delta(\mathbf{y}) \, \langle D \,|\, V_\nu \,|\, B \rangle = F_\nu(t). \tag{B.2}$$

B.2 Invariant coefficients of the $V_{\mu\nu}$ and $A_{\mu\nu}$ in $B^- \to D^{0*} \ell \bar{\nu} \to D^0 \ell \bar{\nu} \gamma$

B.2.1 Contribution to $V_{\mu\nu}^{\mathrm{SD}}$

$$V_1^{D^*} = \frac{2 g_{D^* D\gamma} V^{BD^*}(W^2)\, m_B E_D}{(m_B + m_{D^*})\left((p'+q)^2 - m_{D^*}^2\right)}, \tag{B.3a}$$

$$V_2^{D^*} = \frac{-g_{D^* D\gamma} V^{BD^*}(W^2)\,(m_D^2 + m_{D^*}^2)}{(m_B + m_{D^*})\left((p'+q)^2 - m_{D^*}^2\right)}, \tag{B.3b}$$

$$V_3^{D^*} = 0, \tag{B.3c}$$

$$V_4^{D^*} = \frac{-2 g_{D^* D\gamma} V^{BD^*}(W^2)}{(m_B + m_{D^*})\left((p'+q)^2 - m_{D^*}^2\right)} \tag{B.3d}$$

B.2.2 Contribution to $A_{\mu\nu}$

$$A_1^{D^*} = \frac{-g_{D^* D\gamma}}{\left((p'+q)^2 - m_{D^*}^2\right) W^2} \left[2 m_{D^*} a_0^{BD^*}(W^2) - (m_B + m_{D^*}) a_1^{BD^*}(W^2) + \frac{W^2 + m_B^2 - m_{D^*}^2}{m_B + m_{D^*}} a_2^{BD^*}(W^2) \right] \frac{m_{D^*}^2 - m_D^2}{2}, \tag{B.4a}$$

$$A_2^{D^*} = \frac{g_{D^* D\gamma}}{\left((p'+q)^2 - m_{D^*}^2\right) W^2} \left[2 m_{D^*} p\cdot q\, a_0^{BD^*}(W^2) - (m_B + m_{D^*})(p\cdot q + W^2) a_1^{BD^*}(W^2) + \frac{p\cdot q\,(W^2 + m_B^2 - m_{D^*}^2)}{m_B + m_{D^*}} a_2^{BD^*}(W^2) \right], \tag{B.4b}$$

$$A_3^{D^*} = \frac{-g_{D^* D\gamma}}{\left((p'+q)^2 - m_{D^*}^2\right) W^2} \left[-2 m_{D^*} a_0^{BD^*}(W^2) + (m_B + m_{D^*}) a_1^{BD^*}(W^2) + \frac{W^2 - m_B^2 + m_{D^*}^2}{m_B + m_{D^*}} a_2^{BD^*}(W^2) \right], \tag{B.4c}$$

$$A_4^{D^*} = \frac{-g_{D^* D\gamma}}{\left((p'+q)^2 - m_{D^*}^2\right) W^2} \left[2 m_{D^*} a_0^{BD^*}(W^2) - (m_B + m_{D^*}) a_1^{BD^*}(W^2) + \frac{W^2 + m_B^2 - m_{D^*}^2}{m_B + m_{D^*}} a_2^{BD^*}(W^2) \right] \tag{B.4d}$$

Bibliography

[1] H. Flacher et al., Eur. Phys. J. **C60**, 543 (2009), 0811.0009.

[2] D. J. Gross and R. Jackiw, Phys. Rev. **D6**, 477 (1972).

[3] M. Kobayashi and T. Maskawa, Prog. Theor. Phys. **49**, 652 (1973).

[4] N. Cabibbo, Phys. Rev. Lett. **10**, 531 (1963).

[5] R. D. Peccei, Lect. Notes Phys. **741**, 3 (2008), hep-ph/0607268.

[6] N. G. Deshpande, P. Lo, J. Trampetic, G. Eilam, and P. Singer, Phys. Rev. Lett. **59**, 183 (1987).

[7] J. Charles et al. (CKMfitter Group), Eur. Phys. J. **C41**, 1 (2005), hep-ph/0406184.

[8] R. S. Chivukula and H. Georgi, Phys. Lett. **B188**, 99 (1987).

[9] G. D'Ambrosio, G. F. Giudice, G. Isidori, and A. Strumia, Nucl. Phys. **B645**, 155 (2002), hep-ph/0207036.

[10] G. Isidori (2010), 1001.3431.

[11] K. Abe (Belle) (2007), hep-ex/0703036.

[12] B. Aubert et al. (BABAR) (2007), hep-ex/0703020.

[13] U. Bitenc et al. (BELLE), Phys. Rev. **D77**, 112003 (2008), 0802.2952.

[14] T. Aaltonen et al. (CDF), Phys. Rev. Lett. **100**, 121802 (2008), 0712.1567.

[15] A. Zupanc et al. (Belle), Phys. Rev. **D80**, 052006 (2009), 0905.4185.

[16] N. Isgur and M. B. Wise, Phys. Lett. **B232**, 113 (1989).

[17] N. Isgur and M. B. Wise, Phys. Lett. **B237**, 527 (1990).

[18] K. G. Wilson, Phys. Rev. **179**, 1499 (1969).

[19] K. G. Wilson and W. Zimmermann, Commun. Math. Phys. **24**, 87 (1972).

[20] S. L. Glashow, Nucl. Phys. **22**, 579 (1961).

[21] A. Salam (1968), originally printed in *Svartholm: Elementary Particle Theory, Proceedings Of The Nobel Symposium Held 1968 At Lerum, Sweden*, Stockholm 1968, 367-377.

[22] S. Weinberg, Phys. Rev. Lett. **19**, 1264 (1967).

[23] P. W. Higgs, Phys. Lett. **12**, 132 (1964).

[24] P. W. Higgs, Phys. Rev. Lett. **13**, 508 (1964).

[25] F. Englert and R. Brout, Phys. Rev. Lett. **13**, 321 (1964).

[26] G. S. Guralnik, C. R. Hagen, and T. W. B. Kibble, Phys. Rev. Lett. **13**, 585 (1964).

[27] L. Wolfenstein, Phys. Rev. Lett. **51**, 1945 (1983).

[28] C. Amsler et al. (Particle Data Group), Phys. Lett. **B667**, 1 (2008).

[29] A. J. Buras (1998), `hep-ph/9806471`.

[30] M. E. Peskin and D. V. Schroeder (1995), reading, USA: Addison-Wesley (1995) 842 p.

[31] R. P. Feynman, Rev. Mod. Phys. **20**, 367 (1948).

[32] R. P. Feynman, Phys. Rev. **76**, 769 (1949).

[33] M. Bauer, B. Stech, and M. Wirbel, Z. Phys. **C34**, 103 (1987).

[34] M. Wirbel, B. Stech, and M. Bauer, Z. Phys. **C29**, 637 (1985).

[35] M. Neubert, Phys. Rept. **245**, 259 (1994), `hep-ph/9306320`.

[36] G. 't Hooft, Phys. Rev. Lett. **37**, 8 (1976).

[37] M. Gell-Mann, Phys. Rev. **106**, 1296 (1957).

[38] Y. Ne'eman, Nucl. Phys. **26**, 222 (1961).

[39] J. Goldstone, A. Salam, and S. Weinberg, Phys. Rev. **127**, 965 (1962).

[40] Y. Nambu, Phys. Rev. **117**, 648 (1960).

[41] S. Weinberg, Physica **A96**, 327 (1979).

[42] G. Colangelo and G. Isidori (2000), `hep-ph/0101264`.

[43] S. R. Coleman, J. Wess, and B. Zumino, Phys. Rev. **177**, 2239 (1969).

[44] J. Gasser and H. Leutwyler, Ann. Phys. **158**, 142 (1984).

[45] J. Gasser and H. Leutwyler, Nucl. Phys. **B250**, 465 (1985).

[46] R. Casalbuoni et al., Phys. Rept. **281**, 145 (1997), `hep-ph/9605342`.

[47] B. Aubert et al. (BABAR), Phys. Rev. Lett. **91**, 051801 (2003), hep-ex/0304006.

[48] A. Garmash et al. (Belle), Phys. Rev. **D69**, 012001 (2004), hep-ex/0307082.

[49] B. Aubert et al. (BABAR), Phys. Rev. **D78**, 091102 (2008), 0808.0900.

[50] K. Huitu, D.-X. Zhang, C.-D. Lu, and P. Singer, Phys. Rev. Lett. **81**, 4313 (1998), hep-ph/9809566.

[51] K. Huitu, C.-D. Lu, P. Singer, and D.-X. Zhang, Phys. Lett. **B445**, 394 (1999), hep-ph/9812253.

[52] S. Fajfer and P. Singer, Phys. Rev. **D62**, 117702 (2000), hep-ph/0007132.

[53] S. Fajfer and P. Singer, Phys. Rev. **D65**, 017301 (2002), hep-ph/0110233.

[54] S. Fajfer and P. Singer, Phys. Lett. **B478**, 185 (2000), hep-ph/0001132.

[55] D. Pirjol and J. Zupan (2009), 0908.3150.

[56] S. Fajfer, J. F. Kamenik, and N. Kosnik, Phys. Rev. **D74**, 034027 (2006), hep-ph/0605260.

[57] Y. Grossman, M. Neubert, and A. L. Kagan, JHEP **10**, 029 (1999), hep-ph/9909297.

[58] R. Mohanta and A. K. Giri, Phys. Rev. **D78**, 116002 (2008), 0812.1077.

[59] E. Witten, Nucl. Phys. **B122**, 109 (1977).

[60] A. J. Buras, M. Jamin, and P. H. Weisz, Nucl. Phys. **B347**, 491 (1990).

[61] F. Gabbiani, E. Gabrielli, A. Masiero, and L. Silvestrini, Nucl. Phys. **B477**, 321 (1996), hep-ph/9604387.

[62] M. J. Duncan, Nucl. Phys. **B221**, 285 (1983).

[63] L. J. Hall, V. A. Kostelecky, and S. Raby, Nucl. Phys. **B267**, 415 (1986).

[64] S. Khalil, Phys. Rev. **D72**, 035007 (2005), hep-ph/0505151.

[65] M. Ciuchini et al., PoS **HEP2005**, 221 (2006), hep-ph/0512141.

[66] M. Ciuchini and L. Silvestrini (2006), hep-ph/0603114.

[67] R. Barbier et al., Phys. Rept. **420**, 1 (2005), hep-ph/0406039.

[68] G. R. Farrar and P. Fayet, Phys. Lett. **B76**, 575 (1978).

[69] S. Dimopoulos and L. J. Hall, Phys. Lett. **B207**, 210 (1988).

[70] P. Langacker and M. Plumacher, Phys. Rev. **D62**, 013006 (2000), hep-ph/0001204.

[71] J. Erler and P. Langacker, Phys. Rev. Lett. **84**, 212 (2000), hep-ph/9910315.

[72] A. Ali, G. Kramer, and C.-D. Lu, Phys. Rev. **D58**, 094009 (1998), hep-ph/9804363.

[73] A. J. Buras, Nucl. Phys. **B434**, 606 (1995), hep-ph/9409309.

[74] D. Melikhov and B. Stech, Phys. Rev. **D62**, 014006 (2000), hep-ph/0001113.

[75] S. Fajfer, J. Kamenik, and P. Singer, Phys. Rev. **D70**, 074022 (2004), hep-ph/0407223.

[76] S. Fajfer and J. Zupan, Int. J. Mod. Phys. **A14**, 4161 (1999), hep-ph/9903427.

[77] G. Kramer and W. F. Palmer, Phys. Rev. **D45**, 193 (1992).

[78] A. Kundu and J. P. Saha, Phys. Rev. **D70**, 096002 (2004), hep-ph/0403154.

[79] L. Silvestrini (2005), hep-ph/0510077.

[80] E. Barberio et al. (Heavy Flavor Averaging Group) (2008), 0808.1297.

[81] Y. Nir (2007), hep-ph/0703235.

[82] M. Ciuchini et al. (2007), hep-ph/0703204.

[83] M. Blanke, A. J. Buras, S. Recksiegel, C. Tarantino, and S. Uhlig (2007), hep-ph/0703254.

[84] C.-H. Chen, C.-Q. Geng, and T.-C. Yuan (2007), arXiv:0704.0601[hep-ph].

[85] X.-Q. Li and Z.-T. Wei (2007), arXiv:0705.1821[hep-ph].

[86] E. Golowich, J. Hewett, S. Pakvasa, and A. A. Petrov, Phys. Rev. **D76**, 095009 (2007), 0705.3650.

[87] F. Martinez-Vidal (BaBar) (2009), 0910.5061.

[88] A. F. Falk, Y. Grossman, Z. Ligeti, Y. Nir, and A. A. Petrov, Phys. Rev. **D69**, 114021 (2004), hep-ph/0402204.

[89] A. F. Falk, Y. Grossman, Z. Ligeti, and A. A. Petrov, Phys. Rev. **D65**, 054034 (2002), hep-ph/0110317.

[90] M. Bobrowski, A. Lenz, J. Riedl, and J. Rohrwild (2010), 1002.4794.

[91] G. Burdman, E. Golowich, J. L. Hewett, and S. Pakvasa, Phys. Rev. **D52**, 6383 (1995), hep-ph/9502329.

[92] G. Burdman, E. Golowich, J. Hewett, and S. Pakvasa, Phys. Rev. **D66**, 014009 (2002), hep-ph/0112235.

[93] G. Burdman and I. Shipsey, Ann. Rev. Nucl. Part. Sci. **53**, 431 (2003), hep-ph/0310076.

[94] S. Fajfer and S. Prelovsek, Phys. Rev. **D73**, 054026 (2006), hep-ph/0511048.

[95] S. Fajfer, S. Prelovsek, and P. Singer, Eur. Phys. J. **C6**, 471 (1999), hep-ph/9801279.

[96] S. Fajfer, S. Prelovsek, and P. Singer, Phys. Rev. **D58**, 094038 (1998), hep-ph/9805461.

[97] S. Fajfer, S. Prelovsek, and P. Singer, Phys. Rev. **D64**, 114009 (2001), hep-ph/0106333.

[98] S. Bianco, F. L. Fabbri, D. Benson, and I. Bigi, Riv. Nuovo Cim. **26N7**, 1 (2003), hep-ex/0309021.

[99] S. Prelovsek (2000), hep-ph/0010106.

[100] C. Greub, T. Hurth, M. Misiak, and D. Wyler, Phys. Lett. **B382**, 415 (1996), hep-ph/9603417.

[101] I. I. Y. Bigi, F. Gabbiani, and A. Masiero, Z. Phys. **C48**, 633 (1990).

[102] S. Prelovsek and D. Wyler, Phys. Lett. **B500**, 304 (2001), hep-ph/0012116.

[103] S. Fajfer, P. Singer, and J. Zupan, Eur. Phys. J. **C27**, 201 (2003), hep-ph/0209250.

[104] Q. He et al. (CLEO), Phys. Rev. Lett. **95**, 221802 (2005), hep-ex/0508031.

[105] A. Freyberger et al. (CLEO), Phys. Rev. Lett. **76**, 3065 (1996).

[106] J. M. Link et al. (FOCUS), Phys. Lett. **B572**, 21 (2003), hep-ex/0306049.

[107] E. M. Aitala et al. (E791), Phys. Rev. Lett. **86**, 3969 (2001), hep-ex/0011077.

[108] Q. He et al. (CLEO), Phys. Rev. Lett. **95**, 221802 (2005), hep-ex/0508031.

[109] V. M. Abazov et al. (D0), Phys. Rev. Lett. **100**, 101801 (2008), 0708.2094.

[110] S. Fajfer and S. Prelovsek (2006), hep-ph/0610032.

[111] V. D. Barger, M. S. Berger, and R. J. N. Phillips, Phys. Rev. **D52**, 1663 (1995), hep-ph/9503204.

[112] V. D. Barger, M. S. Berger, and R. J. N. Phillips, Phys. Rev. **D52**, 1663 (1995), hep-ph/9503204.

[113] P. Langacker and D. London, Phys. Rev. **D38**, 886 (1988).

[114] S. A. Abel, M. Masip, and J. Santiago, JHEP **04**, 057 (2003), hep-ph/0303087.

[115] K. Higuchi and K. Yamamoto, Phys. Rev. **D62**, 073005 (2000), hep-ph/0004065.

[116] J. Y. Lee, JHEP **12**, 065 (2004), hep-ph/0408362.

[117] E. Golowich, J. Hewett, S. Pakvasa, and A. A. Petrov, Phys. Rev. **D79**, 114030 (2009), 0903.2830.

[118] B. A. Dobrescu and A. S. Kronfeld, Phys. Rev. Lett. **100**, 241802 (2008), 0803.0512.

[119] I. Dorsner, S. Fajfer, J. F. Kamenik, and N. Kosnik, Phys. Lett. **B682**, 67 (2009), 0906.5585.

[120] R. Benbrik and C.-H. Chen, Phys. Lett. **B672**, 172 (2009), 0807.2373.

[121] A. S. Kronfeld, PoS **LATTICE2008**, 282 (2008), 0812.2030.

[122] S. Fajfer and N. Kosnik, Phys. Rev. **D79**, 017502 (2009), 0810.4858.

[123] P. P. del Amo Sanchez et al. (The BABAR) (2010), 1003.3063.

[124] B. Blossier et al., JHEP **07**, 043 (2009), 0904.0954.

[125] I. Dorsner, S. Fajfer, J. F. Kamenik, and N. Kosnik, Phys. Rev. **D81**, 055009 (2010), 0912.0972.

[126] J. A. Casas and S. Dimopoulos, Phys. Lett. **B387**, 107 (1996), hep-ph/9606237.

[127] S. Fajfer, S. Prelovsek, and P. Singer, Phys. Rev. **D59**, 114003 (1999), hep-ph/9901252.

[128] G. Buchalla, A. J. Buras, and M. E. Lautenbacher, Rev. Mod. Phys. **68**, 1125 (1996), hep-ph/9512380.

[129] B. C. Allanach, A. Dedes, and H. K. Dreiner, Phys. Rev. **D60**, 075014 (1999), hep-ph/9906209.

[130] M. Petric, M. Staric, and f. t. B. Collaboration (2010), 1003.2345.

[131] B. I. Eisenstein et al. (CLEO), Phys. Rev. **D78**, 052003 (2008), 0806.2112.

[132] D. Becirevic and A. B. Kaidalov, Phys. Lett. **B478**, 417 (2000), hep-ph/9904490.

[133] S. Fajfer and J. Kamenik, Phys. Rev. **D71**, 014020 (2005), hep-ph/0412140.

[134] J. Y. Ge et al. (CLEO), Phys. Rev. **D79**, 052010 (2009), 0810.3878.

[135] C. Aubin et al. (Fermilab Lattice), Phys. Rev. Lett. **94**, 011601 (2005), hep-ph/0408306.

[136] N. Isgur and M. B. Wise, Phys. Rev. **D42**, 2388 (1990).

[137] P. Lichard, Acta Phys. Slov. **49**, 215 (1999), hep-ph/9811493.

[138] S. Weinberg, *The Quantum theory of fields. Vol. 1: Foundations* (1995), Cambridge, UK: Univ. Pr. 609 p.

[139] S. Fajfer and J. Kamenik, Phys. Rev. **D72**, 034029 (2005), hep-ph/0506051.

[140] D. Asner (2007), 0711.3044.

[141] D. Atwood, T. Gershon, M. Hazumi, and A. Soni, Phys. Rev. **D71**, 076003 (2005), hep-ph/0410036.

[142] D. Atwood, M. Gronau, and A. Soni, Phys. Rev. Lett. **79**, 185 (1997), hep-ph/9704272.

[143] B. Grinstein, Y. Grossman, Z. Ligeti, and D. Pirjol, Phys. Rev. **D71**, 011504 (2005), hep-ph/0412019.

[144] B. Grinstein and D. Pirjol, Phys. Rev. **D73**, 014013 (2006), hep-ph/0510104.

[145] D. Atwood, T. Gershon, M. Hazumi, and A. Soni (2007), hep-ph/0701021.

[146] S. Nishida et al. (Belle), Phys. Lett. **B610**, 23 (2005), hep-ex/0411065.

[147] B. Aubert et al. (BABAR), Phys. Rev. **D74**, 031102 (2006), hep-ex/0603054.

[148] B. Aubert et al. (BABAR) (2008), 0805.1317.

[149] D. Becirevic et al., PoS **LAT2005**, 212 (2006), hep-lat/0510017.

[150] S. Fajfer and J. F. Kamenik, Phys. Rev. **D74**, 074023 (2006), hep-ph/0606278.

[151] M. Beneke and T. Feldmann, Nucl. Phys. **B592**, 3 (2001), hep-ph/0008255.

[152] J. Charles, A. Le Yaouanc, L. Oliver, O. Pene, and J. C. Raynal, Phys. Rev. **D60**, 014001 (1999), hep-ph/9812358.

[153] P. Ball and R. Zwicky, Phys. Rev. **D71**, 014015 (2005), hep-ph/0406232.

[154] T. Feldmann, P. Kroll, and B. Stech, Phys. Rev. **D58**, 114006 (1998), hep-ph/9802409.

[155] E. Lunghi and A. Soni (2009), 0912.0002.

[156] V. Lubicz (2009), presented at the Lattice 2009 conference, Beijing, China, 25-31 Jul 2009.

[157] C. Bernard et al., Phys. Rev. **D79**, 014506 (2009), 0808.2519.

[158] I. Caprini, L. Lellouch, and M. Neubert, Nucl. Phys. **B530**, 153 (1998), hep-ph/9712417.

[159] G. M. de Divitiis, E. Molinaro, R. Petronzio, and N. Tantalo, Phys. Lett. **B655**, 45 (2007), 0707.0582.

[160] G. M. de Divitiis, R. Petronzio, and N. Tantalo, JHEP **10**, 062 (2007), 0707.0587.

[161] G. M. de Divitiis, R. Petronzio, and N. Tantalo, Nucl. Phys. **B807**, 373 (2009), 0807.2944.

[162] (2009), private communication with Damir Bećirević.

[163] F. Bloch and A. Nordsieck, Phys. Rev. **52**, 54 (1937).

[164] D. Becirevic and B. Haas (2009), 0903.2407.

[165] G. M. de Divitiis, R. Petronzio, and N. Tantalo, Nucl. Phys. **B807**, 373 (2009), 0807.2944.

[166] G. 't Hooft, Nucl. Phys. **B61**, 455 (1973).

[167] G. 't Hooft, Nucl. Phys. **B62**, 444 (1973).

[168] T. Appelquist and J. Carazzone, Phys. Rev. **D11**, 2856 (1975).

[169] A. V. Manohar (1996), hep-ph/9606222.

[170] S. Weinberg, Phys. Lett. **B91**, 51 (1980).

[171] S. Weinberg, *The quantum theory of fields. Vol. 2: Modern applications* (1996), cambridge, UK: Univ. Pr. 489 p.

List of publications

"Light colored scalars from grand unification and the forward-backward asymmetry in top quark pair production"
I. Doršner, S. Fajfer, J. F. Kamenik and N. Košnik
Phys. Rev. D **81**, 055009 (2010) [arXiv:0912.0972 [hep-ph]]

"Can scalar leptoquarks explain the f_{D_s} puzzle?"
I. Doršner, S. Fajfer, J. F. Kamenik and N. Košnik
Phys. Lett. B **682**, 67 (2009) [arXiv:0906.5585 [hep-ph]]

"Leptoquarks in FCNC charm decays"
S. Fajfer and N. Košnik
Phys. Rev. D **79**, 017502 (2009) [arXiv:0810.4858 [hep-ph]]

"On the Dalitz plot analysis of the $B \to K\eta\gamma$ decays"
S. Fajfer, T. N. Pham and N. Košnik
Phys. Rev. D **78**, 074013 (2008) [arXiv:0806.2247 [hep-ph]]

"Updated constraints on new physics in rare charm decays"
S. Fajfer, N. Košnik and S. Prelovšek
Phys. Rev. D **76**, 074010 (2007) [arXiv:0706.1133 [hep-ph]]

"$b \to dd\bar{s}$ transition and constraints on new physics in B^- decays"
S. Fajfer, J. F. Kamenik and N. Košnik
Phys. Rev. D **74**, 034027 (2006) [arXiv:hep-ph/0605260]

Poglavje 8

Razširjeni povzetek disertacije

8.1 Standardni model in njegove razširitve

Standardni model (SM) je preverjena fizikalna teorija veljavna na najmanjših dosegljivih dolžinskih skalah (10^{-15} m). Skladen je s principi posebne relativnosti in kvantne mehanike, ter za osnovne prostostne stopnje uporablja kvantna polja, katerih ekscitacije predstavljajo delce. Vsebuje 19 prostih parametrov, ki kvantitativno razložijo vse eksperimentalne opazljivke na omenjenih skalah v okviru teoretičnih in eksperimentalnih napak. Edina izjema so opažene nevtrinske oscilacije, ki jih SM ne napove, in nakazujejo na masivnost nevtrinov.

Ker v naboru interakcij SM ni gravitacije, je le-ta veljaven najdlje do Planckove energijske skale ($M_P \simeq 10^{19}$ GeV), kjer zagotovo odpove klasičen (nekvanten) opis gravitacije. V zvezi s tem se pojavi tudi *problem hierarhije* med skalo elektrošibkih interakcij (~ 100 GeV) in Planckovo skalo M_P, kjer je težko razumeti, zakaj bi bila masa Higgsovega bozona na šibki skali. To je tudi glavni teoretični argument za veljavnost SM zgolj do skale ~ 1 TeV, ali kvečjemu nekaj TeV. Obstaja mnogo modelov, ki na skali okrog 1 TeV dopolnijo SM in so v literaturi poimenovani *nova fizika*. V disertaciji obravnavamo efekte supersimetričnih razširitev z ohranjeno ali kršeno parnostjo R_p, modelov z dodatnim umeritvenim bozonom Z', dodatnim singletnim kvarkom, ali singletnim leptokvarkom z nabojem $-1/3$.

8.2 Fizika težkih kvarkovskih okusov

Eksperimenti v fiziki kvarkovskih okusov testirajo šibke interakcije, kjer lahko pride do sprememb med šestimi okusi kvarkov [1]. Za to so posebno pripravni šibki razpadi mezonov, vezanih stanj kvarka in antikvarka. Težka mezona sta mezona D in B, ki ustrezata težkima kvarkoma c in b, vezanima z enim od lahkih antikvarkov (u, d, ali s). Torej je kvarkovska sestava težkih mezonov $B = (b\bar{q})$ in $D = (c\bar{q})$, kjer $\bar{q}$ označuje lahki antikvark. Masa težkih mezonov ($\lesssim 5$ GeV) je dva velikostna reda pod šibko skalo, kar omogoča tvorbo parov težkih mezonov v velikih količinah pri relativno nizkih energijah v t.i. tovarnah težkih mezonov (eksperimenta Belle in BaBar). Ti eksperimenti slonijo na veliki statistiki, ki omogoča dobro natančnost pri

[1] Barvna in elektromagnetna interakcija ohranjata okus kvarkov.

meritvi parametrov fizike okusov — 6 mas kvarkov in matrike Cabibbo-Kobayashi-Maskawa (CKM), ki vsebuje 3 kvarkovske mešalne kote in fazni parameter δ.

Pri teoretični obravnavi razpadov je potrebno upoštevati neperturbativne učinke barvnih interakcij, ki se v sistemu težkih mezonov lahko poenostavijo zaradi hierarhije med masama težkega in lahkega kvarka[2]. Zaradi masivnosti so na voljo mnogi šibki razpadni kanali v vezana stanja lažjih kvarkov ter leptonov.

8.2.1 Kvarkovski okusi v SM

Interakcijske člene v Lagrangevi gostoti določa lokalna umeritvena invarianca pod umeritveno grupo $G = SU(3)_c \times SU(2)_W \times U(1)_Y$. Reprezentacije fermionske snovi v SM so leptonske (E, ℓ_R) in kvarkovske (Q, u_R, d_R):

$$\begin{aligned} &E(1,2)_{-1/2} = \begin{pmatrix} \nu_L \\ \ell_L \end{pmatrix}, && \ell_R(1,1)_{-1}, \\ &Q(3,2)_{1/6} = \begin{pmatrix} u_L^1 \\ d_L^1 \end{pmatrix}, \begin{pmatrix} u_L^2 \\ d_L^2 \end{pmatrix}, \begin{pmatrix} u_L^3 \\ d_L^3 \end{pmatrix}, && \\ &u_R(3,1)_{2/3} = \begin{pmatrix} u_R^1 & u_R^2 & u_R^3 \end{pmatrix}, && d_R(3,1)_{-1/3} = \begin{pmatrix} d_R^1 & d_R^2 & d_R^3 \end{pmatrix}, \end{aligned} \tag{8.1}$$

kjer številke v oklepajih označujejo, v katero reprezentacijo grupe G spada posamezno fermionsko polje. Takó polje $E(1,2)_{-1/2}$ označuje singlet grupe $SU(3)_c$, dublet pod šibko grupo $SU(2)_W$, ter hipernaboj $Y = -1/2$. Interakcije med fermioni SM prenašajo umeritveni bozoni s spinom 1. Eksplicitni masni členi uničijo umeritveno invarianco SM, zato simetrijo zlomimo s Higgsovim mehanizmom, ki priskrbi mase šibkim umeritvenim bozonom $W^{\pm}$, Z ter preko Yukawinih sklopitev tudi mase fermionom. Po rotaciji kvarkovskih polj v masno bazo, nam v interakcijskih členih kvarkov z nabitimi šibkimi bozoni ostane unitarna mešalna matrika CKM V s štirimi prostimi parametri:

$$\mathcal{L}_{\text{kin}} \ni -\frac{g}{\sqrt{2}} W_\mu^+ \, \bar{u}_i \gamma^\mu P_L V_{ij} d_j + \text{H.c.}. \tag{8.2}$$

Izmerjena skorajšnja diagonalnost matrike CKM nudi razvoj v vrsto (Wolfensteinova parametrizacija) po elementu $V_{uc} \equiv \lambda$

$$V = \begin{pmatrix} 1 - \frac{\lambda^2}{2} & \lambda & A\lambda^3(\rho - i\eta) \\ -\lambda & 1 - \frac{\lambda^2}{2} & A\lambda^2 \\ A\lambda^3(1 - \rho - i\eta) & -A\lambda^2 & 1 \end{pmatrix} + \mathcal{O}(\lambda^4), \tag{8.3}$$

kjer je $\lambda = 0.226 \pm 0.001$.

Vozlišče nabitega šibkega bozona s šibkim tokom kvarkov poleg spremembe okusa povzroči tudi prehod med spodnjim (naboj $-1/3$) in zgornjim kvarkom (naboj $2/3$). Okus spreminjajoči nevtralni tokovi (FCNC) se v SM pojavijo šele na ravni kvantnih popravkov z virtualnim šibkim bozonom in so dodatno zastrti zaradi unitarnosti matrike CKM preko mehanizma Glashow-Iliopoulos-Maiani (GIM).

[2]Težki mezon je analog vodikovemu atomu, kjer lahko maso jedra v prvem približku vzamemo za neskončno.

Posledično so vsi procesi, ki vključujejo spremembo okusa, a ne naboja, v SM zelo redki. V modelih nove fizike ne pričakujemo mehanizma analognega GIMu, zato je meritev procesov FCNC lahko okno v efekte nove fizike.

8.2.2 Razvoj produkta operatorjev v šibkih razpadih

Okus spreminjajoči kvarkovski procesi vključujejo izmenjavo šibkih bozonov mase ~ 100 GeV ($m_W = 80.4$ GeV, $m_Z = 90.2$ GeV), mnogo večje od značilne energijske skale pri razpadu težkih mezonov ($\sim$ GeV). Izračuni z uporabo elektrošibke teorije postanejo nepraktični, saj je v nizkoenergijskih procesih vzbujanje šibkih prostostnih stopenj zastrto. Zelo pripravno je uporabiti efektivno teorijo, kjer obdržimo le za dani proces relevantne prostostne stopnje, medtem ko propagacijo masivnih prostostnih stopenj (kratkosežnih efektov) skrčimo v točkovno interakcijo. V primeru interakcije 4 fermionov prek izmenjave šibkega bozona imamo v efektivni Lagrangevi gostoti produkt dveh tokov povezanih s propagatorjem šibkega bozona $i\Delta^{\mu\nu}(x,y)$ (glej enačbo (2.18))

$$\frac{-ig^2}{2}\int d^4x\, d^4y\, J^-_\mu(x)\Delta^{\mu\nu}(x,y)J^+_\nu(y), \tag{8.4}$$

ki ga formalno lahko razvijemo v potenčno vrsto okrog točke $m_W = \infty$. Zgornja nelokalna Lagrangeva gostota se tako zapiše kot *razvoj produkta operatorjev*

$$\frac{-ig^2}{2m_W^2}\int d^4x\, d^4y\left[J^-_\mu(x)g^{\mu\nu}\delta(x-y)J^+_\nu(y) + \mathcal{O}(1/m_W^2)\right], \tag{8.5}$$

kjer je razvidno, da je dominanten prispevek točkovna interakcija 4 fermionov, medtem ko so nelokalni operatorji višjih dimenzij zastrti z višjimi potencami $1/m_W^2$. V vodilnem redu razvoja v $1/m_W^2$ dobimo v Lagrangevi gostoti štiri-fermionske operatorje masne dimenzije 6

$$\mathcal{L}_{\text{dim-6}} = -\frac{4G_F}{\sqrt{2}}\sum_i C_i(\mu)Q_i(\mu), \qquad Q_i = (\bar\psi_{i_1}\Gamma_i\psi_{i_2})(\bar\psi_{i_3}\Gamma'_i\psi_{i_4}). \tag{8.6}$$

Brezdimenzijske Wilsonove koeficiente določimo iz *ujemalnih pogojev* (ang. matching conditions), ki zahtevajo enakost štiritočkovnih enodelčno ireducibilnih Greenovih funkcij v efektivni in celotni teoriji. V ujemanje obeh teorij lahko vključimo tudi virtualne popravke barvnih interakcij. Ti v obravnavo uvedejo renormalizacijsko skalo μ, ki razmejuje kratkosežne od dolgosežnih efektov.

8.3 Redek proces $b \to dd\bar s$

V SM kvarkovski proces $b \to dd\bar s$ poteka preko izmenjave dveh bozonov W, ki tvorita škatlasti diagram (Slika 8.1). Ta proces je zaradi dvojne vsote po notranjih gornjih kvarkih dvojno-GIM zastrt, kar ga naredi eksperimentalno nevidnega. V skladu s temi pričakovanji obstaja le zgornja meja na razvejitveno razmerje trodelčnega razpada, ki ga na kvarkovskem nivoju sproži $b \to dd\bar s$

$$\mathcal{B}(B^- \to \pi^-\pi^-K^+) < 9.5\times 10^{-7} \text{ pri } 90\% \text{ intervalu zaupanja}\,. \tag{8.7}$$

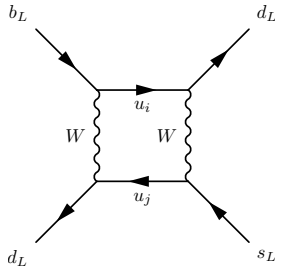

Slika 8.1: Izmenjava dveh bozonov W, ki sproži proces $b \to dd\bar{s}$ v SM.

V nasprotju z napovedmi SM lahko nekateri modeli nove fizike drastično povečajo pogostost procesa $b \to dd\bar{s}$. Analizirali bomo minimalni supersimetrični model z ohranjeno (MSSM) in kršeno ($\not{R}_p$MSSM) parnostjo R_p ter model z dodatnim nevtralnim umeritvenim bozonom Z'.

8.3.1 Inkluzivni razpad

Za dani proces in študirane modele je efektivna Hamiltonova gostota linearna kombinacija

$$\mathcal{H}_{\text{eff.}} = \sum_{n=1}^{5} \left[C_n \mathcal{O}_n + \tilde{C}_n \tilde{\mathcal{O}}_n \right], \tag{8.8}$$

kjer so Wilsonovi koeficienti C_n z masno dimenzijo -2 množijo efektivne operatorje (3.3). V SM je prispevek le k koeficientu C_3, ki vsebuje kvarkovska tokova Lorentzove strukture $(V-A)_\mu$. Perturbativni učinki barvne interakcije so za operator $\mathcal{O}_3$ zanemarljivi. Za inkluzivno razpadno širino $b \to dd\bar{s}$ dobimo

$$\Gamma^{\text{SM}}_{\text{incl.}} = \frac{\left|C_3^{\text{SM}}\right|^2 m_b^5}{384\pi^3}, \qquad C_3^{\text{SM}} \approx 5.3 \times 10^{-13}\ \text{GeV}^{-2}, \tag{8.9}$$

in razvejitveno razmerje je mnogo premajhno za zaznavo v prihodnjih eksperimentih ($\mathcal{B}(b \to dd\bar{s})_{\text{SM}} = (8 \pm 2) \times 10^{-14}$). V modelu MSSM je tako kot v SM neničelen le koeficient C_3, ki se v tem primeru inducira preko škatlastih diagramov s skvarki in gluini, katerih prispevki so bili izračunani za $\Delta S = 2$ procese. Dobimo $|C_3^{\text{MSSM}}| < 1.6 \times 10^{-12}$ GeV^{-2} ter posledično za zgornjo mejo razvejitvenega razmerja 7×10^{-13}. V MSSM torej ni možnosti, da bi ta proces opazili.

Če v modelu MSSM sprostimo zahtevo po ohranitvi parnosti R_p, ki je za vsak delec definirana kot

$$R_p = (-1)^S (-1)^{3B+L} = \begin{cases} +1 & ; \quad \text{SM} \\ -1 & ; \quad \text{SUSY} \end{cases}, \tag{8.10}$$

kjer je S spin, L leptonsko število, in B barionsko število delca, dovolimo člene v Lagrangevi gostoti, ki kršijo leptonsko ali barionsko število. V tem modelu ($\not{R}_p$MSSM) sklopitve λ'_{ijk} kršijo leptonsko število in lahko posredujejo okus spreminjajoče nev-

tralne tokove med kvarki preko izmenjave snevtrina (Slika 8.2)

$$C_4^{\not R_p} = -\sum_{n=1}^{3} \frac{\lambda'_{n31}\lambda'^{*}_{n12}}{m^2_{\tilde\nu_n}}, \tag{8.11}$$

$$\tilde C_4^{\not R_p} = -\sum_{n=1}^{3} \frac{\lambda'_{n21}\lambda'^{*}_{n13}}{m^2_{\tilde\nu_n}}. \tag{8.12}$$

Učinke perturbativnih popravkov barvne interakcije upoštevamo z uporabo re-

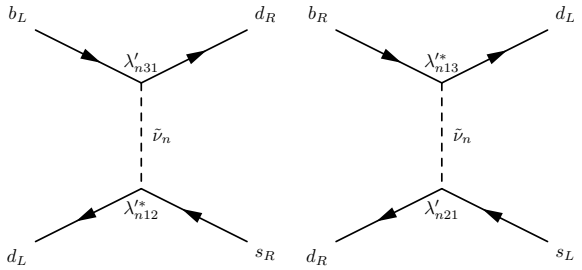

Slika 8.2: Prehod $b \to dd\bar s$ preko izmenjave snevtrina v modelu $\not R_p$MSSM.

normalizacijske grupe, ki v tem primeru na nivoju razpadne širine prispeva faktor f_{QCD}, ki je za mase snevtrinov do 1 TeV približno 2.2.

$$\Gamma^{\not R_p}_{\text{incl.}} = \frac{m_b^5 f^2_{QCD}(m_{\tilde\nu})}{2048\pi^3}\left(|C_4^{\not R_p}|^2 + |\tilde C_4^{\not R_p}|^2\right). \tag{8.13}$$

Zgornja kombinacija parametrov λ'_{ijk} iz drugih procesov še ni znana.

V modelu z dodatnim nevtralnim umeritvenim bozonom Z' so FCNC prav tako inducirani na drevesnem redu in njihove prispevke upoštevamo v koeficientih

$$C_1^{Z'} = -4\sqrt{2}G_F y B_{12}^{d_L} B_{13}^{d_R}, \qquad \tilde C_1^{Z'} = -4\sqrt{2}G_F y B_{12}^{d_R} B_{13}^{d_L}, \tag{8.14a}$$

$$C_3^{Z'} = -4\sqrt{2}G_F y B_{12}^{d_L} B_{13}^{d_L}, \qquad \tilde C_3^{Z'} = -4\sqrt{2}G_F y B_{12}^{d_R} B_{13}^{d_R}. \tag{8.14b}$$

Mešanje operatorjev zaradi barvnih interakcij generira tudi končen C_2, in za $m_{Z'} = 500$ GeV so koeficienti na skali mase kvarka b sledeči:

$$C_1^{Z'}(m_b) = 0.90 C_1^{Z'}, \qquad C_3^{Z'}(m_b) = 0.81 C_3^{Z'}, \tag{8.15}$$

$$C_2^{Z'}(m_b) = 0.47 C_1^{Z'}. \tag{8.16}$$

Na enak način se mešajo koeficienti $\tilde C_{1,2,3}$. Meje na zgornje Wilsonove koeficiente bomo izpeljali iz zgornje meje razpadne širine $B^- \to K^+\pi^-\pi^-$.

8.3.2 Ekskluzivni razpadi mezona B^-

Za izračun hadronske amplitude moramo upoštevati učinke neperturbativnih barvnih interakcij pri računanju razpadnih amplitud. Efektivno Lagrangevo gostoto je potrebno izvrednotiti med začetnim in končnim stanjem hadronov. Najprej uporabimo približek saturacije z vakuumom kot edinega vmesnega stanja. Amplituda

se tako faktorizira v produkt dveh hadronskih matričnih elementov. V primeru za razpad v tri psevdoskalarne mezone preko operatorja $\mathcal{O}_3$ dobimo

$$\begin{aligned}\left\langle P_2(p_2)P_1(p_1)\left|\,\bar{d}\gamma_\mu s\,\right|0\right\rangle\left\langle P(p)\left|\,\bar{d}\gamma^\mu b\,\right|B^-(p_B)\right\rangle = \\ = (t-u)F_1^{P_2P_1}(s)F_1^{PB}(s) \\ + \frac{(m_{P_1}^2-m_{P_2}^2)(m_B^2-m_P^2)}{s}\left[F_1^{P_2P_1}(s)F_1^{PB}(s)-F_0^{P_2P_1}(s)F_0^{PB}(s)\right],\end{aligned} \tag{8.17}$$

kjer smo uvedli Mandelstamove kinematske spremenljivke $s=(p_B-p)^2$, $t=(p_B-p_1)^2$ in $u=(p_B-p_2)^2$. Funkcije F so oblikovni faktorji, ki vsebujejo učinke neperturbativnih barvnih interakcij. Definirani so v poglavju 2.3.1. Njihove funkcijske odvisnosti od kinematičnega parametra vzamemo iz literature. Za oblikovne faktorje $B\to\pi(\rho)$ uporabimo vrednosti izračunane v relativističnem konstituentnem kvarkovskem modelu [74]. Za prehoda $D_s\to D$ in $K\to\pi$ obstaja napoved narejena v efektivni teoriji težkih kvarkov in kiralne perturbacijske teorije [75, 76].

Izračunali smo razvejitvena razmerja nekaterih dvo- in trodelčnih razpadnih kanalov mezona B^- (Tabela 8.1). Kot je bilo razvidno že iz inkluzivnih razvejitvenih

Razpadni kanal	SM	MSSM	$\not{R}_p$MSSM	Z'
$B^-\to\pi^-\pi^-K^+$	1×10^{-15}	1×10^{-14}	omejitev par.	omejitev par.
$B^-\to\pi^-D^-D_s^+$	6×10^{-21}	6×10^{-20}	9×10^{-9}	4×10^{-9}
$B^-\to\pi^-K^0$	3×10^{-16}	3×10^{-15}	5×10^{-8}	2×10^{-7}
$B^-\to\rho^-K^0$	3×10^{-16}	3×10^{-15}	5×10^{-8}	4×10^{-7}
$B^-\to\pi^-K^{*0}$	5×10^{-16}	5×10^{-15}	—	5×10^{-7}
$B^-\to\rho^-K^{*0}$	6×10^{-16}	6×10^{-15}	—	6×10^{-7}

Tabela 8.1: Razvejitvena razmerja za $\Delta S=-1$ hadronske razpade mezona B^-, izračunana v SM, MSSM, $\not{R}_p$MSSM in modelu z bozonom Z'. Iz eksperimentalne zgornje meje za razpad $\mathcal{B}(B^-\to\pi^-\pi^-K^+)<9.5\times10^{-7}$ smo določili zgornje meje parametrov modela $\not{R}_p$MSSM (četrti stolpec) in Z' (peti stolpec).

razmerij, je model MSSM nemogoče opaziti v teh razpadih, saj poveča razvejitvena razmerja glede na SM le za red velikosti. Veliki prispevki so možni v modelih $\not{R}_p$MSSM in Z', kjer smo iz zgornje meje $\mathcal{B}(B^-\to\pi^-\pi^-K^+)<9.5\times10^{-7}$ določili meje na parametre. Za $\not{R}_p$MSSM ta meja ustreza

$$\left|\sum_{n=1}^{3}\left(\frac{100\text{ GeV}}{m_{\tilde{\nu}_n}}\right)^2\left(\lambda'_{n31}\lambda'^*_{n12}+\lambda'_{n21}\lambda'^*_{n13}\right)\right|<6.6\times10^{-5}, \tag{8.18}$$

medtem ko v modelu Z' izpeljemo

$$y\left|B_{12}^{d_L}B_{13}^{d_R}+B_{12}^{d_R}B_{13}^{d_L}\right|<3.2\times10^{-4}, \tag{8.19a}$$

$$y\left|B_{12}^{d_L}B_{13}^{d_L}+B_{12}^{d_R}B_{13}^{d_R}\right|<5.2\times10^{-4}. \tag{8.19b}$$

Neenačbe (8.18) in (8.19) ustrezajo napovedim v zadnjih dveh stolpcih Tabele 8.1. V Z' je največ možnosti za zaznavo dvodelčnih razpadov v K^{0*}, medtem ko so faktorizabilni prispevki k tem razpadom v $\not{R}_p$MSSM ničelni, kanali s K^0 pa so za velikostni razred manjši.

8.4 Nevtralni tokovi čarobnega kvarka in razpad $D \to P\ell^+\ell^-$

Čarobni mezoni so edini hadronski sistem za opazovanje nevtralnih kvarkovskih tokov med gornjimi kvarki. Pomemben proces z nevtralnim tokom je $c \to u\gamma$, kjer je lahko γ realen ali tvori par leptonov $\ell^+\ell^-$ in žene proces $c \to u\ell^+\ell^-$. V luči nedavno izmerjenih parametrov mešanja nevtralnih mezonov D^0

$$x \equiv \frac{\Delta m_D}{\bar{\Gamma}_D} = (0.98 \pm 0.25) \times 10^{-2}, \tag{8.20a}$$

$$y \equiv \frac{\Delta \Gamma_D}{2\bar{\Gamma}_D} = (0.83 \pm 0.16) \times 10^{-2}, \tag{8.20b}$$

bomo raziskali njihov vpliv na razpade $c \to u\gamma$ in razpade mezona D v psevdoskalar in leptonski par ($D \to P\ell^+\ell^-$, $\ell = e, \mu$). Razpade bomo analizirali v SM, MSSM, $\not{R}_p$MSSM, modelu s singletnim gornjim kvarkom, ter modelu z leptokvarkom. Gornji meji za kanal s pionom in elektronom ali mionom sta znani

$$\mathcal{B}(D^+ \to \pi^+ e^+ e^-) < 7.4 \times 10^{-6} \qquad [108], \tag{8.21a}$$

$$\mathcal{B}(D^+ \to \pi^+ \mu^+ \mu^-) < 3.9 \times 10^{-6} \qquad [109]. \tag{8.21b}$$

8.4.1 Razpad $c \to u\gamma$ v MSSM

V SM ima inkluzivni $c \to u\gamma$ razvejitveno razmerje $\Gamma(c \to u\gamma)/\Gamma_{D^0} = 2.5 \times 10^{-8}$ [100]. V minimalnem supersimetričnem SM (MSSM) ta proces posredujejo diagrami z virtualnimi gluini, kjer se okus zamenja v prvem redu masnih vstavkov (ang. mass insertions). Prispevata le masna vstavka $(\delta^u_{12})_{LR}$ in $(\delta^u_{12})_{RL}$ [101, 102], ki prav tako generirata mešanje mezonov D^0–$\bar{D}^0$. Iz zahteve, da vakuumsko stanje MSSM ni niti električno niti barvno nabito, dobimo pogoje $(\delta^u_{12})_{LR,RL} \leq \sqrt{3} m_c/m_{\tilde{q}}$ [126], kjer $\tilde{q}$ označuje maso skvarkov. Primerjava mej iz mešanja in stabilnosti vakuuma za degenerirane mase skvarkov in gluinov je prikazana v Tabeli 8.2. Če privzamemo

$m_{\tilde{q}} = m_{\tilde{g}}$	$\max\lvert(\delta^u_{12})_{LR,RL}\rvert$ omejitev iz Δm_D	$\max\lvert(\delta^u_{12})_{LR,RL}\rvert$ omejitev iz stabilnosti vakuuma
350 GeV	0.007	0.006
500 GeV	0.01	0.004
1000 GeV	0.02	0.002

Tabela 8.2: Zgornje meje na masne vstavke $|(\delta^u_{12})_{LR,RL}|$ dobljene iz Δm_D in omejitev na stabilnost vakuuma [126].

mase gluinov in skvarkov $m_{\tilde{q}} = m_{\tilde{g}} = 350$ GeV in uporabimo mejo iz Tabele 8.2 dobimo v MSSM

$$\Gamma(c \to u\gamma)/\Gamma_{D^0} \leq 8 \times 10^{-7}, \tag{8.22}$$

kar je en red velikosti nad napovedjo SM, vendar so hadronski razpadi $D \to V\gamma$ povsem zasičeni z dolgosežnimi prispevki barvne interakcije.

8.4.2 Kratkosežni prispevki k $c \to u\ell^+\ell^-$

SM

V SM nam proces $c \to u\ell^+\ell^-$ generira efektivna Lagrangeva gostota na skali m_c kvarka [103]

$$\mathcal{L}_{\text{eff}}^{\text{SM}} = -\frac{4G_F}{\sqrt{2}}\left[\lambda_d \sum_{i=1,2} C_i(\mu_c)Q_i^d + \lambda_s \sum_{i=1,2} C_i(\mu_c)Q_i^s - \lambda_b \sum_{i=3,\ldots,10} C_i(\mu_c)Q_i\right], \tag{8.23}$$

z operatorji definiranimi na strani 55. Dominantni prispevek je generiran z vstavitvijo operatorja Q_2 in dodatnim virtualnim gluonom. Končna amplituda je sorazmerna z operatorjem Q_7 s koeficientom [100, 103]

$$\hat{C}_7^{\text{eff}} = \lambda_s(0.007 + 0.020i)(1 \pm 0.2). \tag{8.24}$$

Dodaten singleten kvark z nabojem $2/3$

V celem razredu modelov [94, 110] nastopajo šibko-singletni kvarki z nabojem $2/3$, ki lahko inducirajo okus spreminjajoče nevtralne tokove na drevesnem redu. Gornji kvarki se mešajo z mešalno matriko Ω_{ij}

$$J_{W^3}^{\mu} = \bar{Q}_{iL}\gamma^{\mu}\frac{\tau_3}{2}\Omega_{ij}Q_{jL} = \frac{1}{2}\bar{u}_{iL}\gamma^{\mu}\Omega_{ij}u_{jL} - \frac{1}{2}\bar{d}_{iL}\gamma^{\mu}d_{iL}. \tag{8.25}$$

Prispevek je k dvema operatorjema, ki sta v SM zanemarljiva:

$$V_{ub}V_{cb}^*\delta C_9 = \frac{4\pi}{\alpha}\Omega_{uc}(4\sin^2\theta_W - 1), \tag{8.26a}$$

$$V_{ub}V_{cb}^*\delta C_{10} = \frac{4\pi}{\alpha}\Omega_{uc}\,. \tag{8.26b}$$

Isti parameter mešalne matrike nastopa v mešanju nevtralnih mezonov in iz izmerjenih parametrov dobimo $\Omega_{uc} < 2.8 \times 10^{-4}$ [116].

MSSM in $\not{R}_p$**MSSM**

V MSSM bi naivno pričakovali, da bodo prispevki ojačani pri majhnih q^2 zaradi propagatorja fotona, vendar nam za končna stanja s psevdoskalarjem nastopa še dodaten faktor q^2. Zato se tu osredotočimo le na model $\not{R}_p$MSSM, kjer zaradi sklopitev λ'_{ijk} dolnji skvarki $\tilde{d}$ sklapljajo gornje kvarke in leptone. V vodilnem redu razvoja v $1/m_{\tilde{d}}^2$ nam ti generirajo efektivna operatorja $Q_{9,10}$ z Wilsonovima koeficientoma

$$V_{cb}^*V_{ub}\delta C_9 = -V_{cb}^*V_{ub}\delta C_{10} = \frac{\sin^2\theta_W}{2\alpha^2}\sum_{k=1}^{3}\left(\frac{m_W}{m_{\tilde{d}_{kR}}}\right)^2 \tilde{\lambda}'_{i2k}\tilde{\lambda}'^*_{i1k}. \tag{8.27}$$

Skalarni leptokvark v reprezentaciji $(3,1,-1/3)$

Sklaplja par lepton-kvark, kjer sta oba ali šibka singleta (desnoročna) ali šibka dubleta (levoročna). Za vse prispevke je potrebno razširiti nabor operatorjev tudi na tenzorske tokove, vendar so ti zaradi močnih mej iz meritev $D^0 \to e^+e^-, \mu^+\mu^-$ zelo zastrti. Dominantni prispevki so le k operatorjema $Q_{9,10}$ in njunima kiralno obrnjenima partnerjema $\tilde{Q}_{9,10}$

$$V_{ub}V_{cb}^*\delta C_9 = -V_{ub}V_{cb}^*\delta C_{10} = \frac{\sin^2\theta_W}{2\alpha^2}\frac{m_W^2}{m_\Delta^2}Y_L^{2i}Y_L^{1i*}, \tag{8.28a}$$

$$V_{ub}V_{cb}^*\delta \tilde{C}_9 = V_{ub}V_{cb}^*\delta \tilde{C}_{10} = \frac{\sin^2\theta_W}{2\alpha^2}\frac{m_W^2}{m_\Delta^2}Y_R^{2i}Y_R^{1i*}. \tag{8.28b}$$

8.4.3 Dolgosežni prispevki v $D \to P\ell^+\ell^-$

V amplitudi razpada $D \to P\ell^+\ell^-$ lahko dobimo pole v spremenljivki q^2 zaradi vezanih stanj, ki se sklapljajo z operatorjema Q_1 in Q_2. Takšni resonančni efekti so posledica vezanih stanj barvne interakcije in jih lahko modeliramo z Breit-Wignerjevo obliko. Prispevek vektorskih resonanc, ki razpadajo v par lepton-antilepton zapišemo

$$\mathcal{A}^{\mathrm{LD}}\left[D \to KV \to K\ell^-\ell^+\right] = e^{i\phi_V}\frac{a_V}{q^2 - m_V^2 + im_V\Gamma_V}\,\bar{u}(p_-)\not{p}\,v(p_+), \tag{8.29}$$

kjer sta $p_\pm$ gibalni količini leptonov, m_V, Γ_V masa in razpadna širina resonance, in a_V prost brezdimenzijski parameter. Prispevajo nevtralne vektorske resonance $V = \rho, \omega, \phi$, za katere lahko parametre a_V določimo iz eksperimentalno znanih širin $\Gamma_{D\to PV}$ in $\Gamma_{V\to\ell^+\ell^-}$. Ker so resonance vse relativno ozke $\Gamma_V \ll m_V$, velja približek

$$\mathcal{B}\left[D \to PV \to P\ell^-\ell^+\right] \simeq \mathcal{B}\left[D \to PV\right] \times \mathcal{B}\left[V \to \ell^-\ell^+\right]. \tag{8.30}$$

8.4.4 Primerjava resonančnih in kratkosežnih spektrov

Izkaže se, da je model z dodatnim singletnim kvarkom preostro omejen iz meritev parametrov mešanja nevtralnih D mezonov in nanj spekter in razpadna širina nista občutljiva. Po drugi strani model $\not{R}_p$MSSM in model z leptokvarkom lahko rezultirata v opazljivih prispevkih tako v kanalu $D^+ \to \pi^+e^+e^-$, kot tudi $D^+ \to \pi^+\mu^+\mu^-$. Sklopitve λ', ki nastopajo v razpadu z elektroni v končnem stanju so omejene iz testov univerzalnosti nabitih tokov in meritev breznevtrinskega dvojnega β razpada. Po drugi strani pa je za kanal z mioni eksperimentalna zgornja meja (8.21b) močnejša od mej na relevantne parametre λ' v literaturi in iz nje izpeljemo

$$\sum_{k=1}^{3}\frac{\left|\tilde{\lambda}'_{22k}\tilde{\lambda}'^*_{21k}\right|}{(m_{\tilde{d}_{kR}}/100\ \mathrm{GeV})^2} < 1.0\times10^{-3}. \tag{8.31}$$

Za sklopitve leptokvarkov dobimo

$$\frac{\left|Y_{L(R)}^{21}Y_{L(R)}^{11*}\right|}{(m_\Delta/100\ \mathrm{GeV})^2} < 1.6\times10^{-3}, \qquad \frac{\left|Y_{L(R)}^{22}Y_{L(R)}^{12*}\right|}{(m_\Delta/100\ \mathrm{GeV})^2} < 1.0\times10^{-3}. \tag{8.32}$$

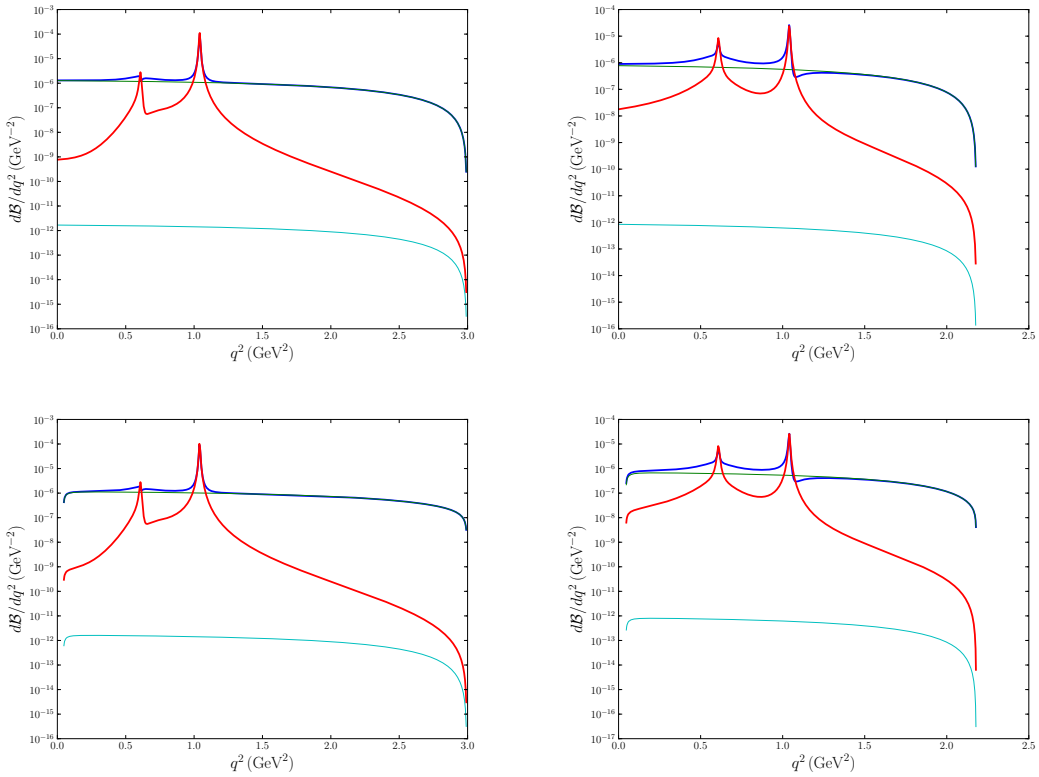

Slika 8.3: Distribucija razpadne širine po invariantni masi leptonov q^2 za razpad $D^+ \to \pi^+\ell^+\ell^-$ (levo) in $D_s \to K^+\ell^+\ell^-$ (desno). V zgornji vrsti je $\ell = e$, v spodnji $\ell = \mu$. Rdeče črte predstavljajo resonančni Breit-Wigner prispevek, temno modre črte pa maksimalni prispevek v modelu $\not{R}_p$MSSM. Svetle modre črte predstavljajo kratkosežni prispevek SM.

Za analizo razpadov čarobno-čudnega mezona D_s, v primeru ko je končno stanje $K^+\mu^+\mu^-$, uporabimo mejo (8.31). Za končno stanje z elektroni uporabimo enake sklopitve, kot smo jih za razpade $D \to Pe^+e^-$.

Vsa razvejitvena razmerja so zbrana v Tabelah 8.3 in 8.4, značilno ojačanje spektrov izven resonančnega območja pa je vidno na grafih 8.3.

razpad	eksperiment	res.	res.+$\not{R}_p$MSSM/LQ
$D^+ \to \pi^+e^+e^-$	$< 7.4 \times 10^{-6}$	1.7×10^{-6}	$< 4.2 \times 10^{-6}$
$D^+ \to \pi^+\mu^+\mu^-$	$< 3.9 \times 10^{-6}$	1.7×10^{-6}	omejitev sklopitev λ'

Tabela 8.3: Primerjava eksperimentalnih mej in predikcij za razvejitvena razmerja razpadov mezona D^+. Zadnja dva stolpca vsebujeta napovedi za resonančni spekter in celoten spekter v modelu $\not{R}_p$MSSM ali modelu leptokvarkov.

razpad	eksperiment	res.	res. + $\not{R}_p$MSSM/LQ
$D_s^+ \to K^+e^+e^-$	$< 1.6 \times 10^{-3}$	6.0×10^{-7}	$< 1.9 \times 10^{-6}$
$D_s^+ \to K^+\mu^+\mu^-$	$< 2.6 \times 10^{-5}$	6.0×10^{-7}	$< 1.8 \times 10^{-6}$

Tabela 8.4: Primerjava eksperimentalnih mej in napovedi za razvejitvena razmerja razpadov mezona D_s^+. Zadnja dva stolpca vsebujeta napovedi za resonančni spekter in celoten spekter v modelu $\not{R}_p$MSSM ali modelu leptokvarkov.

8.5 Analiza Dalitzovega diagrama za razpad $B \to K\eta\gamma$

Razpad $b \to s\gamma$ z realnim fotonom v SM poteka preko pingvinskega diagrama, kjer k kromomagnetnem dipolnem operatorju

$$Q_7 = \frac{e}{8\pi^2}\left[m_b\bar{s}\sigma_{\mu\nu}(1+\gamma_5)b + m_s\bar{s}\sigma_{\mu\nu}(1-\gamma_5)b\right]F^{\mu\nu}. \tag{8.33}$$

dominantno prispevata kvark t in šibki bozonom W v zanki. Najbolje raziskan razpadni kanal za meritev velikosti pripadajočega Wilsonovega koeficienta C_7 je razpad $B \to K^*\gamma$. V tem razdelku bomo analizirali razpad $B \to K\eta\gamma$ v kinematičnem območju z energetskim fotonom in enim od lahkih mezonov. Razvejitveni razmerji naslednjih dveh razpadov sta že izmerjeni

$$\mathcal{B}(B^0 \to K^0\eta\gamma) = (7.1^{+2.1}_{-2.0} \pm 0.4) \times 10^{-6}, \tag{8.34a}$$

$$\mathcal{B}(B^+ \to K^+\eta\gamma) = (7.7 \pm 1.0 \pm 0.4) \times 10^{-6}. \tag{8.34b}$$

8.5.1 Pristop z efektivnimi teorijami kvantne kromodinamike

Za emisijo nizkoenergijskega mezona iz težkega mezona B uporabimo kiralno perturbacijsko teorijo težkih mezonov, kjer amplitude razvijemo v potenčno vrsto po dveh majhnih parametrih: $\Lambda_{\rm QCD}/m_b$ in p/Λ_χ (p je gibalna količina lahkega mezona, Λ_χ skala zlomitve kiralne simetrije ~ 1 GeV). Vodilni člen v Lagrangevi gostoti te efektivne teorije je

$$\mathcal{L}_{\rm eff} = g\left\langle H_a(v)\mathcal{A}^\mu_{ab}\gamma_\mu\gamma_5\bar{H}_b(v)\right\rangle. \tag{8.35}$$

Natančna definicija polj težkih in lahkih mezonov je dana v razdelku 2.3.3. Za preostali nadaljnji razpad težkega mezona B na energetska γ in lahki mezon upoštevamo, da sta oba delca v končnem stanju zaradi njune majhne mase skoraj na svetlobnem stožcu. V limiti, ko je njuna energija zelo velika, lahko oblikovne funkcije za prehod $B^* \to K$ preko Q_7 izrazimo z oblikovnimi funkcijami vektorskega toka

$$\left\langle \bar{K}^0(k) \,\middle|\, \bar{s} q_\mu \sigma^{\mu\nu}(1+\gamma_5) h_v \,\middle|\, B^*(v,\eta) \right\rangle = F_+^{BK}(0) \Big[2M \epsilon^{\nu\mu\rho\sigma} v_\mu k_\rho \eta_\sigma + iM^2 \eta^\nu - i\eta \cdot q (Mv+k)^\nu \Big]. \tag{8.36}$$

Naš pristop deluje za nizkoenergijski η ali K, kjer sta (Slika 8.4) Feynmanova diagrama za oba primera različna.

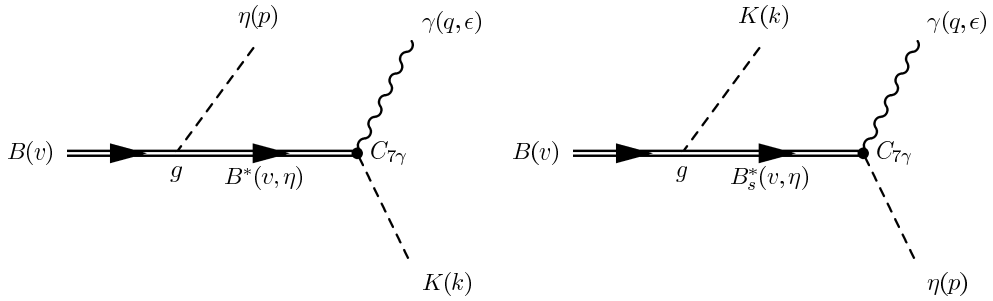

Slika 8.4: Diagram na levi je vodilni prispevek v kinematičnem območju z nizkoenergijskim mezonom η, na desni pa vodilni prispevek za nizkoenergijski mezon K.

8.5.2 Fotonski spektri

Možnost resonančnih prispevkov nudijo vmesna stanja na masni lupini $B \to K_2^*(1430)\gamma$ ali $B \to K_3^*(1780)\gamma$, vendar lahko iz znanih razvejitvenih razmerij teh resonanc [28] ugotovimo, da je resonančno ozadje majhno. Prav tako v eksperimentalnih spektrih teh razpadov [146, 148] ni evidentnih resonančnih prispevkov.

Napovedi fotonskih spektrov razpadov so dobljene v efektivnem pristopu, opisanem v prejšnjem razdelku. Za opis mešanja η in η' uporabimo pristop [154], kjer je mešalni kot θ med $SU(3)$ oktetom η_8 in singletom η_1 enak $-15.4°$. Spektri z η v končnem stanju so vidni na Sliki 8.5. Ko pointegriramo spektra po obeh območjih ($E_K < 1.2$ GeV ali $E_\eta < 1.2$ GeV) za razpad $\bar{B}^0 \to \bar{K}^0 \eta\gamma$ zagotovimo približno 10% razpadne širine (8.34a). Z naraščajočo natančnostjo eksperimentov bo v prihodnosti možno študirati velikost C_7 tudi v omenjenih kinematičnih območjih razpadov $B \to K\eta\gamma$.

8.6 Ozadje mehkih fotonov v razpadih $B \to D\ell\nu$

Meritve ekskluzivnih razpadov $B \to D\ell\nu$ so pomembne za ekstrakcijo elementa V_{cb} matrike CKM, še posebej zavoljo trenutnega razhajanja rezultatov med inkluzivno in ekskluzivno metodo določanja V_{cb}. Vrednost V_{cb} postaja dominanten izvor napake

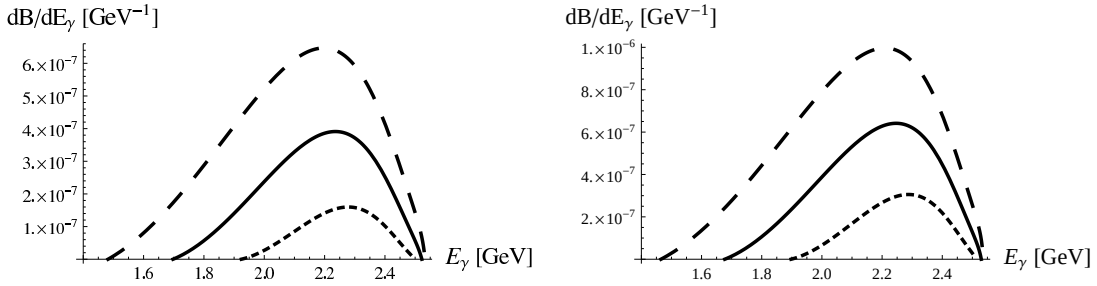

Slika 8.5: Spektra razpada $\bar{B}^0 \to \bar{K}^0\eta\gamma$. Na levi fotonski spekter v območju $E_\eta < 0.8$ GeV (kratko črtkana črta), $E_\eta < 1.0$ GeV (neprekinjena črta) in $E_\eta < 1.2$ GeV (dolgo črtkana črta). Na desni iste oznake za nizkoenergijski K, $E_K < 0.8, 1.0, 1.2$ GeV.

pri teoretični napovedi parametra ϵ_K

$$|\epsilon_K| \propto \hat{B}_K \eta |V_{cb}|^2 \lambda^2. \tag{8.37}$$

kjer je λ zelo natančno znan kosinus Cabibbovega kota. Napaka parametra vreče $\hat{B}_K$ iz simulacij kvantne kromodinamike na mreži je trenutno $\sim 5\%$ in postaja primerljiva z napako V_{cb}. Inkluzivna in ekskluzivna metoda imata do velike mere neodvisne sistematične efekte. Za meritve V_{cb} v ekskluzivnih razpadih $B \to D\ell\nu$ je v prihajajočih tovarnah okusa pričakovana relativna natančnost $\sim 1\%$, kjer lahko pridejo do izraza majhni sistematični efekti. Ker je tipičen eksperiment občutljiv le na fotone do neke najmanjše energije, se lahko za foton γ pod to mejo zgodi, da eksperiment napačno prepozna razpad $B \to D\ell\nu\gamma$ kot $B \to D\ell\nu$.

8.6.1 Enodelčna vmesna stanja

Amplitude za radiacijski razpad se zapiše kot

$$\begin{aligned}&\mathcal{A}(B(p) \to D(p')\ell(p_l)\bar{\nu}(k)\gamma(\epsilon, q)) = \\ &= \frac{eG_F V_{cb}}{\sqrt{2}} \epsilon^{*\mu}\, \bar{u}(p_l)\Big[- \frac{F_\nu(t)}{2p_l \cdot q}\gamma_\mu(\not{p}_l + \not{q} + m_l) + V_{\mu\nu} - A_{\mu\nu}\Big]\gamma^\nu(1-\gamma_5)v(k),\end{aligned} \tag{8.38}$$

kjer je $F_\nu(t)$ matrični element vektorskega toka za prehod $B \to D$ in ustreza izsevu fotona iz leptona, medtem ko je tenzor $V_{\mu\nu} - A_{\mu\nu}$ hadronski korelator elektromagnetnega in šibkega toka. Divergentni prispevki (odvisni le od nabojev hadronov) se v limiti $E_\gamma \to 0$ pokrajšajo z virtualnimi elektromagnetnimi popravki na nivoju razpadne širine, medted ko so strukturno odvisni prispevki v limiti $E_\gamma \to 0$ končni. V hadronskem korelatorju nam vmesna enodelčna stanja generirajo pole v invariantnih masah. V našem primeru bo zaradi majhne razlike mas med stanji D^{0*} in D^0 dominantno prispeval ravno D^{0*}, ki lahko nastane na masni lupini, tako da nam generira resonančno obliko amplitude

$$\frac{i\,\langle D(p')\,|\,J_\mu\,|\,D^*(\mathbf{p}'+\mathbf{q})\rangle\,\langle D^*(\mathbf{p}'+\mathbf{q})\,|\,V_\nu\,|\,B(p)\rangle}{(p'+q)^2 - m_{D^*}^2 + i m_{D^*}\Gamma_{D^*}}. \tag{8.39}$$

8.6.2 Spekter mehkega fotona

Prehod $D^{*0} \to D^0\gamma$ v realni foton nam določa neperturbativni parameter $g_{D^{0*}D^0\gamma}$, ki je bil izračunan na mreži, kot so bile tudi oblikovne funkcije (aksialno-)vektorskega prehoda $B \to D^*$ (za nabor oblikovnih funkcij glej razdelek 2.3.1). Spekter se v celoti nahaja pod 350 MeV, z energijo večine fotonov v intervalu od 100 do 200 MeV. Če bi bil torej eksperiment slep za fotone pod 350 MeV, bi v vzorec dogodkov

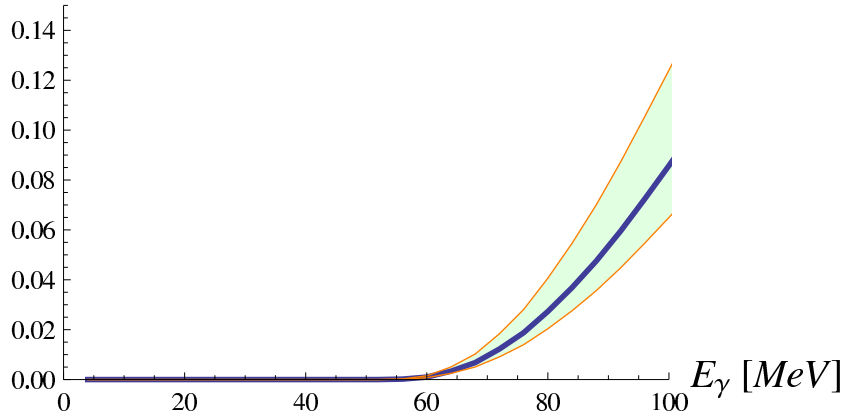

Slika 8.6: Delež napačno prepoznanih radiacijskih dogodkov kot funkcija najmanjše še zaznavne energije fotona.

$B \to D\ell\nu$ zajel še vse dogodke $B \to D^*\ell\nu \to D\gamma\ell\nu$. Na Sliki 8.6 je razvidno, da resolucija eksperimenta 80 MeV ustreza približno 1% relativni napaki na V_{cb} *samo zaradi mehkih fotonov.*

8.7 Zaključek

Fizika okusov, eksperimentalna in teoretična, je igrala pomembno vlogo pri preverbi Yukawinega sektorja standardnega modela. Mehanizem mešanja kvarkovskih okusov Cabibbo-Kobayashi-Maskawa je potrjen na nivoju 10% natančnosti in jasno je, da so efekti nove fizike velikostnega reda tipično nekaj odstotkov ali manj.

V disertaciji smo analizirali razpade težkih mezonov, za katere je pričakovana razpadna širina v okviru standardnega modela majhna, in so tako bolj občutljivi za prispevke nove fizike. V tem kontekstu smo izpostavili modele nove fizike in razpadne kanale, ki še ponujajo možnost za eksperimentalna iskanja. V drugem delu disertacije smo predlagali metodi za preverjanje napovedi samega standardnega modela, ki lahko kaj kmalu pokažejo na nekonsistenco meritev z napovedmi standardnega modela in tako posredno kažejo na novo fiziko. Fizika okusov bo igrala pomembno vlogo tudi v interpretaciji podatkov iz Velikega hadronskega trkalnika (LHC), saj bo potrebno za odkritje novih delcev na LHC njihov vpliv najti in preveriti tudi v virtualnih efektih, kjer do izraza pridejo drugi nabori parametrov nove fizike. V tem oziru pričakujemo komplementarnost prihodnjih tovarn okusa in velikega hadronskega trkalnika v iskanju fizike onkraj standardnega modela.

IZJAVA O AVTORSTVU

Spodaj podpisani Nejc Košnik izjavljam, da je pričujoča disertacija plod lastnega dela in raziskav.

Ljubljana, 16. april 2010 Nejc Košnik